SEISMIC PARTIAL COHERENCY STUDY

28 April 1965

Prepared For

AIR FORCE TECHNICAL APPLICATIONS CENTER
WASHINGTON, D. C.

By

James C. Bradford
UED EARTH SCIENCES DIVISION
TELEDYNE, INC.

And

L. D. Enochson and G. P. Thrall
MEASUREMENT ANALYSIS CORPORATION

Under

Project VELA UNIFORM

Sponsored By

ADVANCED RESEARCH PROJECTS AGENCY
Nuclear Test Detection Office
ARPA Order No. 624

SEISMIC PARTIAL COHERENCY STUDY

28 April 1965

SEISMIC DATA LABORATORY REPORT NO. 121

AFTAC Project No.:	VELA T/2037
Project Title:	Seismic Data Labora cy
ARPA Order No.:	624
ARPA Program Code No.:	5810
Name of Contractor:	UED EARTH SCIENCES DIVISION TELEDYNE, INC.
Contract No.:	AF 33(657) 12447
Date of Contract:	17 August 1963
Amount of Contract:	$5,257,624
Contract Expiration Date:	17 February 1966
Project Manager:	Robert Van Nostrand (703) 836-7644

P. O. Box 334, Alexandria, Virginia

This research was supported by the Advanced Research Projects Agency, Nuclear Test Detection Office, and was monitored by the Air Force Technical Applications Center under Contract AF 33(657) 12447.

TABLE OF CONTENTS

TABLE OF CONTENTS (Continued)

ABSTRACT

Computational experiments have been conducted on a digital computer to illustrate numerically the usefulness of partial coherence techniques. The numerical results obtained demonstrate the necessity of employing partial coherence functions when a multi-input-single output linear system is involved.

Two seismic noise traces were randomly selected from available Seismic Data Lab sources and were combined in various ways to obtain two correlated input traces and an output trace. From this data, gain factors and coherence functions were computed in two ways. First, just one input and one output were employed in the computations. Second, both inputs were accounted for. The numerical results vividly illustrate the biased answers obtained when only the single input and output are considered. This is contrasted with the correct results obtained via the proper model of a two input system.

These procedures were also extended to a three input-single output system where the third input was ignored. In this case the application of partial coherence functions as an indicator of the existence of the third neglected seismic data source is illustrated.

SEISMIC PARTIAL COHERENCY STUDY

1. INTRODUCTION

This report presents the results of a preliminary investigation into the application of partial coherency techniques to the problem of processing seismic data. Ultimately, these techniques will be applied to the detection of the presence or absence of unidentified components in seismic noise, determination of filter responses between two time series, and description of seismic noise fields.

A specific application of partial coherencies to seismology would be the modeling of a seismic noise field. If a noise field has only one component propagating across an area, then the output of one seismometer should suffice to predict the output of a second. If there are two components in the field, then two element outputs are required to predict a third. If there are n components, n elements are required to predict the output of one additional element. As will be seen below, the methods of partial coherencies can be used to determine when sufficiently many inputs are being used to predict an output. Thus, it will be possible, by using partial coherencies, to determine the number of major noise components present and the minimum number of elements required to study the noise field.

However, before the development of a general program, it was necessary to study partial coherence techniques applied to the solution of relatively simple problems under controlled conditions.

The application of power spectra and cross-spectra to determine frequency response functions for simple linear systems, where a single input and output are clearly defined, is well

established. Application of these ideas to more complex systems such as the earth where there are many input and output points is not so well known. Thus, a brief review of these topics is presented below.

Consider the case of a simple linear system with a well-defined single input (excitation) point and single output (response) point. If the input $x(t)$ is a stationary random process with zero mean, then the output $y(t)$ is also a stationary random process with zero mean. Now, if $G_x(f)$ and $G_y(f)$ are the one-sided power spectral density functions, and $G_{xy}(f)$ the cross-power spectral density for the input and output; then the frequency response function for the linear system, $H(f)$ is completely determined by the two relations

$$G_y(f) = |H(f)|^2 G_x(f) \tag{1}$$

$$G_{xy}(f) = H(f) G_x(f) \tag{2}$$

A quantity of particular importance in more complicated situations is the coherence function which is defined by

$$\gamma^2_{xy}(f) = \frac{|G_{xy}(f)|^2}{G_x(f) G_y(f)} \tag{3}$$

It is easily shown that $0 \leq \gamma_{xy}(f) \leq 1$, and for a linear system, $\gamma^2_{xy}(f) = 1$. Thus, the coherence function may be thought of as a measure of linear relationship in the sense that the function attains a theoretical maximum of unity for all frequencies in a linear system. Therefore, if the coherence function is less than unity, one possible cause might be the lack of complete linear dependence between the input and output.

Another application of coherence functions to single input-single output systems is to determine the effect of measurement noise on frequency response function measurements. Without going into the mathematical details, the coherence function in this case is

$$\gamma_{xy}^2(f) = \frac{1}{1 + \beta_i + \beta_o + \beta_i\beta_o} \leq 1 \qquad (4)$$

where β_i is the measurement noise to signal ratio at the input and β_o is the corresponding ratio at the output. Hence, if the coherence function is found to be significantly less than unity, one possible cause might be that the measurement noise effects are not negligible and must be taken into account in determining the frequency response function.

As indicated above, coherence functions are useful aids in the analysis of single input-single output linear systems. However, the area of major application is in the analysis of multiple input-multiple output linear systems which, for example, could represent the response of the earth to internal excitations as measured at several different points. This would be the case when an array of seismic instruments is employed. If it is assumed that the earth has a linear response, and that measurement noise is negligible, then a low coherence function between two points will serve to indicate the presence of other factors which contribute to the output but are not being considered.

In classical statistics, if $\{x_i\}$ is a sequence of random variables, then the residual random variables $\{\Delta x_i\}$ are defined as the result of subtracting a linear least squares prediction of x_i from x_i. Using these residuals, partial correlation coefficients, $\rho_{ij\cdot k}$ can be computed. The notation $\rho_{ij\cdot k}$ stands

for the correlation between x_i and x_j when the effect of x_k has been removed. Partial correlation coefficients are useful in determining the true correlation between two random variables which might otherwise be obscured by the effect of the third random variable.

By analogy, a partial coherence function $\gamma^2_{ij\cdot k}$ can be defined as the coherence function between $x_i(t)$ and $x_j(t)$ after a least squares prediction of $x_k(t)$ has been subtracted out. It should be understood that the subscripts i, j, and k may indicate either inputs or outputs. The utility of partial coherence functions is similar to that of partial correlation coefficients. That is, a high ordinary coherence between two variables could indicate a linear relationship, but in reality this may be a spurious relation due to correlation of one of the variables with a third variable. If the partial coherence function is calculated, the more realistic low coherence would be uncovered. Alternately, the opposite effect may occur where the partial coherence will be larger than the ordinary coherence. This occurs, for example, when two separate inputs both pass through linear systems and make up the single output. Then the partial coherence between either one of the inputs and the output is unity due to the linear relations, but the ordinary coherence will be less than unity. This follows because each input contributes to the output and this fact is not accounted for in the computation of the ordinary coherence function between the output and a single output.

2. SIMULATION MODEL

In order to investigate partial coherence techniques under controlled conditions, two demonstration cases were developed. These are described briefly below

Case 1. Given $x_1(t)$, $x_2(t)$, and $y(t) = a_1x_1(t)+a_2x_2(t-T)$. Determine a_1 , a_2 , and T in the case where x_1 , x_2 are independent and in the case where x_1 , x_2 are correlated.

Case 2. Given $x_1(t)$, $x_2(t)$, and $y(t) = a_1x_1(t)+a_2x_2(t-T)+a_3x_3(t)$. Determine a_1 , a_2 , T , and the presence of x_3 under various conditions of dependence and independence between x_1 , x_2 , and x_3 .

Detailed procedures for generating cases 1 and 2 are presented in Appendix I and are not repeated here. Equations used in calculating expected results are also given in Appendix I.

3. ILLUSTRATIVE EXAMPLE

To show the effect of partial coherence techniques in the analysis of a linear system, one example will not be discussed. This example plus five others are reviewed in detail in Appendix III.

Consider the linear system sketched below.

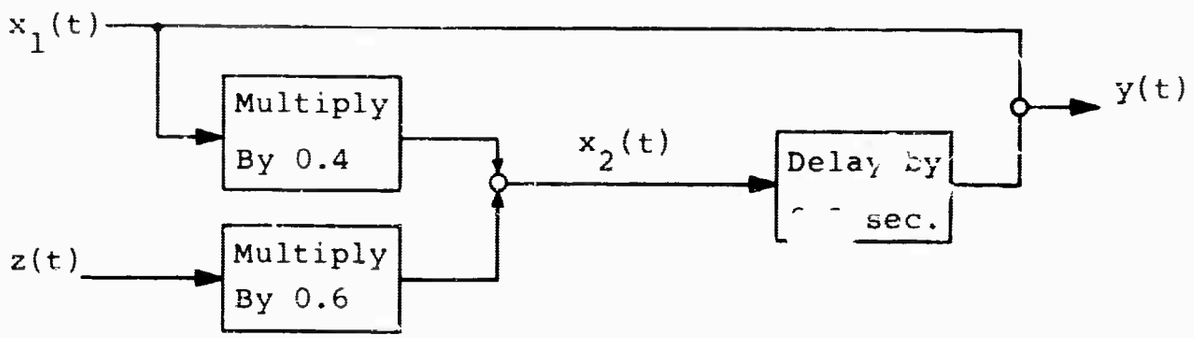

Two independent seismic sources, $x_1(t)$ and $z(t)$, are combined to form a new process, $x_2(t)$, such that

$$x_2(t) = 0.4x_1(t) + 0.6z(t) \tag{5}$$

Secondly, $x_2(t)$ is delayed in time by 0.2 second relative to $x_1(t)$, and finally combined with $x_1(t)$ to form $y(t)$. Thus

$$y(t) = x_1(t) + x_2(t - 0.2) \tag{6}$$

The power spec ra of $x_1(t)$, $x_2(t)$, and $y(t)$ are shown in Figure 1. Because of the way $x_2(t)$ and $y(t)$ were formed, the cross-spectra are given by

$$G_{12}(f) = 0.4G_{11}(f) \tag{7}$$

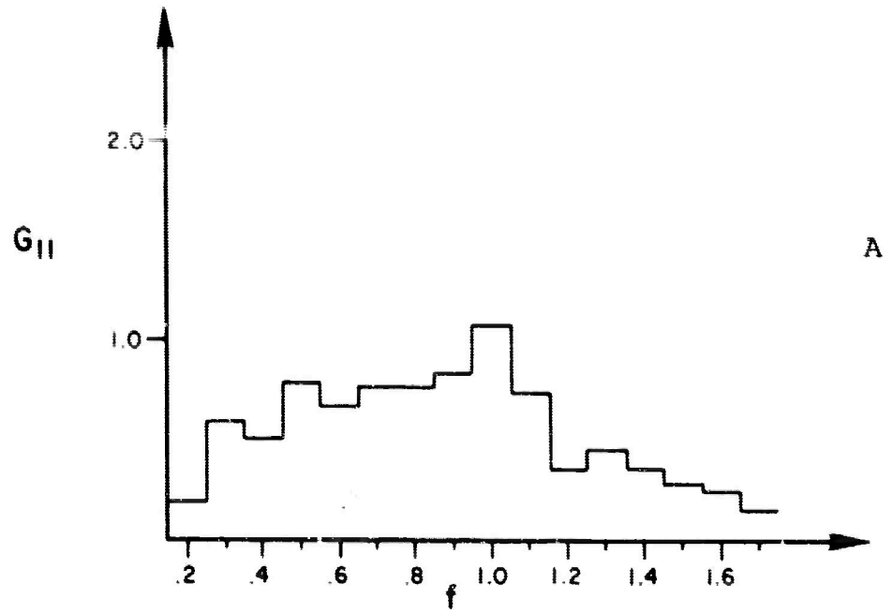

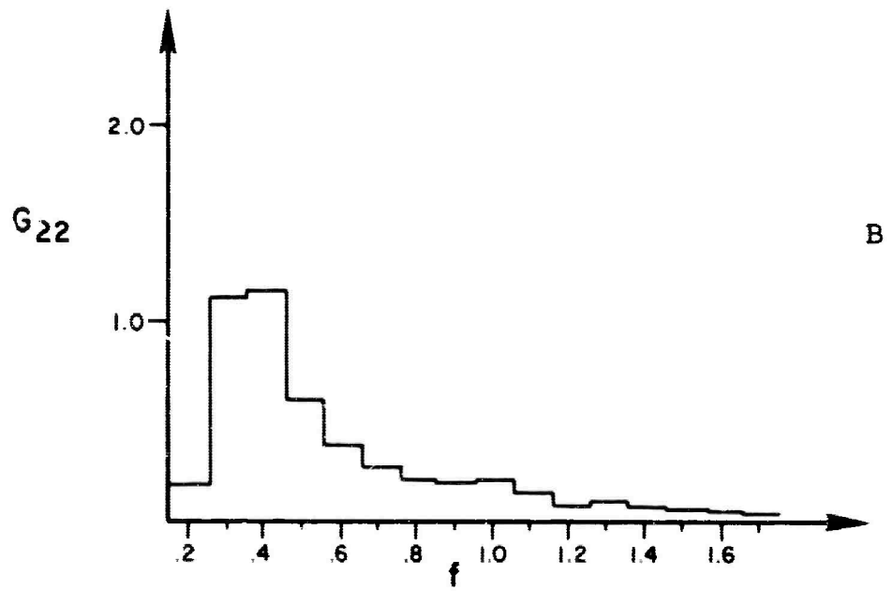

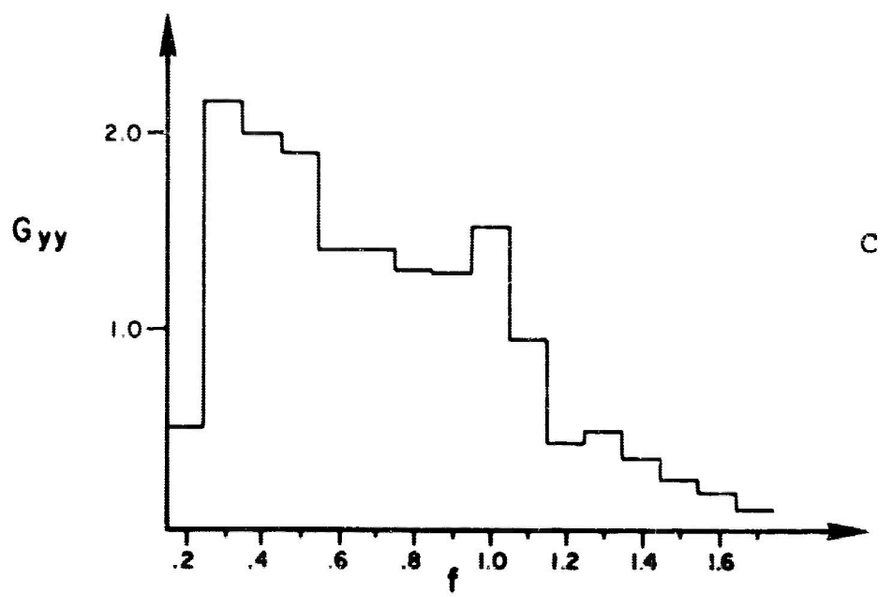

Power Spectra

Figure 1

$$G_{1y}(f) = \left\{1 + 0.4\left[\cos(0.4\pi f) - j\sin(0.4\pi f)\right]\right\} G_{11}(f) \quad (8)$$

$$G_{2y}(f) = 0.4G_{11}(f) + \left[\cos(0.4\pi f) - j\sin(0.4\pi f)\right]G_{22}(f) \quad (9)$$

If the transfer functions between the two inputs and the output, denoted by $H_{1M}(f)$ and $H_{2M}(f)$, are computed (see Appendix I for appropriate equation) without taking into account the correlation between $x_1(t)$ and $x_2(t)$ completely erroneous results are obtained, as shown in Figure 2. It should be noted that transfer functions are complex quantities in general. They are denoted here by gain and phase variables

$$H(f) = |H(f)|e^{j\Phi(f)} \quad (10)$$

where $|H(f)|$ is the gain factor and $\Phi(f)$ is the phase factor. The corresponding true transfer functions are shown in Figure 3. These are computed using the proper multidimensional formulas which take into account all the known variables.

The ordinary coherence functions are plotted in Figure 4. If used by themselves to infer the nature of the system being investigated, one would tend to conclude that high measurement noise was present or that nonlinear effects were present. The true nature of the system is exhibited when the partial coherencies are computed, as shown in Figure 5. The fact that all three functions are equal to one over the frequency range indicates the true linear relationships which exist between $x_1(t)$, $x_2(t)$, and $y(t)$.

As mentioned before, more detailed evaluations of this and five other cases are presented in Appendix III.

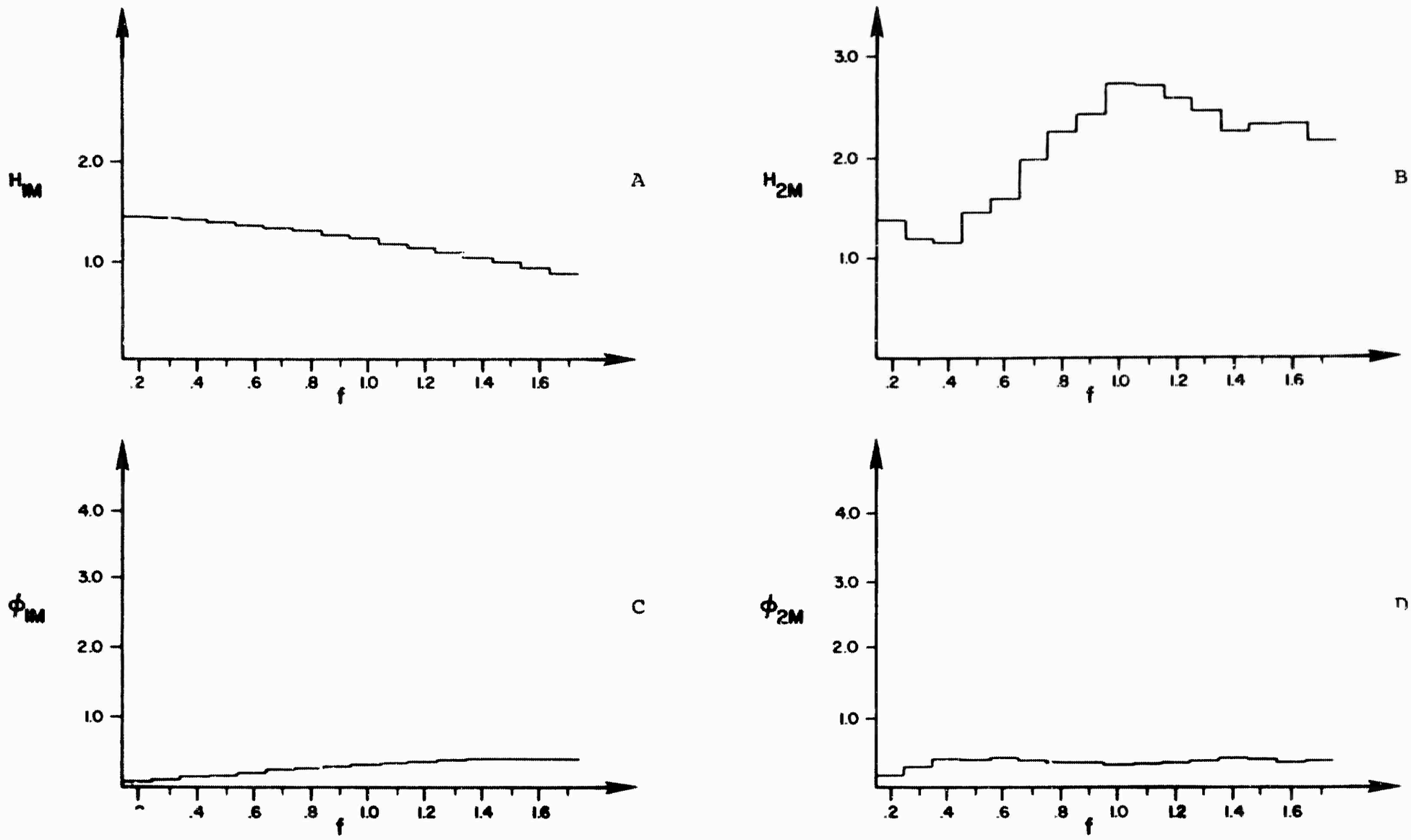

Measured System Response Functions

Figure 2

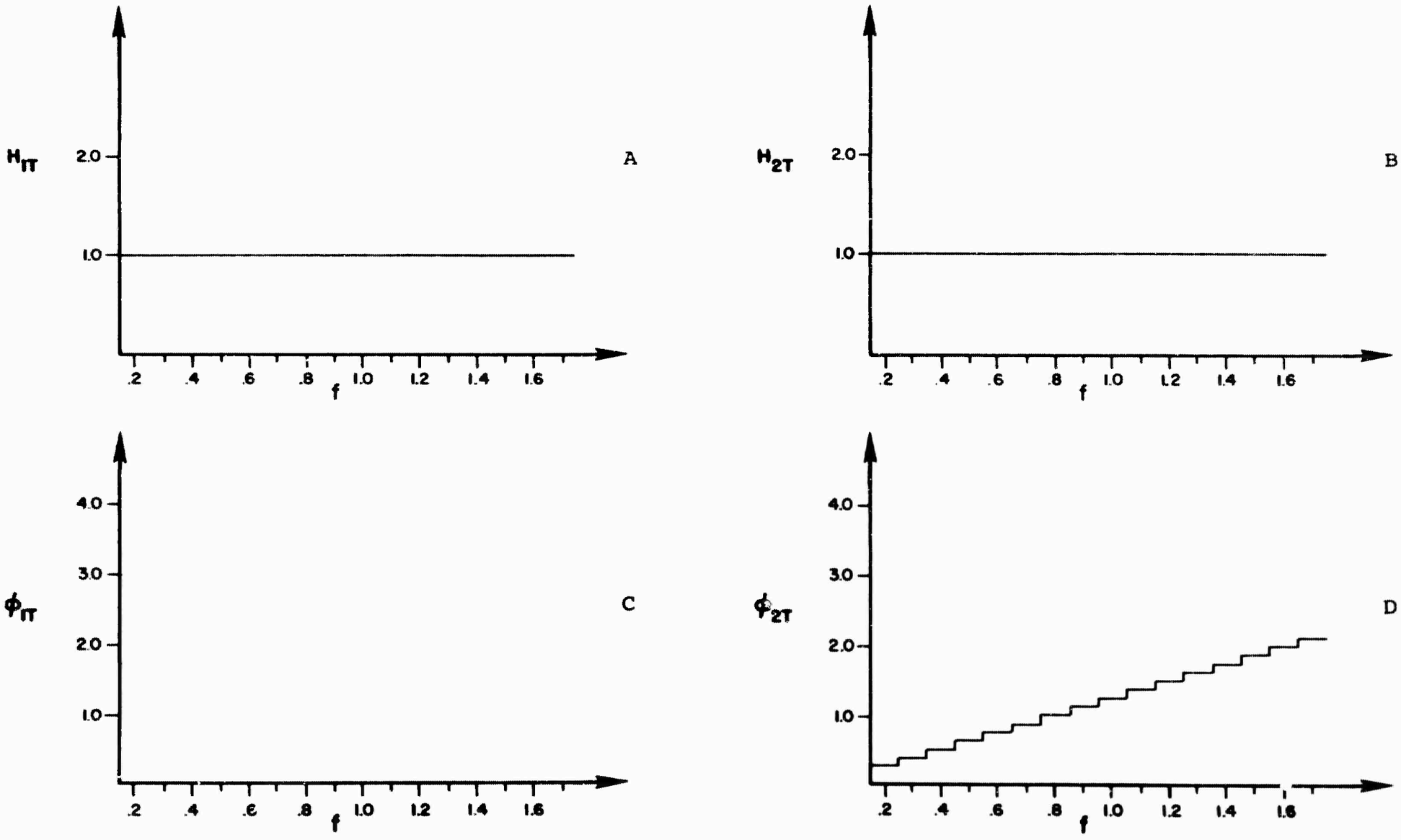

True System Response Functions

Figure 3

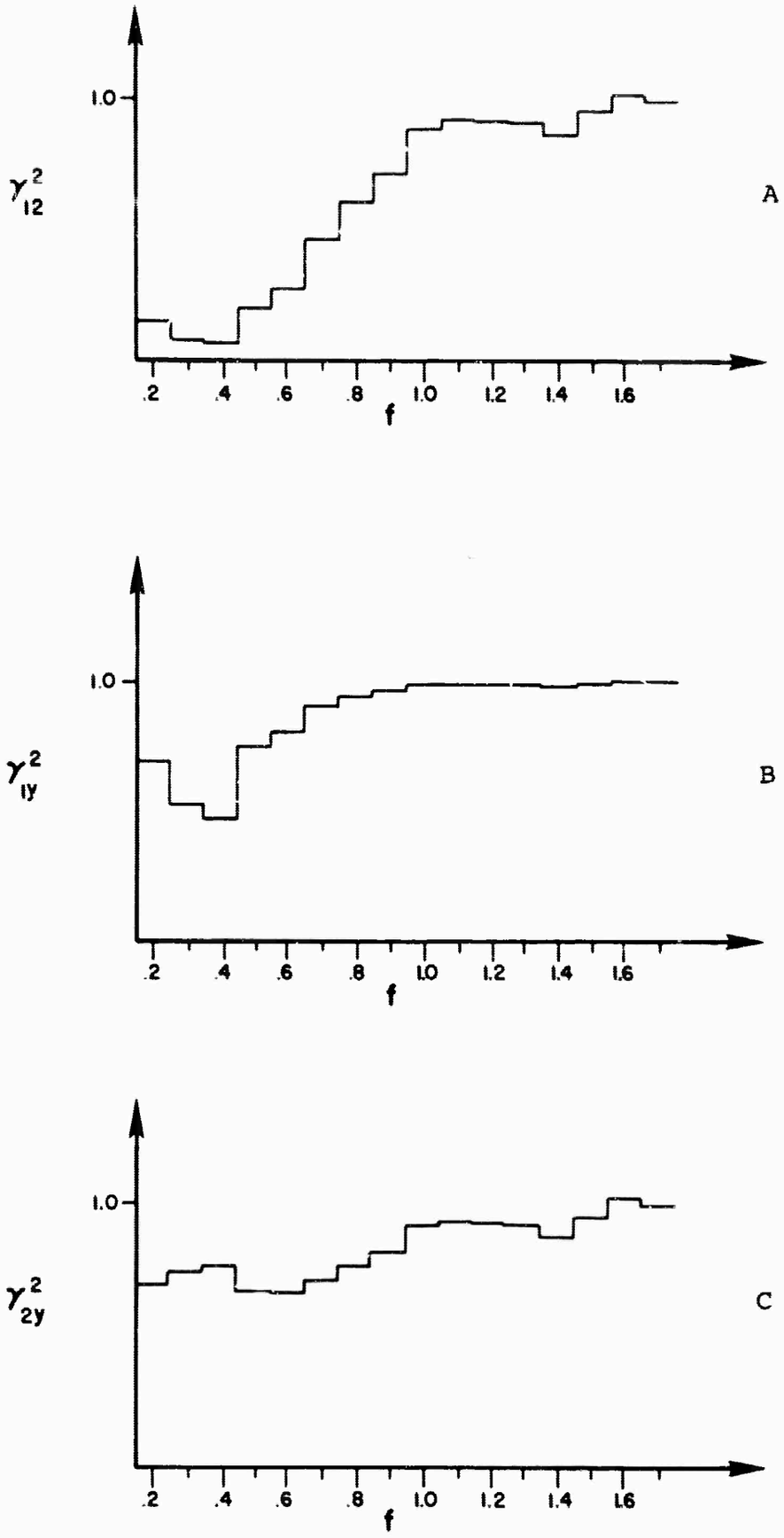

Ordinary Coherence Functions

Figure 4

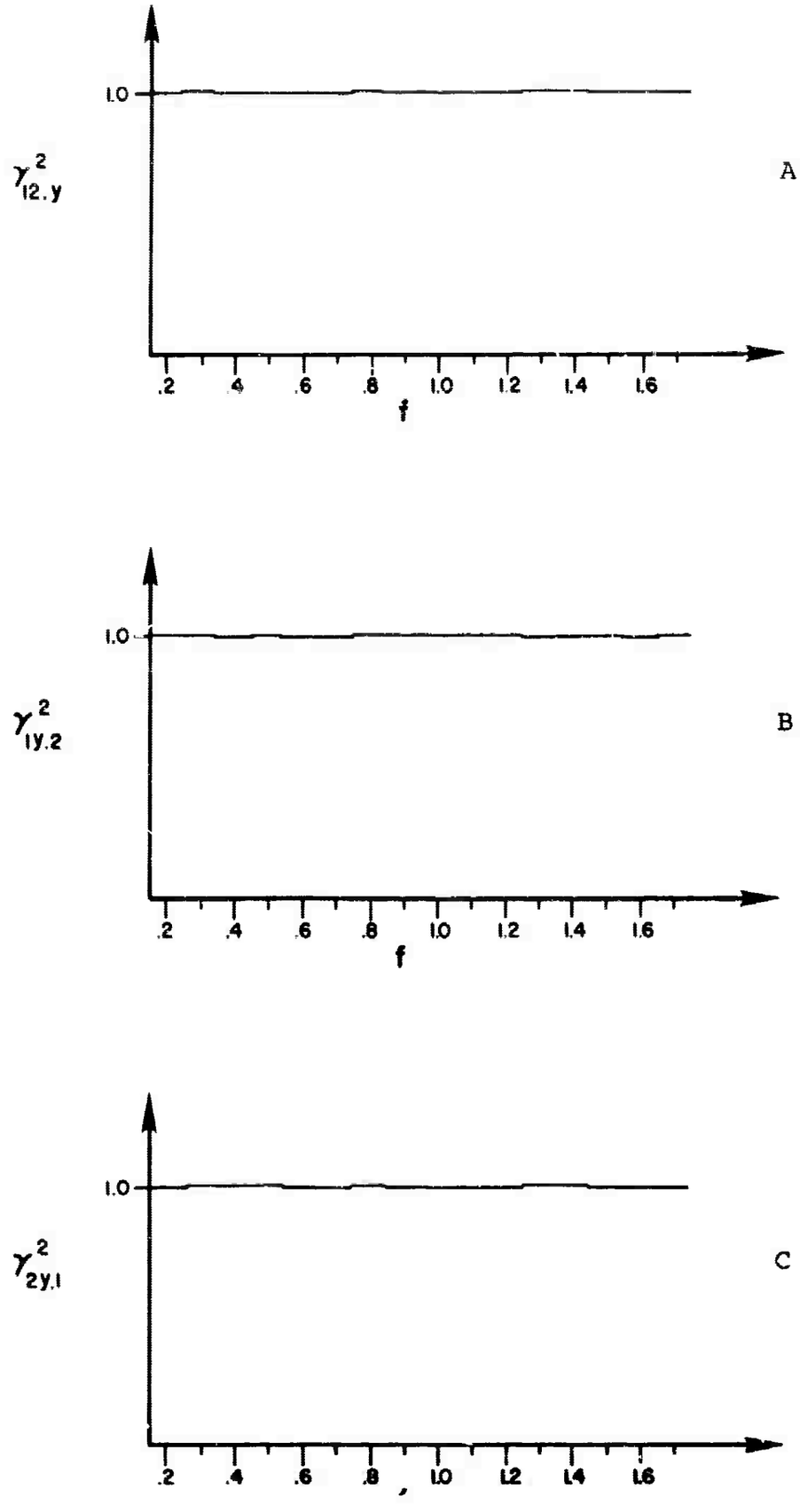

Partial Coherence Functions

Figure 5

4. CONCLUSIONS AND EXTENSIONS

The demonstration cases investigated through the aid of computer simulation methods illustrate the usefulness of partial coherency techniques in analyzing multiple input-multiple output systems. The fact that correct values of transfer functions and coherence functions are obtained when all inputs are properly taken into account has been numerically illustrated.

The next step in the investigation will be to use the computational procedures described in Appendix II to compute transfer and coherence functions completely from actual data. These can then be compared with the expected results discussed in this report. Questions of statistical accuracy which will be limited by sampling errors in the spectral computations can then be explored. Another area for future study is the trade-offs between statistical accuracy, number of inputs, and computation time.

Finally, a general program must be developed for the multi-input case and applied to the measurement and interpretation of seismic noise in large arrays.

APPENDIX I

EXPECTED RESULTS FOR SEISMIC COHERENCY EXPERIMENT

EXPECTED RESULTS FOR SEISMIC COHERENCY EXPERIMENT

1. INTRODUCTION

The following equations and input data form the basis from which expected experimental results were obtained by machine computation. The results of these computations provided mathematical checks on the computer simulation work. The defining equations for Case I are presented in Section 2 while the modifications required to run Case II are given in Section 3.

The two demonstration cases were based on data constructed in the following manner:

I. A signal of seismic noise y(t) is composed of two other known statistically independent seismic traces $x_1(t)$ and $x_2(t)$ where

$$y(t) = a_1x_1(t) + a_2x_2(t - T) \tag{1}$$

(a) The two signals $x_1(t)$ and $x_2(t)$ are independent.

(b) The two signals $x_1(t)$ and $x_2(t)$ are statistically correlated.

II. The signal of seismic noise y(t) generated as indicated above in (I) was modified by the addition of a third component $x_3(t)$. For this case, the formula for y(t) is

$$y(t) = a_1x_1(t) + a_2x_2(t - T) + a_3x_3(t) \tag{2}$$

(a) The three signals, $x_1(t)$, $x_2(t)$, and $x_3(t)$ are independent.

(b) The two signals $x_1(t)$ and $x_2(t)$ are correlated, but $x_3(t)$ is independent of $x_1(t)$ and $x_2(t)$.

(c) The two signals $x_1(t)$ and $x_2(t)$ are independent, but $x_3(t)$ is correlated with $x_1(t)$.

(d) The two signals $x_1(t)$ and $x_2(t)$ are correlated and $x_3(t)$ is correlated with $x_1(t)$ but independent of $x_2(t)$.

2. CALCULATION FOR CASE I

A block diagram of Case I is shown in Figure 1. Referring to the diagram, $x_1(t)$ and $z_1(t)$ are samples from independent random processes. The process $x_2(t)$ is formed by a linear combination of $x_1(t)$ and $z_1(t)$, thus

$$x_2(t) = \alpha x_1(t) + (1 - \alpha) z_1(t) \tag{3}$$

The random process y(t) is obtained by applying gain factors a_1 and a_2 to $x_1(t)$ and $x_2(t)$, respectively, and by delaying $x_2(t)$ by an amount T so that

$$y(t) = a_1 x_1(t) + a_2 x_2(t - T) \tag{4}$$

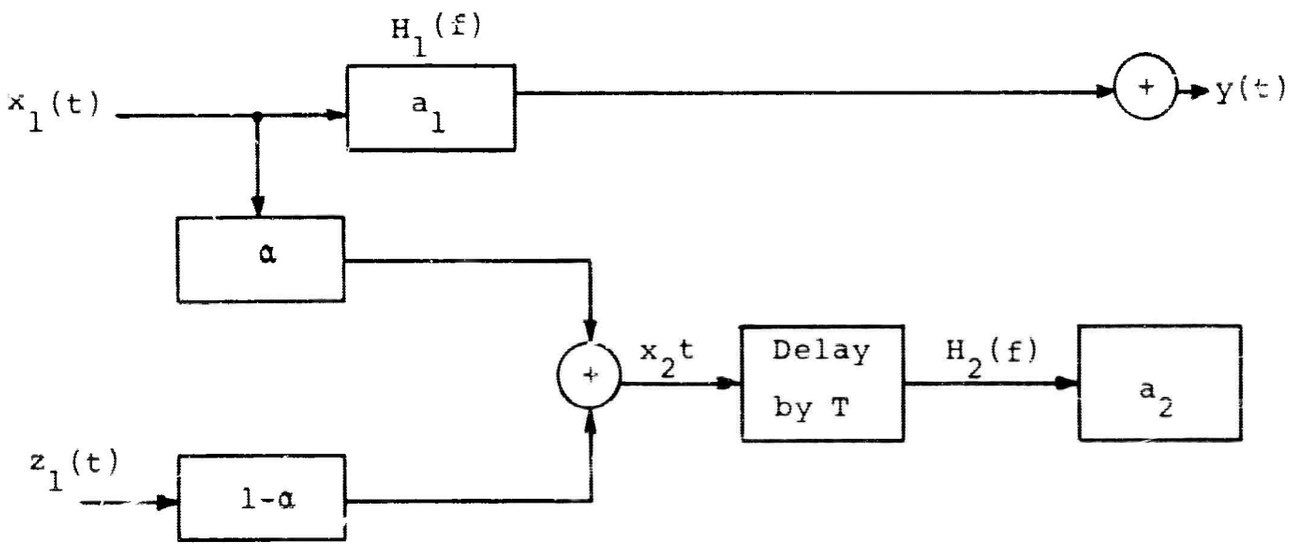

a. $x_1(t)$ and $z_1(t)$ independent

b. $x_2(t) = \alpha x_1(t) + (1 - \alpha) z_1(t)$

c. $y(t) = a_1 x_1(t) + a_2 x_2(t - T)$

d. $H_1(f) = a_1$

e. $H_2(f) = a_2 e^{-j2\pi fT}$

Figure 1. Block Diagram of Method for Construction of Case 1 Signals

For computation of the various coherence and frequency response functions, the following format was used. Notation used follows that employed in Ref. [1].

In the computations described below, "true" and "measured" frequency response functions are calculated. The measured frequency response functions $H_{iM}(f)$, $i = 1, 2$ are defined as the functions which would be calculated only from knowledge of one input and one output. These functions are incorrect when additional inputs exist which are not accounted for. The true function $H_{iT}(f)$, $i = 1, 2$ are defined as the versions computed using the proper multidimensional formulas which account for all the known variables. Hence, the difference between the true and measured frequency response functions will reflect the advantage in using the proper computational formulas.

1. Specify $G_{11}(f)$ and $G_{zz}(f)$ in the frequency interval 0.5 to 2.0 cps at 0.1 cps increments.

2. Compute $G_{22}(f)$ using

$$G_{22}(f) = \alpha^2 G_{11}(f) + (1 - \alpha)^2 G_{zz}(f) \qquad (5)$$

3. Compute $G_{yy}(f)$ using

$$G_{yy}(f) \quad \left[a_1^2 + 2a_1 a_2 \alpha \cos(2\pi fT)\right] G_{11}(f) + a_2^2 G_{22}(f) \qquad (6)$$

4. Compute $G_{12}(f)$ using

$$G_{12}(f) = \alpha G_{11}(f) \qquad (7)$$

5. Compute $G_{1y}(f) = C_{1y}(f) - jQ_{1y}(f) = |G_{1y}(f)| e^{-j\Phi_{1y}(f)}$

$$C_{1y}(f) = \left[a_1 + \alpha a_2 \cos(2\pi fT)\right] G_{11}(f) \qquad (8a)$$

$$Q_{1y}(f) = \alpha a_2 \sin(2\pi fT)\, G_{11}(f) \qquad (8b)$$

and $$|G_{1y}(f)| = \sqrt{C_{1y}^2(f) + Q_{1y}^2(f)} \qquad (9a)$$

$$\Phi_{1y}(f) = \tan^{-1} \frac{Q_{1y}(f)}{C_{1y}(f)} \qquad (9b)$$

6. Compute $G_{2y}(f)$ using

(10a)

$$C_{2y}(f) = a_1 \alpha G_{11}(f) + a_2 \cos(2\pi f T) G_{22}(f)$$

$$Q_{2y}(f) = a_2 \sin(2\pi f T) G_{22}(f) \qquad (10b)$$

and

$$|G_{2y}(f)| = \sqrt{C_{2y}^2(f) + Q_{2y}^2(f)} \qquad (11a)$$

$$\Phi_{2y}(f) = \tan^{-1} \frac{Q_{2y}(f)}{C_{2y}(f)} \qquad (11b)$$

7. Compute the "true" frequency response functions, $H_{1T}(f)$ and $H_2T(f)$, using

$$\mathrm{Re}H_{1T}(f) = \frac{G_{22}(f)C_{1y}(f) - G_{12}(f)C_{2y}(f)}{G_{11}(f)G_{22}(f) - G_{12}^2(f)} \qquad (12a)$$

$$\mathrm{Im}H_{1T}(f) = \frac{G_{12}(f)Q_{2y}(f) - G_{22}(f)Q_{1y}(f)}{G_{11}(f)G_{22}(f) - G_{12}^2(f)} \qquad (12b)$$

$$\mathrm{Re}H_{2T}(f) = \frac{G_{12}(f)C_{2y}(f) - G_{12}(f)C_{1y}(f)}{G_{11}(f)G_{22}(f) - G_{12}^2(f)} \qquad (13a)$$

$$\mathrm{Im}H_{2T}(f) = \frac{G_{12}(f)Q_{1y}(f) - G_{11}(f)Q_{2y}(f)}{G_{11}(f)G_{22}(f) - G_{12}^2(f)} \qquad (13b)$$

and

$$|H_{1T}(f)| = \sqrt{ReH_{1T}(f)^2 + ImH_{1T}(f)^2} \qquad (14a)$$

$$\Phi_{1T}(f) = -\tan^{-1} \frac{ImH_{1T}(f)}{ReH_{1T}(f)} \qquad (14b)$$

$$|H_{2T}(f)| = \sqrt{ReH_{2T}(f)^2 + ImH_{2T}(f)^2} \qquad (15a)$$

$$\Phi_{2T}(f) = -\tan^{-1} \frac{ImH_{2T}(f)}{ReH_{2T}(f)} \qquad (15b)$$

8. Compute the "measured" frequency response functions, $H_{1M}(f)$ and $H_{2M}(f)$, using

$$|H_{1M}(f)| = \frac{|G_{1y}(f)|}{G_{11}(f)} \qquad (16a)$$

$$\Phi_{1M}(f) = \Phi_{1y}(f) \qquad (16b)$$

$$|H_{2M}(f)| = \frac{|G_{2y}(f)|}{G_{22}(f)} \qquad (17a)$$

$$\Phi_{2M}(f) = \Phi_{2y}(f) \qquad (17b)$$

9. Compute $\gamma_{12}^2(f)$ using

$$\gamma_{12}^2(f) = \alpha^2 \frac{G_{11}(f)}{G_{22}(f)} \qquad (18)$$

10. Compute $\gamma_{1y}^2(f)$ using

$$\gamma_{1y}^2(f) = \frac{|G_{1y}(f)|^2}{G_{11}(f)G_{yy}(f)} \tag{19}$$

11. Compute $\gamma_{2y}^2(f)$ using

$$\gamma_{2y}^2(f) = \frac{|G_{2y}(f)|^2}{G_{22}(f)G_{yy}(f)} \tag{20}$$

12. Compute the following residual spectra

$$G_{11\cdot 2}(f) = G_{11}(f)\left[1 - \gamma_{12}^2(f)\right] \tag{21}$$

$$G_{11\cdot y}(f) = G_{11}(f)\left[1 - \gamma_{12}^2(f)\right] \tag{22}$$

$$G_{22\cdot 1}(f) = G_{22}(f)\left[1 - \gamma_{2y}^2(f)\right] \tag{23}$$

$$G_{22\cdot y}(f) = G_{22}(f)\left[1 - \gamma_{2y}^2(f)\right] \tag{24}$$

$$G_{yy\cdot 1}(f) = G_{yy}(f)\left[1 - \gamma_{2y}^2(f)\right] \tag{25}$$

$$G_{yy\cdot 2}(f) = G_{yy}(f)\left[1 - \gamma_{2y}^2(f)\right] \tag{26}$$

13. Compute the following quantities: (Note that the argument, f, has been dropped from all functions for simplicity.)

$$|G_{12\cdot y}|^2 = \left[G_{12} - \frac{C_{1y}C_{2y} + Q_{1y}Q_{2y}}{G_{yy}}\right]^2 + \left[\frac{C_{2y}Q_{1y} - C_{1y}Q_{2y}}{G_{yy}}\right]^2 \quad (27)$$

$$|G_{1y\cdot 2}|^2 = \left[C_{1y} - \frac{G_{12}C_{2y}}{G_{22}}\right]^2 + \left[Q_{1y} - \frac{G_{12}Q_{2y}}{G_{22}}\right]^2 \quad (28)$$

$$|G_{2y\cdot 1}|^2 = \left[C_{2y} - \frac{G_{12}C_{1y}}{G_{11}}\right]^2 + \left[Q_{2y} - \frac{G_{12}Q_{1y}}{G_{11}}\right]^2 \quad (29)$$

14. Compute $\gamma^2_{12\cdot y}(f)$ using

$$\gamma^2_{12\cdot y}(f) = \frac{|G_{12\cdot y}(f)|^2}{G_{11\cdot y}(f)G_{22\cdot y}(f)} \quad (30)$$

15. Compute $\gamma^2_{1y\cdot 2}(f)$ using

$$\gamma^2_{1y\cdot 2}(f) = \frac{|G_{1y\cdot 2}(f)|^2}{G_{11\cdot 2}(f)G_{yy\cdot 2}(f)} \quad (31)$$

16. Compute $\gamma^2_{2y\cdot 1}(f)$ using

$$\gamma^2_{2y\cdot 1}(f) = \frac{|G_{2y\cdot 1}(f)|^2}{G_{22\cdot 1}(f)G_{yy\cdot 1}(f)} \quad (32)$$

3. COMPUTATIONAL PROCEDURE MODIFICATIONS FOR CASE II

The block diagram for Case II is shown in Figure 2. The addition of a third process, $z_2(t)$ which is combined with $x_1(t)$ to form $x_3(t)$ is the only change from Case I.

The computational procedure presented previously was modified as follows for Case II:

2. Compute $G_{22}(f)$ and $G_{33}(f)$ using

$$G_{22}(f) = \alpha^2 G_{11}(f) + (1 - \alpha)^2 G_{z_1 z_1}(f) \qquad (5'a)$$

$$G_{33}(f) = \beta^2 G_{11}(f) + (1 - \beta)^2 G_{z_2 z_2}(f) \qquad (5'b)$$

3. Compute $G_{yy}(f)$ using

$$G_{yy}(f) = \left[a_1^2 + 2a_1 a_2\, \alpha \cos(2\pi fT) + 2a_1 a_3 \beta + 2a_2 a_3\, \alpha\beta \cos(2\pi fT)\right] G_{11}(f) + a_2^2 G_{22}(f) + a_3^2 G_{33}(f) \qquad (6')$$

5. Compute $G_{1y}(f) = C_{1y}(f) - jQ_{1y}(f)$

$$C_{1y}(f) = \left[a_1 + a_2\, \alpha \cos(2\pi fT) + a_3 \beta\right] G_{11}(f) \qquad (8'a)$$

$$Q_{1y}(f) = a_2 \alpha \sin(2\pi fT) G_{11}(f) \qquad (8'b)$$

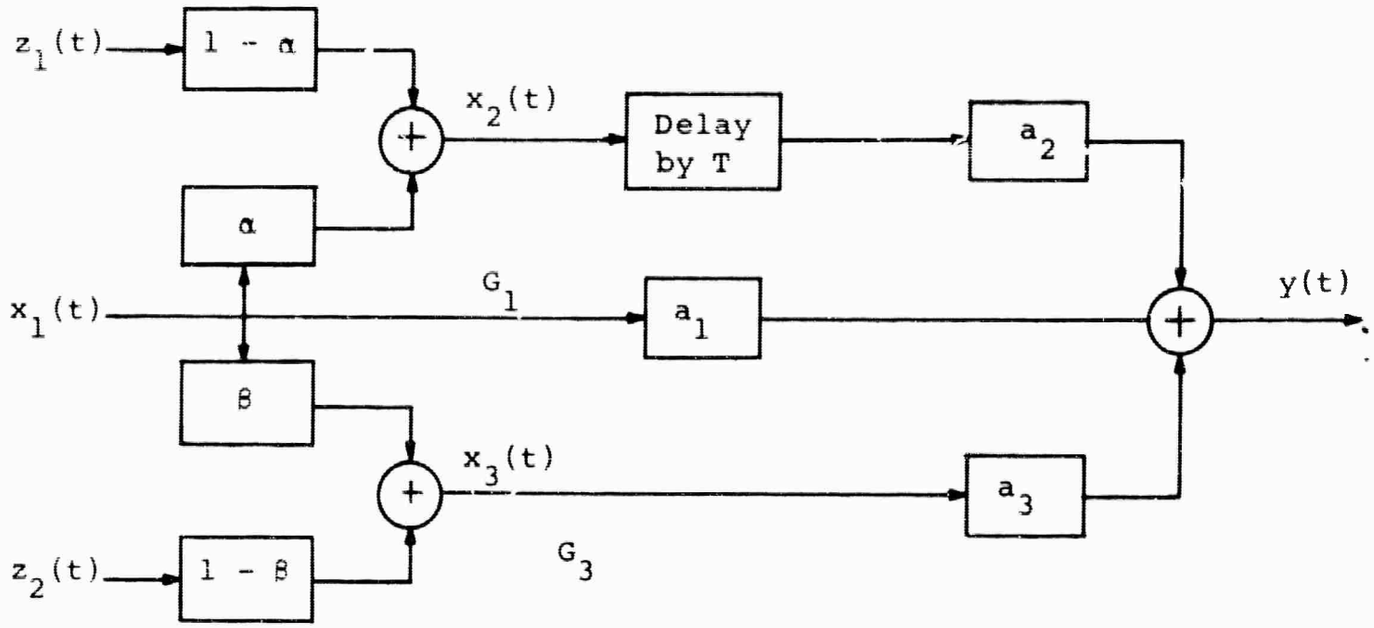

a. $x_1(t)$, $z_1(t)$, $z_2(t)$ INDEPENDENT

b. $x_2(t) = \alpha x_1(t) + (1 - \alpha)\ z_1(t)$

c. $x_3(t) = \beta x_1(t) + (1 - \beta)\ z_2(t)$

d. $H_1(f) = a_1$

e. $H_2(f) = a_2\ e^{-j2\pi fT}$

f. $H_3(f) = a_3$

Figure 2. Block Diagram for Method of Construction of Case II Signals

and

$$|G_{1y}(f)| = \sqrt{C_{1y}^2(f) + Q_{1y}^2(f)} \qquad (9'a)$$

$$\Phi_{1y}(f) = \tan^{-1} \frac{Q_{1y}(f)}{C_{1y}(f)} \qquad (9'b)$$

6. Compute $G_{2y}(f)$ using

$$C_{2y}(f) = \left[a_1\alpha + \alpha_3\alpha\beta\right] G_{11}(f) + a_2\cos(2\pi fT)\, G_{22}(f) \qquad (10'a)$$

$$Q_{2y}(f) = a_2 \sin(2\pi fT)\, G_{22}(f) \qquad (10'b)$$

and

$$|G_{2y}(f)| = \sqrt{C_{2y}^2(f) + Q_{2y}^2(f)} \qquad (11'a)$$

$$\Phi_{2y}(f) = \tan^{-1} \frac{Q_{2y}(f)}{C_{2y}(f)} \qquad (11'b)$$

All other computations were unchanged.

REFERENCES - APPENDIX I

1. Enochson, L. D., "Frequency Response Functions and Coherence Functions for Multiple Input Linear Systems," NASA Cr-32, prepared under contract NAS-5-4590. April 1964.

APPENDIX II

COMPUTATIONAL PROCEDURES FOR SEISMIC COHERENCY EXPERIMENTS

COMPUTATIONAL PROCEDURES FOR SEISMIC COHERENCY EXPERIMENTS

The computational procedures here are intended to give correct results when the proper physical model is a two input-single output time invariant linear system. This model is depicted in Figure 1.

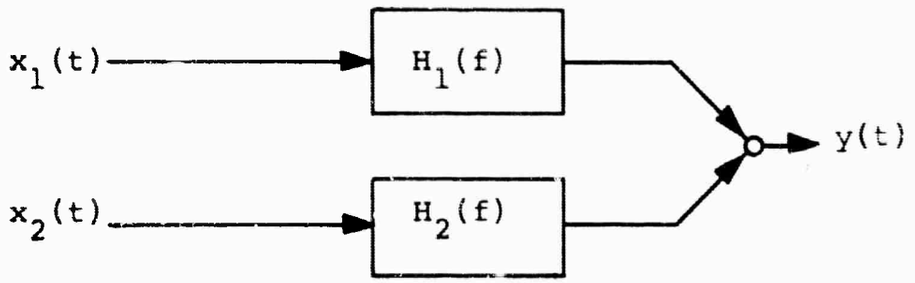

Figure 1. Two Input Single Output Linear System

The two input processes $x_1(t)$ and $x_2(t)$ both are assumed to be stationary with zero mean but need not be statistically independent.

The procedures described naturally separate into three basic steps. There are:

(1) Compute auto and cross-correlation functions.

(2) Transform the weighted correlation function to obtain the spectral densities where either or both the Hanning and Parzen weighting functions have been applied.

(3) Compute the frequency response functions, ordinary coherence functions, and partial coherence functions.

The discrete digi ized points of the zero mean stationary processes are denoted as follows:

$$\begin{aligned} x_1(t) &: x_1(i) \quad i = 1,2,\ldots,N \\ x_2(t) &: x_2(i) \quad i = 1,2,\ldots,N \\ y(t) &: y(i) \quad i = 1,2,\ldots,N \end{aligned} \tag{1}$$

The quantity N represents the number of discrete data points for each seismic data record. The symbol m will be used to designate the maximum number of lags at which the correlation functions are computed defined by $m\Delta\tau = \tau_{max}$. It is expected that the digitizing rate is 20 cps, and the desired bandwidth B of the spectral density estimates is 0.1 cps. Hence, since $B = 1/\tau_{max}$, one must have $m = 200$. Also, $\tau_{max} = 10$ sec so to satisfy a requirement of $10\tau_{max} \leq T$, a record length of T = 100 sec would be required.

1. COMPUTATION OF THE CORRELATION FUNCTIONS AND RAW SPECTRAL DENSITIES

1.1 Autocorrelation and Cross-Correlation functions

$$\begin{aligned} R_{11}(\tau) &= \frac{1}{N}\sum_{i=1}^{N-\tau} x_1(i)x_1(i+\tau) \\ R_{22}(\tau) &= \frac{1}{N}\sum_{i=1}^{N-\tau} x_2(i)x_2(i+\tau) \\ R_{yy}(\tau) &= \frac{1}{N}\sum_{i=1}^{N-\tau} y(i)y(i+\tau) \end{aligned} \tag{2}$$

$$R_{12}(\tau) = \frac{1}{N} \sum_{i=1}^{N-\tau} x_1(i)x_2(i+\tau)$$

$$R_{21}(\tau) = \frac{1}{N} \sum_{i=1}^{N-\tau} x_2(i)x_1(i+\tau)$$

$$R_{1y}(\tau) = \frac{1}{N} \sum_{i=1}^{N} x_1(i)y(i+\tau)$$

$$R_{y1}(\tau) = \frac{1}{N} \sum_{i=1}^{N-\tau} y(i)x_1(i+\tau)$$

$$R_{2y}(\tau) = \frac{1}{N} \sum_{i=1}^{N-\tau} x_2(i)y(i+\tau)$$

$$R_{y2}(\tau) = \frac{1}{N} \sum_{i=1}^{N-\tau} y(i)x_2(i+\tau)$$

$$\tau = 0,1,2,\ldots,m=200$$

1.2 Determination of a Peak in the Cross-Correlation Function

For each of $R_{12}(\tau)$, $R_{21}(\tau)$, $R_{1y}(\tau)$, $R_{y1}(\tau)$, $R_{2y}(\tau)$, and $R_{y2}(\tau)$, the maximum statistically significant peak (if one exists) is to be found and the cross-correlation functions translated appropriately. This search for a significant peak should be limited to an interval of time $[-\tau,\tau]$ which corresponds to maximum physically meaningful time delays. This translation

of the correlation function corresponds to a crude "prewhitening" of the cross-spectral density. Hence, if some more general prewhitening for the cross-spectral computations was employed, this translation need not be performed.

Let $R_{ij}(\tau)$ and $R_{ji}(\tau)$ represent the two parts of any of the three cross-correlation functions. Note that $R_{ij}(-\tau) = R_{ji}(\tau)$. Determine the maximum function value of these two parts. That is,

$$R_{max} = \max_{\tau} \left[|R_{ij}(\tau)|, |R_{ji}(\tau)|, \tau = 0,1,\ldots,m \right] \quad (4)$$

Next calculate the maximum correlation coefficient

$$r_{max} = \frac{R_{max}}{\sqrt{R_{ii}(0)R_{jj}(0)}} \quad (5)$$

As a reasonable test of statistical significance, it is suggested that r_{max} be compared against $\rho = 0.25$. To perform this test, compute

$$z = \frac{1}{2} \ell n \frac{1 + |r_{max}|}{1 - |r_{max}|} \quad (6)$$

which may be assumed to be norma ly distributed with mean ζ and variance $1/(n-3)$ where

$$\zeta = \frac{1}{2} \ell n \frac{1 + \rho}{1 - \rho}$$

$$= \frac{1}{2} \ell n \frac{1 + 0.25}{1 - 0.25} = .255 \qquad (7)$$

and the effective sample size is given by

$$n = 2BT$$

It is assumed that the record length T will be about 100 sec or longer. The signal bandwidth is B and a reasonable value for B should be 1.5 cps in which case $n = 3T$. Hence, if

$$Z = \tan h^{-1} |r_{max}| \geq .255 + \frac{2.33}{\sqrt{3(T - 1)}} = .255 + \frac{1.34}{\sqrt{T-1}} \qquad (8)$$

then the hypothesis that r_{max} is larger than 0.25 or a negative r_{max} is less than -0.25 is accepted at the 1% level of significance. The quantity 2.33 is the 99th percentile of the normal distribution function.

1.3 Translation of the Cross-Correlation Function

Let $\tau_0 = s_0 \Delta\tau$ represent the time point at which a statistically significant r_{max} for $x_1(t)$ and $x_2(t)$ occurs. This value is $\tau_0 = 0$ if no significant peak in the sample cross-correlation function exists. Then, the quantities $A_{12}(\tau)$, $B_{12}(\tau)$ as defined below are computed:

$$A_{12}(\tau) = \frac{1}{2} \left[R_{12}(\tau + s_0) + R_{21}(\tau - s_0) \right] \qquad (9a)$$

$$B_{12}(\tau) = \frac{1}{2} \left[R_{12}(\tau + s_0) - R_{21}(\tau - s_0) \right] \qquad (9b)$$

Let $\tau_1 = s_1 \Delta\tau$ and $\tau_2 = s_2 \Delta\tau$ represent delay values determined for the cross-correlations between $x_1(t)$ and $y(t)$ and $x_2(t)$ and $y(t)$, respectively. Also compute

$$A_{1y}(\tau) = \frac{1}{2}\left[R_{1y}(\tau + s_1) + R_{y1}(\tau - s_1)\right] \quad (10a)$$

$$B_{1y}(\tau) = \frac{1}{2}\left[R_{1y}(\tau + s_1) - R_{y1}(\tau - s_1)\right] \quad (10b)$$

$$A_{2y}(\tau) = \frac{1}{2}\left[R_{2y}(\tau + s_2) + R_{y2}(\tau - s_2)\right] \quad (11a)$$

$$B_{2y}(\tau) = \frac{1}{2}\left[R_{2y}(\tau + s_2) - R_{y2}(\tau - s_2)\right] \quad (11b)$$

2. COMPUTATION OF WEIGHTED FOURIER TRANSFORMS

Two different weighting functions are to be allowed in the computation of the power spectral density function. These are the Hanning weighting $D_1(\tau)$ and the Parzen weighting $D_2(\tau)$. This weighting may be performed in a slightly more computationally efficient method by smoothing of the raw spectrum estimates. However, for convenience in varying weighting functions, it would seem desirable to multiply the correlation functions by the weighting function.

Hence, compute the weighting function values

$$D_1(\tau) = \frac{1}{2}\left(1 + \cos\frac{\pi\tau}{m}\right) \quad , \quad , \quad \tau = 0,1,2,\ldots m \quad (12)$$

$$D_2(\tau) = \begin{cases} 1 - 6\left(\frac{\tau}{m}\right)^2\left(1 - \frac{\tau}{m}\right), & \tau = 0,1,2,\ldots,m/2 \\ 2\left(1 - \frac{\tau}{m}\right)^3, & \tau = \frac{m}{2}+1,\ldots,m \end{cases} \quad (13)$$

Compute the spectral density estimates by Fourier transforming the correlation functions. If the necessary sine and cosine values for the transform are not precomputed and stored, they should be generated from the following recursion formula where sin (π/m) and cos (π/m) are necessary to get started.

$$\begin{bmatrix} \cos\,(i+1)\pi/m \\ \sin\,(i+1)\pi/m \end{bmatrix} = \begin{bmatrix} \cos\,i\pi/m & -\sin\,i\pi/m \\ \sin\,i\pi/m & \cos\,i\pi/m \end{bmatrix} \begin{bmatrix} \cos\,\pi/m \\ \sin\,\pi/m \end{bmatrix} \quad (14)$$

$$i=1,2\ldots,\frac{m^2}{2}$$

The Fourier transform equations for the autocorrelation functions are

$$G_i(k) = 2\Delta\tau\left[R(0) + 2\sum_{\tau=1}^{m-1} D_1(\tau)R(\tau)\cos\frac{\pi\tau k}{m}\right] \quad k=4,6,\ldots,34 \quad (15)$$

where it is tacitly understood that $R(\tau)$ stands for any of the three autocorrelation functions $R_{11}(\tau)$, $R_{22}(\tau)$, and $R_{yy}(\tau)$. The evaluation of the above equation is therefore performed a total of six times; two different weighting functions for each of three autocorrelation functions. The spectral density is evaluated at the 16 values of k which correspond to frequencies f = 0.2, 0.3,...,1.7.

The transform for the cross-correlation function consists of a real part C(k) and an imaginary part Q(k). The equations

employ the special A's and B's defined by Eqs. (9), (10), and (11). If $G_{uv}(k)$ represents the cross-spectral density between some arbitrary u and v, then

$$\mathrm{Re}\left[G_{uv}(k)\right] = C_i(k) = 2\Delta\tau \left[A(0) + 2\sum_{\tau=1}^{m-1} A(\tau)D_i(\tau)\cos\frac{\pi\tau k}{m}\right]$$

$$\mathrm{Im}\left[G_{uv}(k)\right] = Q_i(k) = 4\Delta\tau \sum_{\tau=1}^{m-1} B(\tau)D_i(\tau)\sin\frac{\pi\tau k}{m} \qquad (16)$$

$$k = 4, 6, \ldots, 34$$

Again, Eqs. (16) are evaluated a total of six times. The quantities $A(\tau)$ and $B(\tau)$ represent $A_{12}(\tau)$ and $B_{12}(\tau)$, $A_{1y}(\tau)$ and $B_{1y}(\tau)$ and $A_{2y}(\tau)$ and $B_{2y}(\tau)$. These quantities are each used twice, once with $D_1(\tau)$ and once with $D_2(\tau)$.

At this point, all the necessary spectral densities have been evaluated. These are

$$G_{11}(k),\ G_{22}(k),\ G_{yy}(k)$$

$$G_{12}(k) = C_{12}(k) - jQ_{12}(k)$$

$$G_{1y}(k) = C_{1y}(k) - jQ_{1y}(k)$$

$$G_{2y}(k) = C_{2y}(k) - jQ_{2y}(k)$$

Each of the quantities are available in two forms corresponding to the two different weighting functions.

At this point, the cross-spectral densities should be adjusted to account for the time translation that was applied

to the cross-correlation functions. This translation by time $s_i \Delta\tau$ amounts to a multiplication of the cross-spectrum by

$$e^{j2\pi f s_i \Delta\tau}$$

Hence, the sample cross-spectrum must be multiplied by $e^{-j2\pi f s_i \Delta\tau}$ to readjust. The adjusted cross-spectra will be temporarily denoted with a prime ('). The equations are

$$C'_{12}(k) = C_{12}(k) \cos 2\pi f s_o \Delta\tau - Q_{12}(k) \sin 2\pi f s_0 \Delta\tau$$

$$Q'_{12}(k) = C_{12}(k) \sin 2\pi f s_0 \Delta\tau + Q_{12}(k) \cos 2\pi f s_0 \Delta\tau$$

$$C'_{1y}(k) = C_{1y}(k) \cos 2\pi f s_1 \Delta\tau - Q_{1y}(k) \sin 2\pi f s_1 \Delta\tau$$

$$Q'_{1y}(k) = C_{1y}(k) \sin 2\pi f s_1 \Delta\tau + Q_{1y}(k) \cos 2\pi f s_1 \Delta\tau$$

$$C'_{2y}(k) = C_{2y}(k) \cos 2\pi f s_2 \Delta\tau - Q_{2y}(k) \sin 2\pi f s_2 \Delta\tau$$

$$Q'_{2y}(k) = C_{2y}(k) \sin 2\pi f s_2 \Delta\tau + Q_{2y}(k) \cos 2\pi f s_2 \Delta\tau$$

Note that these computations are performed at the usual 16 frequency values. Subsequently, the primes will be dropped and the adjusted spectra will simply be denoted by $G_{12}(k)$, $G_{1y}(k)$, and $G_{2y}(k)$.

3. COMPUTATION OF FREQUENCY RESPONSE FUNCTIONS, ORDINARY COHERENCE FUNCTIONS, AND PARTIAL COHERENCE FUNCTIONS

The computations to follow will give a "true" and "measured" frequency response function $H_{iT}(k)$ and $H_{iM}(k)$ as defined in the discussion on experimental results. Then the ordinary coherence function formulas will be given followed by the partial coherence function formulas. It is to be understood that all formulas are evaluated twice, once for each weighting function,

Several of the subsequent formulas correspond exactly to formulas appearing in the write-up on expected results calculations. In each case where this occurs a special mention is made so that separate subroutines could be common to both programs.

3.1 Frequency Response Functions

(1) First compute the "measured" frequency response functions. These formulas correspond to Step 8 of the expected results computations.

$$H(k) = \mathrm{Re}H(k) + j\ \mathrm{Im}\ H(k) = |H(k)|\ e^{j\phi(k)}$$

$$\mathrm{Re}H_{1M}(k) = \frac{C_{1y}(k)}{G_{11}(k)}$$

$$k = 4,\ 6,\ \ldots\ ,\ 34 \qquad (18)$$

$$\mathrm{Im}H_{1M}(k) = -\frac{Q_{1y}(k)}{G_{11}(k)}$$

Compute the gain and phase factors

$$|H_1M(k)| = \sqrt{\left[ReH_{1M}(k)\right]^2 + \left[ImH_{1M}(k)\right]^2} \quad , \quad \Phi_{1M}(k) = -\tan^{-1} \frac{ImH_{1M}(k)}{ReH_{1M}(k)}$$

In subsequent formulas the k will be dropped for notational convenience and it will be understood that all computations are performed at 16 values, k = 4,6,...,34.

$$ReH_{2M} = \frac{C_{2y}}{G_{22}}$$

$$ImH_{2M} = -\frac{Q_{2y}}{G_{22}} \qquad (19)$$

Compute the gain and phase factors

$$|H_{1M}(k)| = \sqrt{(ReH_{2M})^2 + (ImH_{2M})^2} \quad , \quad \Phi_{1M}(k) = -\tan^{-1} \frac{ImH_{2M}}{ReH_{2M}}$$

(2) Computation of the "true" frequency response function. First, compute the squared magnitudes of the cross-spectra for later use.

$$|G_{12}|^2 = C_{12}^2 + Q_{12}^2$$

$$|G_{1y}|^2 = C_{1y}^2 + Q_{1y}^2 \qquad (20)$$

$$|G_{2y}|^2 = C_{2y}^2 + Q_{2y}^2$$

$$\Delta = G_{11}G_{22} - |G_{12}|^2 \tag{21}$$

$$\begin{aligned} \mathrm{ReH}_{1T} &= \frac{G_{22}C_{1y} - C_{12}C_{2y} \pm Q_{12}Q_{2y}}{\Delta} \\ \mathrm{ImH}_{1T} &= \frac{-G_{22}Q_{1y} + C_{12}Q_{2y} + Q_{12}C_{2y}}{\Delta} \end{aligned} \tag{22}$$

$$|H_{1T}| = \sqrt{(\mathrm{ReH}_{1T})^2 + (\mathrm{ImH}_{1T})^2}\ , \quad \Phi_{1T} = -\tan^{-1}\frac{\mathrm{ImH}_{1T}}{\mathrm{ReH}_{2T}}$$

$$\begin{aligned} \mathrm{ReH}_{2T} &= \frac{G_{11}C_{2y} - C_{12}C_{1y} - Q_{12}Q_{1y}}{\Delta} \\ \mathrm{ImH}_{2T} &= \frac{-G_{11}Q_{2y} + C_{12}Q_{1y} \pm Q_{12}C_{1y}}{\Delta} \end{aligned} \tag{23}$$

$$|H_{2T}| = \sqrt{(\mathrm{ReH}_{2T})^2 + (\mathrm{ImH}_{2T})^2}\ , \quad \Phi_{2T} = -\tan^{-1}\frac{\mathrm{ImH}_{2T}}{\mathrm{ReH}_{2T}}$$

(3) Computation of the ordinary coherence functions

$$\begin{aligned} \gamma_{12}^2 &= \frac{|G_{12}|^2}{G_{11}G_{22}} \\ \gamma_{1y}^2 &= \frac{|G_{1y}|^2}{G_{11}G_{yy}} \\ \gamma_{2y}^2 &= \frac{|G_{2y}|^2}{G_{22}G_{yy}} \end{aligned} \tag{24}$$

(4) Computation of the partial coherence functions. First, the residual spectra are computed which corresponds to Step 12 of the expected results computations.

$$
\begin{aligned}
G_{11\cdot 2} &= G_{11}\left[\,1 - \gamma_{12}^{2}\,\right] \\
G_{11\cdot y} &= G_{11}\left[\,1 - \gamma_{1y}^{2}\,\right] \\
G_{22\cdot 1} &= G_{22}\left[\,1 - \gamma_{12}^{2}\,\right] \\
G_{22\cdot y} &= G_{22}\left[\,1 - \gamma_{2y}^{2}\,\right] \\
G_{yy\cdot 1} &= G_{yy}\left[\,1 - \gamma_{1y}^{2}\,\right] \\
G_{yy\cdot 2} &= G_{yy}\left[\,1 - \gamma_{2y}^{2}\,\right]
\end{aligned}
\tag{25}
$$

Compute the residual cross-spectra:

$$
\begin{aligned}
G_{12\cdot y} &= C_{12\cdot y} - jQ_{12\cdot y} \\
C_{12\cdot y} &= C_{12} - \frac{C_{1y}C_{2y} + Q_{1y}Q_{2y}}{G_{yy}} \\
Q_{12\cdot y} &= -Q_{12} - \frac{C_{1y}Q_{2y} - Q_{1y}C_{2y}}{G_{yy}}
\end{aligned}
\tag{26}
$$

$$G_{1y\cdot 2} = C_{1y\cdot 2} - jQ_{1y\cdot 2}$$

$$C_{1y\cdot 2} = C_{1y} - \frac{C_{12}C_{2y} - Q_{12}Q_{2y}}{G_{22}} \qquad (27)$$

$$Q_{1y\cdot 2} = -Q_{1y} + \frac{C_{12}Q_{2y} + Q_{12}C_{2y}}{G_{22}}$$

$$G_{2y\cdot 1} = C_{2y\cdot 1} - jQ_{2y\cdot 1}$$

$$C_{2y\cdot 1} = C_{2y} - \frac{C_{12}C_{1y} + Q_{12}Q_{1y}}{G_{11}} \qquad (28)$$

$$Q_{2y\cdot 1} = -Q_{2y} + \frac{C_{12}Q_{1y} - Q_{12}C_{1y}}{G_{11}}$$

Compute the partial coherence functions. This is identical to Steps 14, 15, and 16 of the expected results computations.

$$\gamma^2_{12\cdot y} = \frac{|G_{12\cdot y}|^2}{G_{11\cdot y}G_{22\cdot y}}$$

$$\gamma^2_{1y\cdot 2} = \frac{|G_{1y\cdot 2}|^2}{G_{11\cdot 2}G_{yy\cdot 2}} \qquad (29)$$

$$\gamma^2_{2y\cdot 1} = \frac{|G_{2y\cdot 1}|^2}{G_{22\cdot 1}G_{yy\cdot 1}}$$

This concludes the basic computations. The output format duplicates that of the expected results computations. This allows a one-to-one comparison of the experimental results with the theoretically expected results. In addition, the power spectral density functions $G_{11}(f)$, $G_{22}(f)$, and $G_{yy}(f)$ and the partial coherence functions $\gamma^2_{12\cdot y}(f)$, $\gamma^2_{1y\cdot 2}(f)$, $\gamma^2_{2y\cdot 1}(f)$ are output to compare with known values.

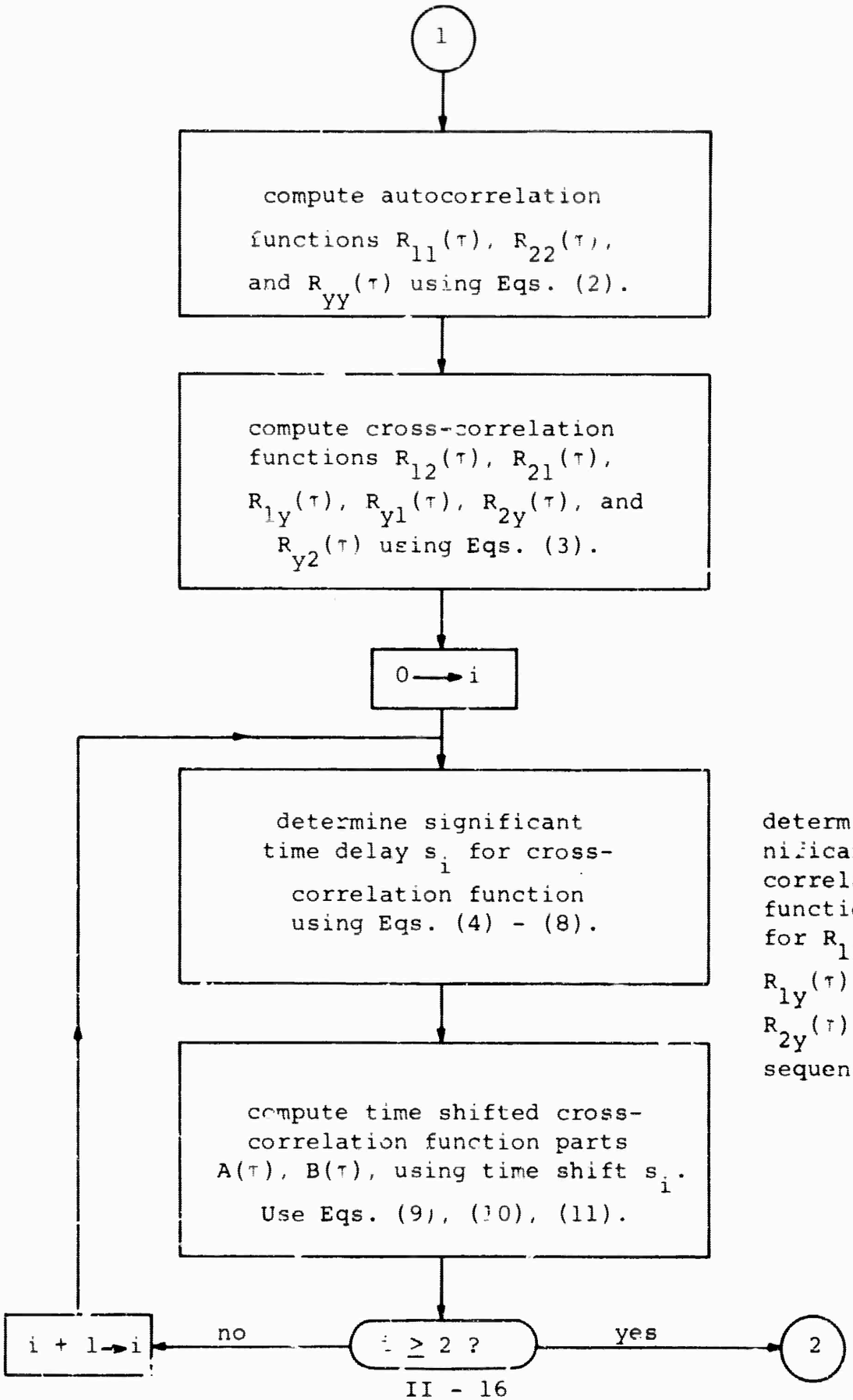
1
compute autocorrelation functions $R_{11}(\tau)$, $R_{22}(\tau)$, and $R_{yy}(\tau)$ using Eqs. (2).
compute cross-correlation functions $R_{12}(\tau)$, $R_{21}(\tau)$, $R_{1y}(\tau)$, $R_{y1}(\tau)$, $R_{2y}(\tau)$, and $R_{y2}(\tau)$ using Eqs. (3).
0 → i
determine significant time delay s_i for cross-correlation function using Eqs. (4) - (8).
determine significant cross-correlation function peaks for $R_{12}(\tau)$, $R_{1y}(\tau)$, and $R_{2y}(\tau)$ in sequence.
compute time shifted cross-correlation function parts $A(\tau)$, $B(\tau)$, using time shift s_i. Use Eqs. (9), (10), (11).
i ≥ 2 ?
no
yes
i + 1 → i
2

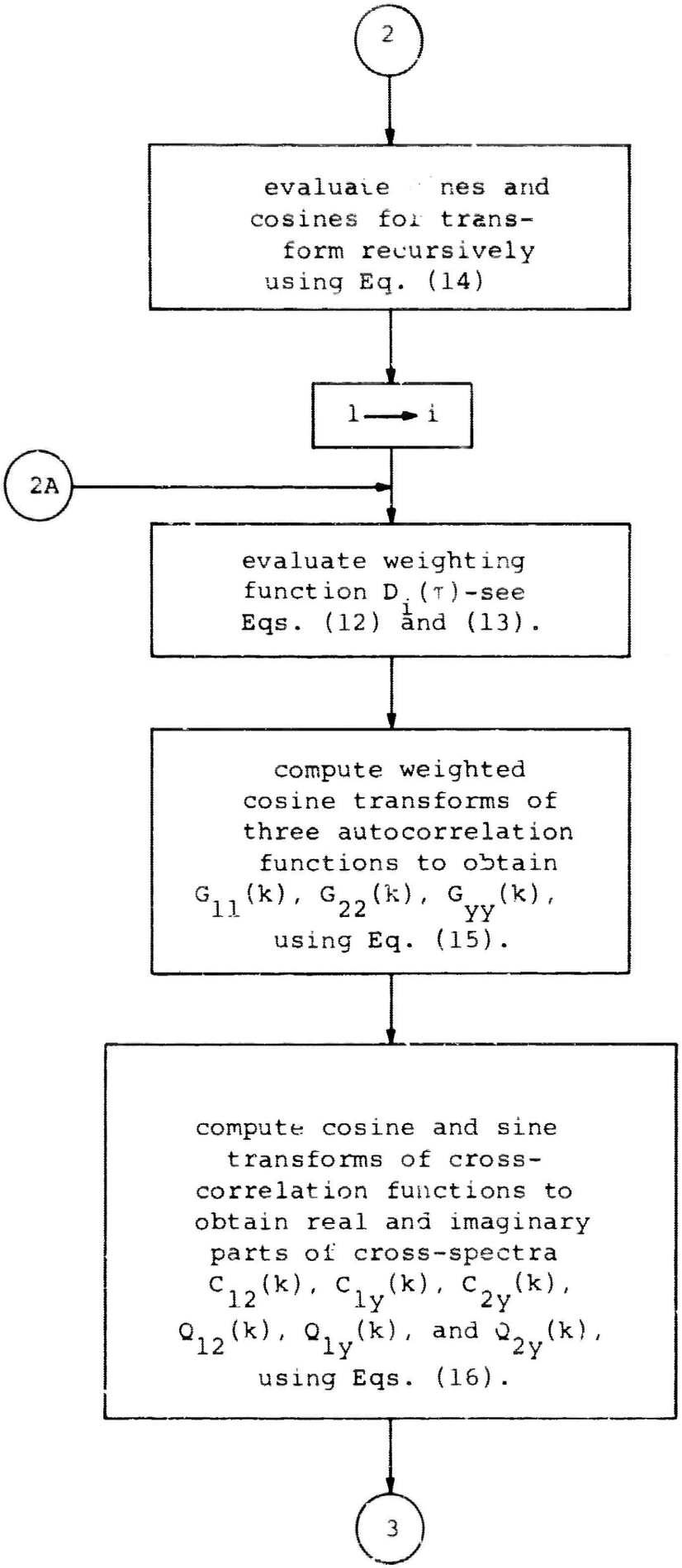
2
evaluate sines and cosines for transform recursively using Eq. (14)
1 → i
2A
evaluate weighting function $D_i(\tau)$-see Eqs. (12) and (13).
compute weighted cosine transforms of three autocorrelation functions to obtain $G_{11}(k)$, $G_{22}(k)$, $G_{yy}(k)$, using Eq. (15).
compute cosine and sine transforms of cross-correlation functions to obtain real and imaginary parts of cross-spectra $C_{12}(k)$, $C_{1y}(k)$, $C_{2y}(k)$, $Q_{12}(k)$, $Q_{1y}(k)$, and $Q_{2y}(k)$, using Eqs. (16).
3

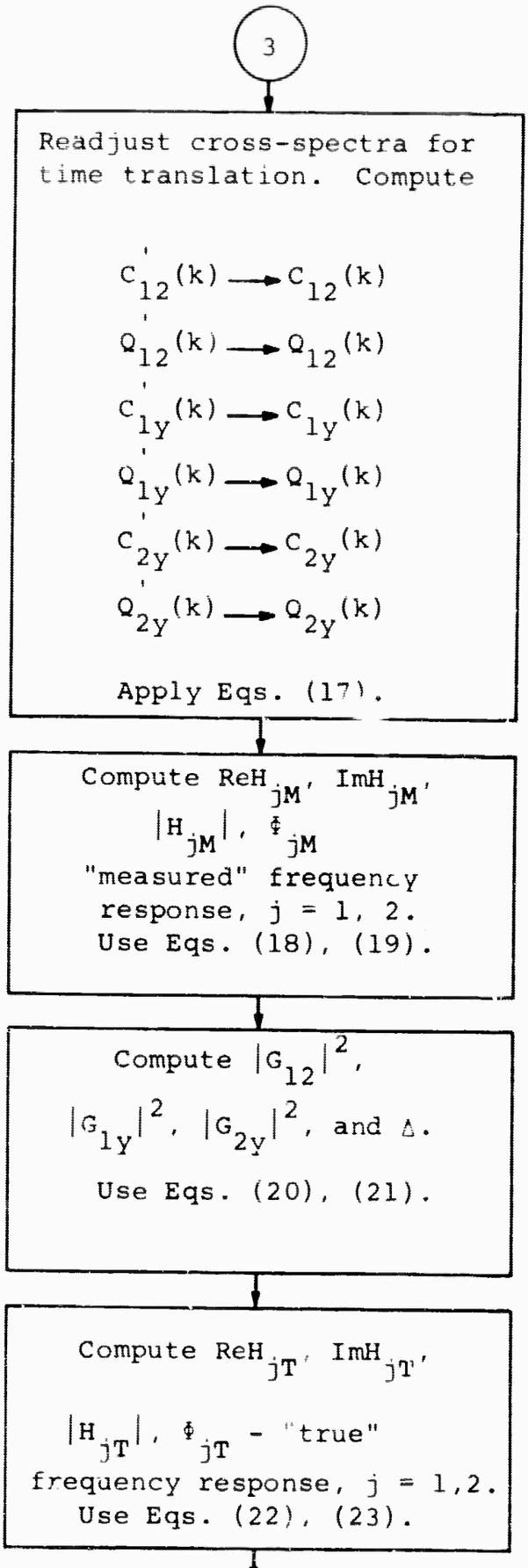
3
Readjust cross-spectra for time translation. Compute
$C'_{12}(k) \rightarrow C_{12}(k)$
$Q'_{12}(k) \rightarrow Q_{12}(k)$
$C'_{1y}(k) \rightarrow C_{1y}(k)$
$Q'_{1y}(k) \rightarrow Q_{1y}(k)$
$C'_{2y}(k) \rightarrow C_{2y}(k)$
$Q'_{2y}(k) \rightarrow Q_{2y}(k)$
Apply Eqs. (17).
Compute ReH_{jM}, ImH_{jM}, $|H_{jM}|$, Φ_{jM} "measured" frequency response, j = 1, 2. Use Eqs. (18), (19).
Compute $|G_{12}|^2$, $|G_{1y}|^2$, $|G_{2y}|^2$, and Δ. Use Eqs. (20), (21).
Compute ReH_{jT}, ImH_{jT}, $|H_{jT}|$, Φ_{jT} - "true" frequency response, j = 1,2. Use Eqs. (22), (23).
4

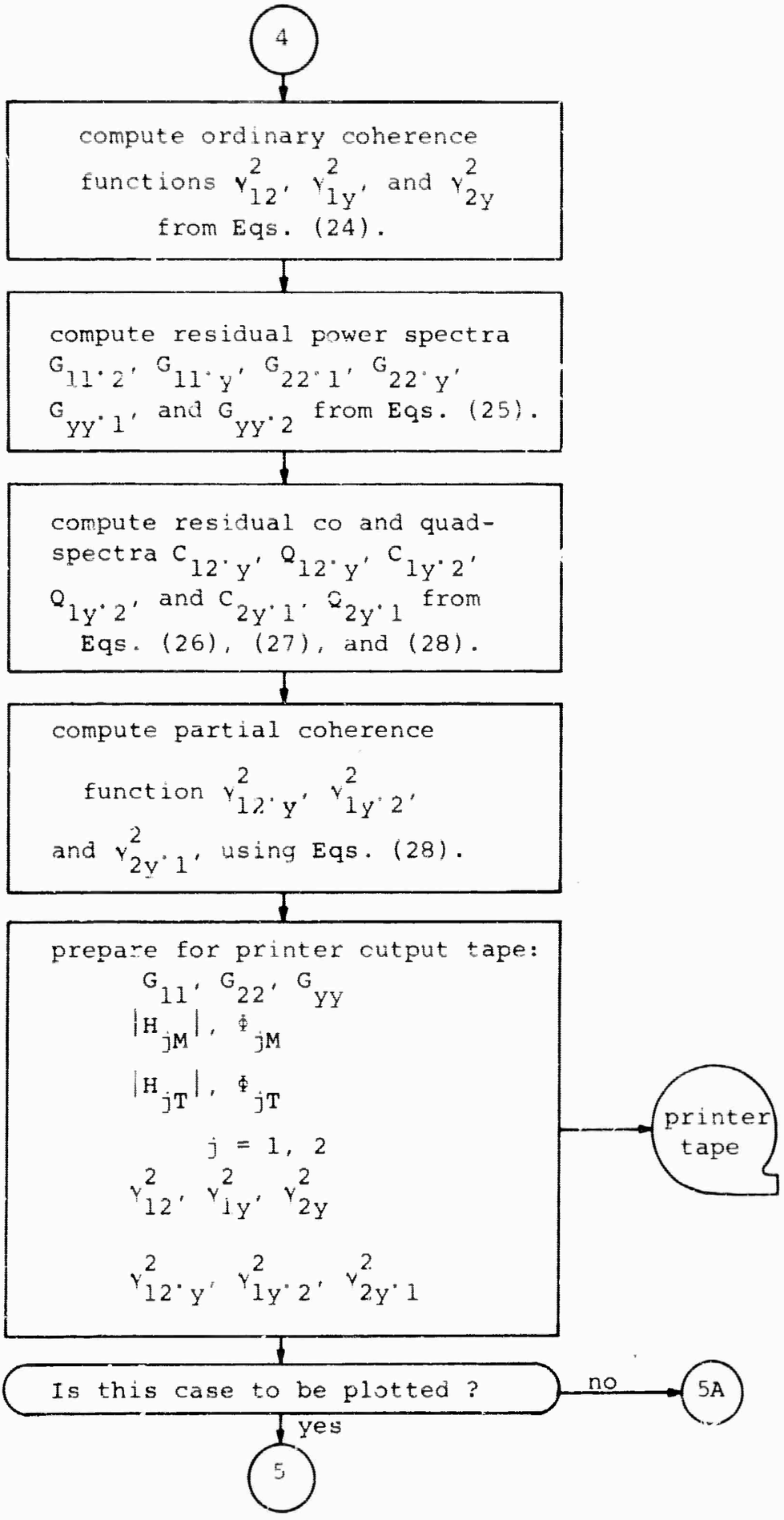
4
compute ordinary coherence functions γ^2_{12}, γ^2_{1y}, and γ^2_{2y} from Eqs. (24).
compute residual power spectra $G_{11\cdot 2}$, $G_{11\cdot y}$, $G_{22\cdot 1}$, $G_{22\cdot y}$, $G_{yy\cdot 1}$, and $G_{yy\cdot 2}$ from Eqs. (25).
compute residual co and quad-spectra $C_{12\cdot y}$, $Q_{12\cdot y}$, $C_{1y\cdot 2}$, $Q_{1y\cdot 2}$, and $C_{2y\cdot 1}$, $Q_{2y\cdot 1}$ from Eqs. (26), (27), and (28).
compute partial coherence function $\gamma^2_{12\cdot y}$, $\gamma^2_{1y\cdot 2}$, and $\gamma^2_{2y\cdot 1}$, using Eqs. (28).
prepare for printer output tape:
G_{11}, G_{22}, G_{yy}
$|H_{jM}|$, Φ_{jM}
$|H_{jT}|$, Φ_{jT}
j = 1, 2
γ^2_{12}, γ^2_{1y}, γ^2_{2y}
$\gamma^2_{12\cdot y}$, $\gamma^2_{1y\cdot 2}$, $\gamma^2_{2y\cdot 1}$
printer tape
Is this case to be plotted ?
no
5A
yes
5

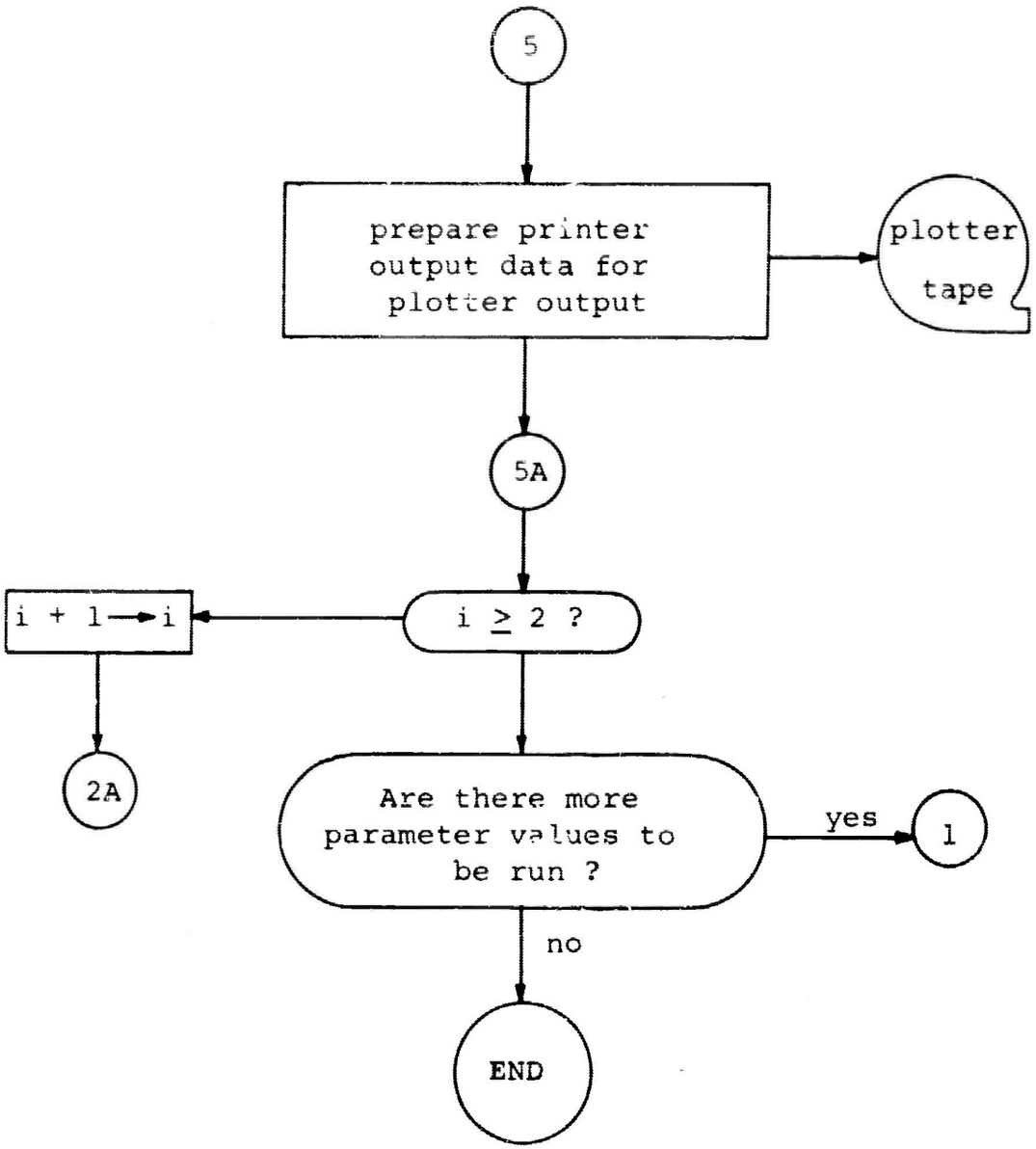
5
prepare printer output data for plotter output
plotter tape
5A
i + 1 → i
i ≥ 2 ?
2A
Are there more parameter values to be run ?
yes
1
no
END

APPENDIX III

ANALYSIS OF RESULTS OF COMPUTATIONAL EXPERIMENTS

ANALYSIS OF RESULTS OF COMPUTATIONAL EXPERIMENTS

1. INTRODUCTION

The purpose and general results of the computational experiments are described in the main body of the text, but certain pertinent details will be reviewed here. The over-all objective of the computational experiments is to develop a numerical feeling for the magnitude effects of various data parameters on the results of interest. A side benefit is gaining familiarity and experience with the general computational procedures required in the analysis of multi-dimensional linear systems.

These preliminary numerical experiments provide results which are not influenced by statistical variability so that an over-all impression of the effectiveness of the theory may be gained. The computations are based on actual seismic data so that some of the physical details of the problem are reflected in the experiments even though the statistical variability which is encountered in actual data analysis has been avoided in these initial evaluations.

As mentioned in the main body of the report, two basic cases were examined. Case I, a two input-single output linear system, was modeled in which one portion of the system represented a unit gain and the other portion of the system represented a unit gain and a time delay. Three cases are analyzed here where the correlation or the coherence of the inputs has been varied. The second type of experiment involved a three input-single output linear system where the

third input was, in effect, treated as noise. That is, the computations are performed as if the third input was not known to exist and the amount of its correlation with the other inputs was varied and its effect on the output was investigated. Three additional instances are described here for Case II in which the gain factor for the third system was varied. Hence, a total of six cases, three of type I and three of type II were run for the computational experiments.

The next extension to these computational experiments will be to include computations of the output spectra and cross-spectra directly from the generated data rather than as a direct analytical function of the input data. This type of result will be one step more realistic in that they will contain statistical variability. After those basic experiments on small dimensional cases, the second extension will be to higher dimensional cases to further evaluate the more varied and more complicated cases. The computational results of six illustrative cases will now be described. Case I, the two input-single output model will be covered first, followed by Case II the three input-single output model.

2. CASE I RESULTS

Some general comments will first be made. In digital spectral analysis, one can occasionally actually obtain negative spectral estimates when certain underlying assumptions are not perfectly fulfilled. This will never happen in the analog case since an analog instrument always filters and then squares which assures that a positive quantity is obtained. However, the smoothing filters which are involved in the digital analysis occasionally have negative side lobes which can contribute negative power to the digital estimates. This can sometimes result in coherencies being larger than 1 or less than 0, even though in theory they are restricted to the range 0 to 1. Problems such as these will often arise either where the spectrum is rapidly changing, or where it is close to zero. This, in fact, has occurred in some of the computational experiments performed for this report. Plots of the power spectra of the basic input processes $G_{11}(f)$ and $G_{zz}(f)$ are illustrated in Figure III-1. The near zero power in the higher frequency range of $G_{zz}(f)$ did actually result in some negative spectral estimates and some coherencies larger than 1 at the higher frequency points. The spectra are plotted at frequency points of 0.2 to 1.7 cps, and the bandwidth of the estimates is .1 cps. Hence, these are statistically independent spectral points which are plotted.

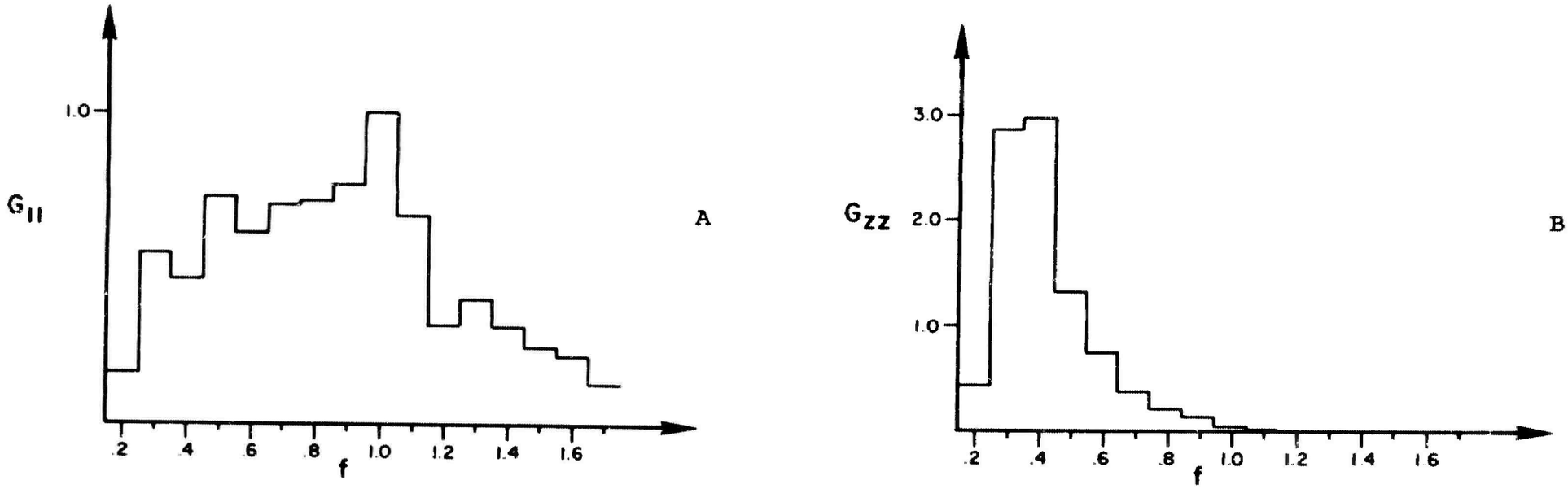

Input Power Spectra

Figure III-1

2.1 CASE I(a) RESULTS

For Case I(a), the parameter α was taken as equal to zero which results in the two inputs being uncorrelated or incoherent. For this situation, theory indicates that both the "true" and "measured" frequency response function estimates are equal. That is, one can use either the correct two-dimensional theory or the incorrect one-dimensional theory to obtain unbiased frequency response function estimates. This is illustrated numerically in Figure III-2 which gives plots of the gain and phase factors for the true and measured versions of the frequency response functions. The linear phase shift which appears in the phase angle plot indicates the time delay that was induced for the second input. The facet of the theory that is not illustrated by these plots is the fact that the statistical variability is increased when there is a second uncorrelated input which is being neglected. The statistical accuracy of the results can be shown to be proportional to the coherency between the input and the output. Hence, if one thinks of the second input as noise, a large noise-to-signal power ratio will decrease the coherency between the first input and the output, and hence, decrease the statistical accuracy of the results.

The coherencies between the first input and the output, and the second input and the output are illustrated in Figure III-3, and reflect the equation given below which applies for this case of unit gain factors. As can be seen from this equation, the noise-to-signal power ratio appears in the

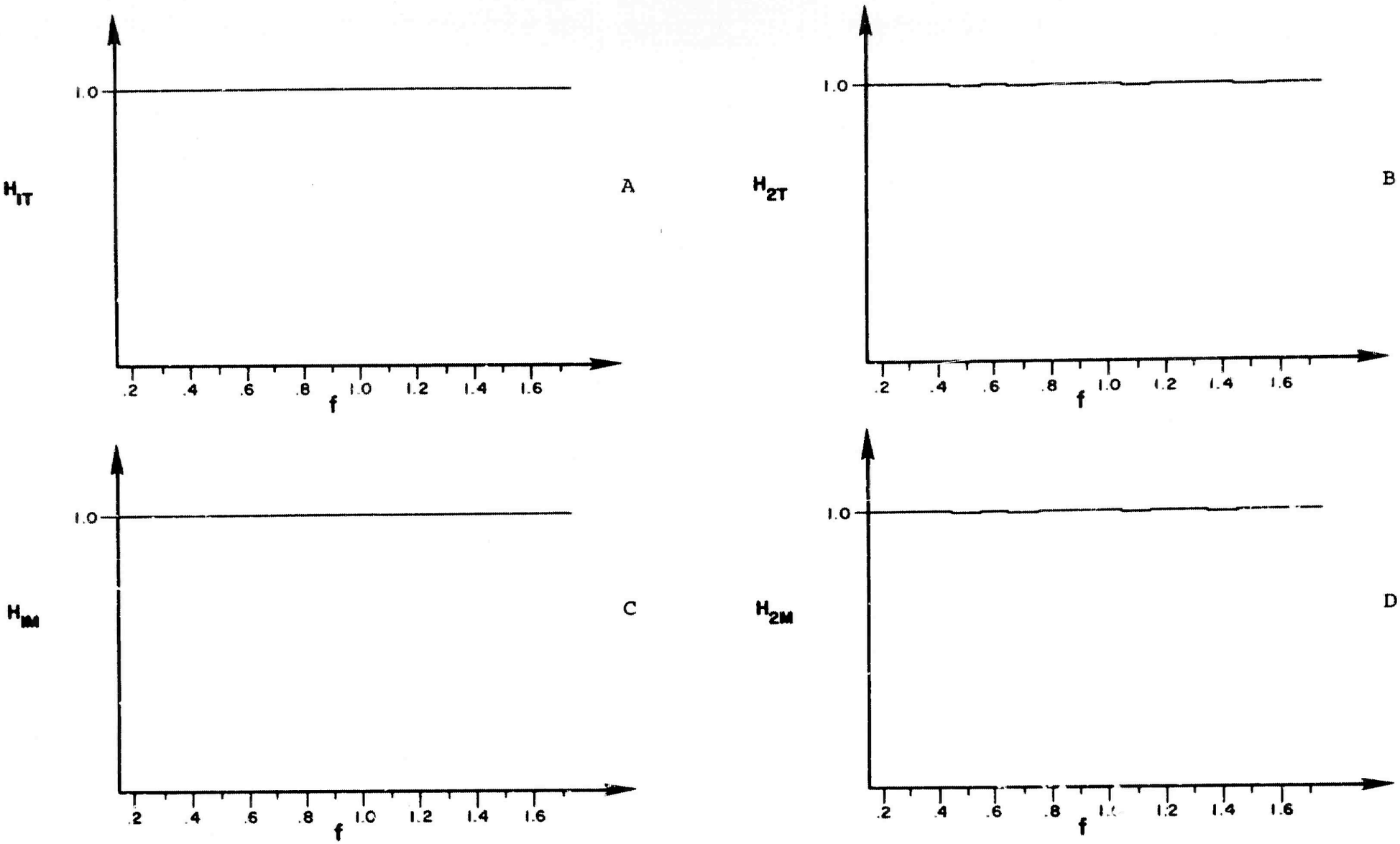

Frequency Response Functions for Case I(a)

Figure III-2A

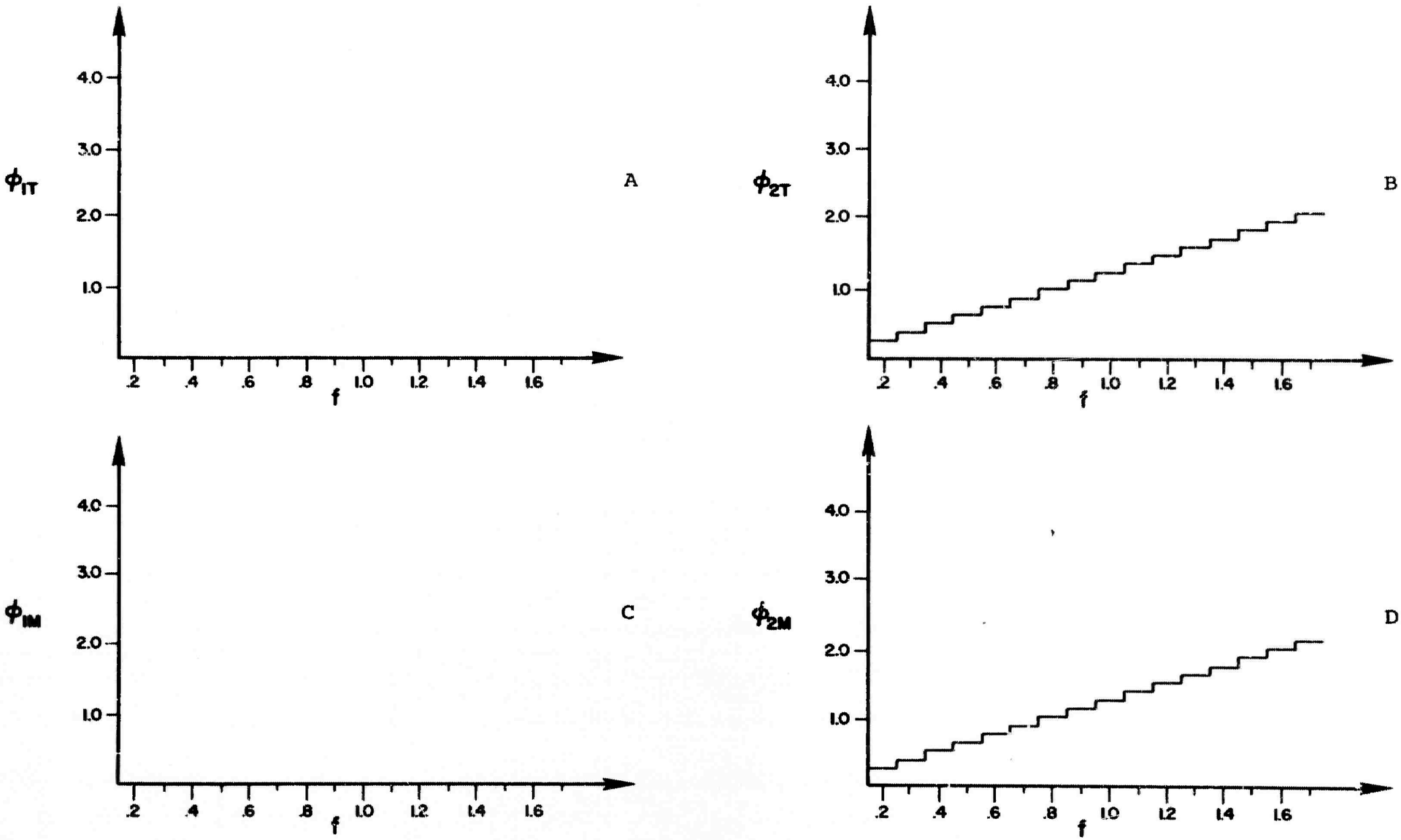

Figure III-2B

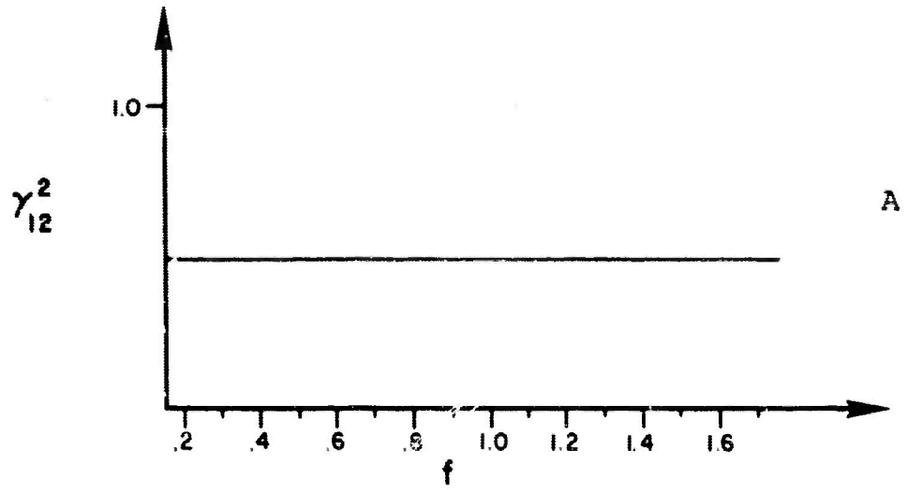

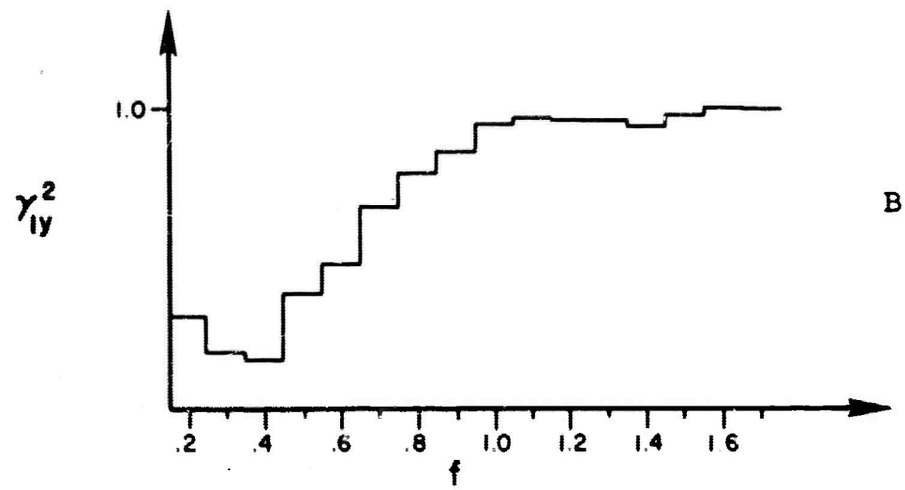

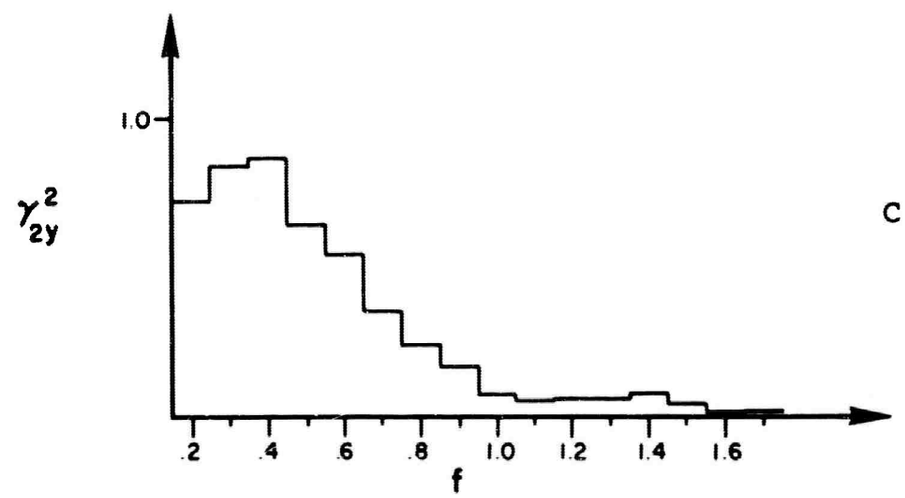

Ordinary Coherence Functions for Case I(a)

Figure III-3

denominator, and hence as this becomes large, the coherency becomes small.

$$\gamma^2_{1y}(f) = \frac{1}{1 + \frac{G_{22}(f)}{G_{11}(f)}} \qquad (1)$$

The output v(t) in this case is considered to be made up of a signal $x_1(t)$ and a noise process $x_2(t)$. By comparing Figure III-3 with Figure III-1, one sees that as $G_{zz}(f)$, which is in this case equal to $G_{22}(f)$, becomes small, then the coherency becomes large. Conversely, when the coherency between the second input and y(t) is computed, the reverse happens, as is illustrated in the second part of Figure III-3.

The ordinary coherencies between the inputs and the output indicated in Figure III-3 can, of course, be misleading since there are, in fact, linear relations between each input and the output, and hence, the coherency is really 1. This true linear relation is illustrated by the plots of the partial coherencies given in Figure III-4 which are, in fact, 1. The reason these go to 1 is that they are coherencies between the input and the output after the best linear estimate of the remaining variable is subtracted out. In the case of the partial coherency between $x_1(t)$ and y(t), the effect of $x_2(t)$ is subtracted out of y(t) which means that the residual portion of y(t) will be directly linearly related to the input $x_1(t)$, and this is illustrated by the partial coherency between $x_1(t)$ and y(t). The exact same reasoning applies to the partial coherencies between $x_2(t)$ and y(t).

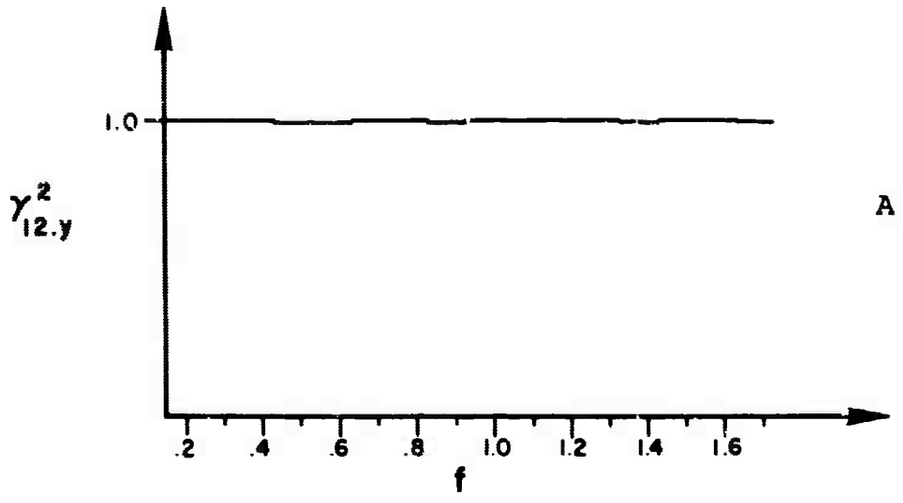

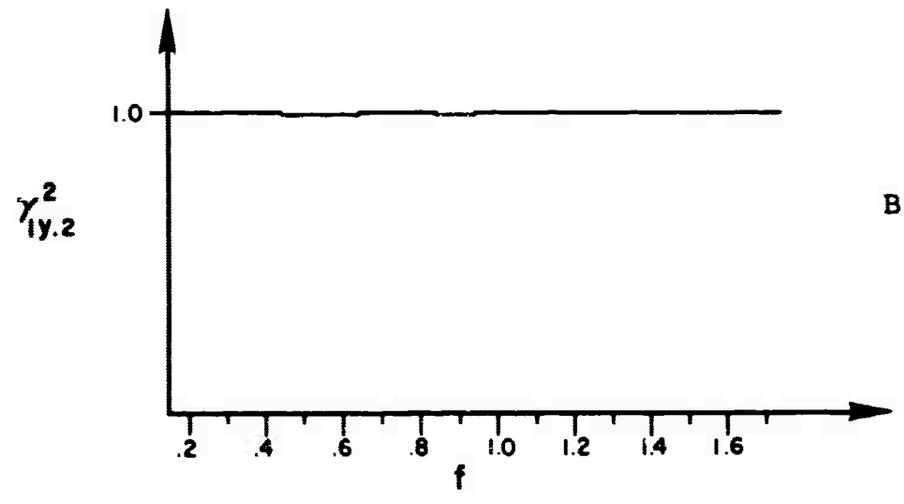

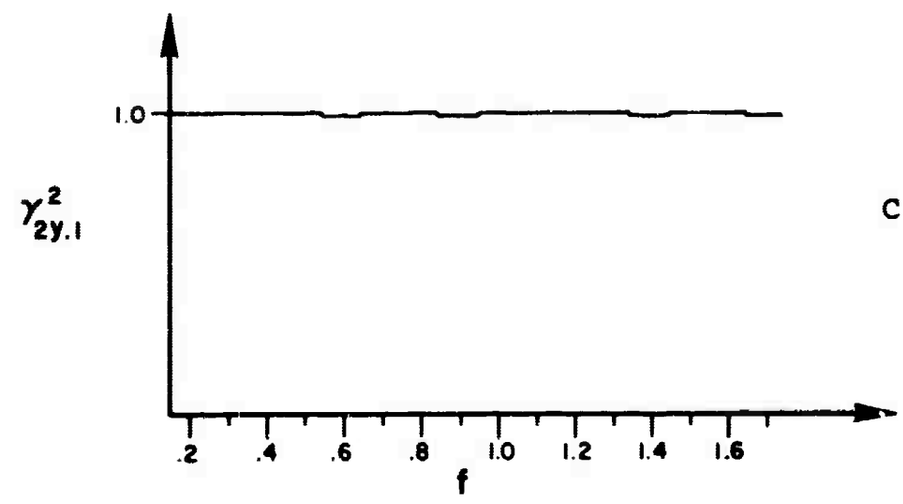

Partial Coherence Functions for Case I(a)

Figure III-4

The interpretation of the partial coherency between the two inputs $x_1(t)$ and $x_2(t)$ becoming unity is slightly more involved. The fact that this partial coherency becomes 1 even though there is no apparent direct linear relation between $x_1(t)$ and $x_2(t)$ reflects the fact that there is an indirect path via $y(t)$ through which $x_1(t)$ and $x_2(t)$ are related. Hence, although one could not detect a relation between x_1 and x_2 if one was measuring only these two variables, a relation between them does exist when the third variable y is measured which is related to both of them.

2.2 CASE I(b) RESULTS

The parameters for this case are the same as for Case I(a) except that now the inputs are moderately correlated. The parameter α which relates x_1 and x_2 was chosen to be 0.4 which results in the second input $x_2(t)$ being made up of 0.4 $x_1(t)$ plus 0.6 $z(t)$. The major differences that will occur here are errors in the computed values of the frequency response function if just two signals are used, that is, the single input and a single output and the effects of a third are ignored. Now, not only the statistical variability of the results is increased but also there are outright bias errors that occur in the computations.

As can be seen from Figure III-5, the differences between the true and measured gain factors for the $x_1(t)$ - $y(t)$ relation definitely exist but $|H_{1M}(f)|$ is not grossly in error. This reflects the fact of the significant but moderate correlation between the two inputs. Considerable error occurs in the frequency response function between the second input x(t) and

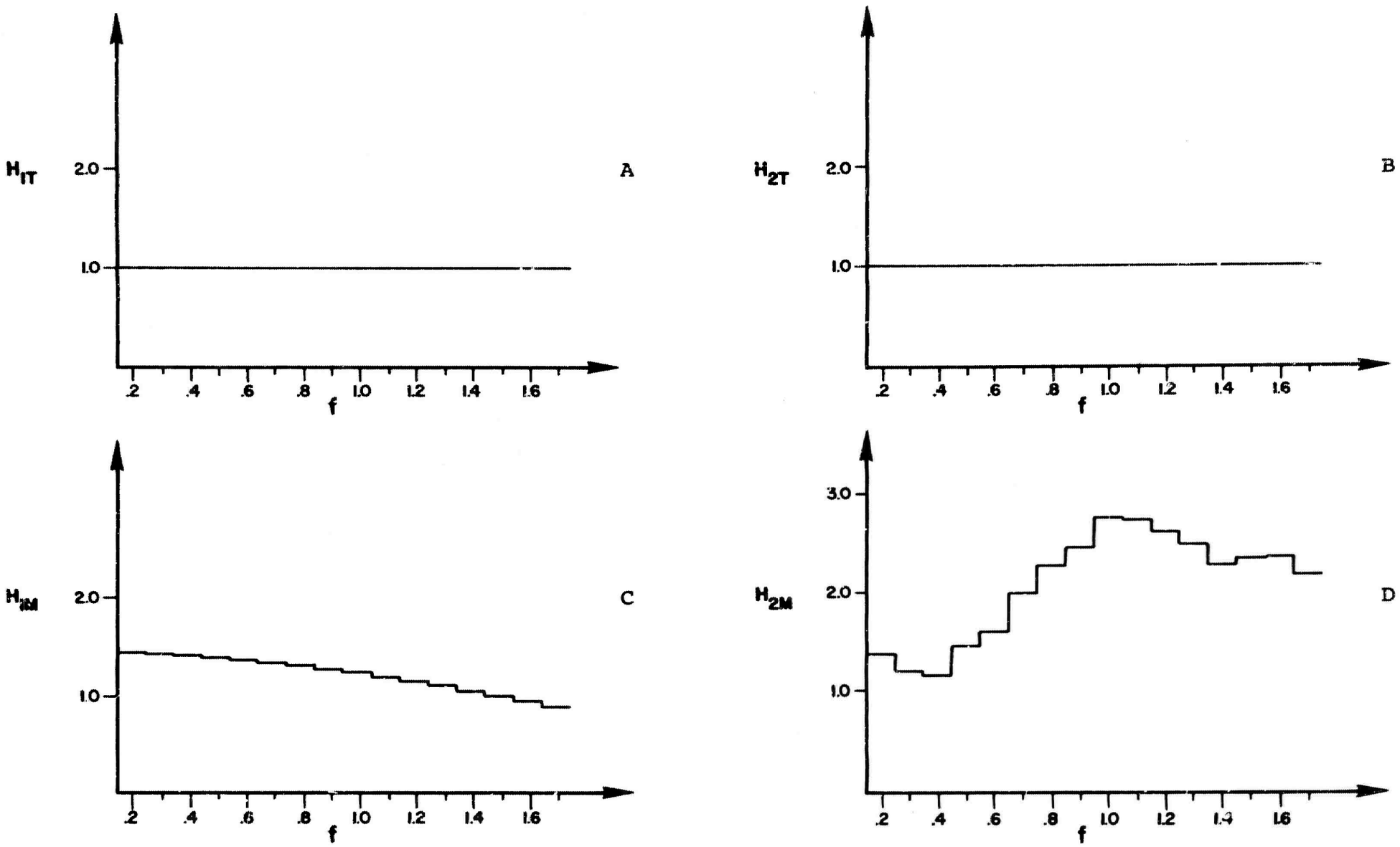

Frequency Response Functions for Case I(b)

Figure III-5A

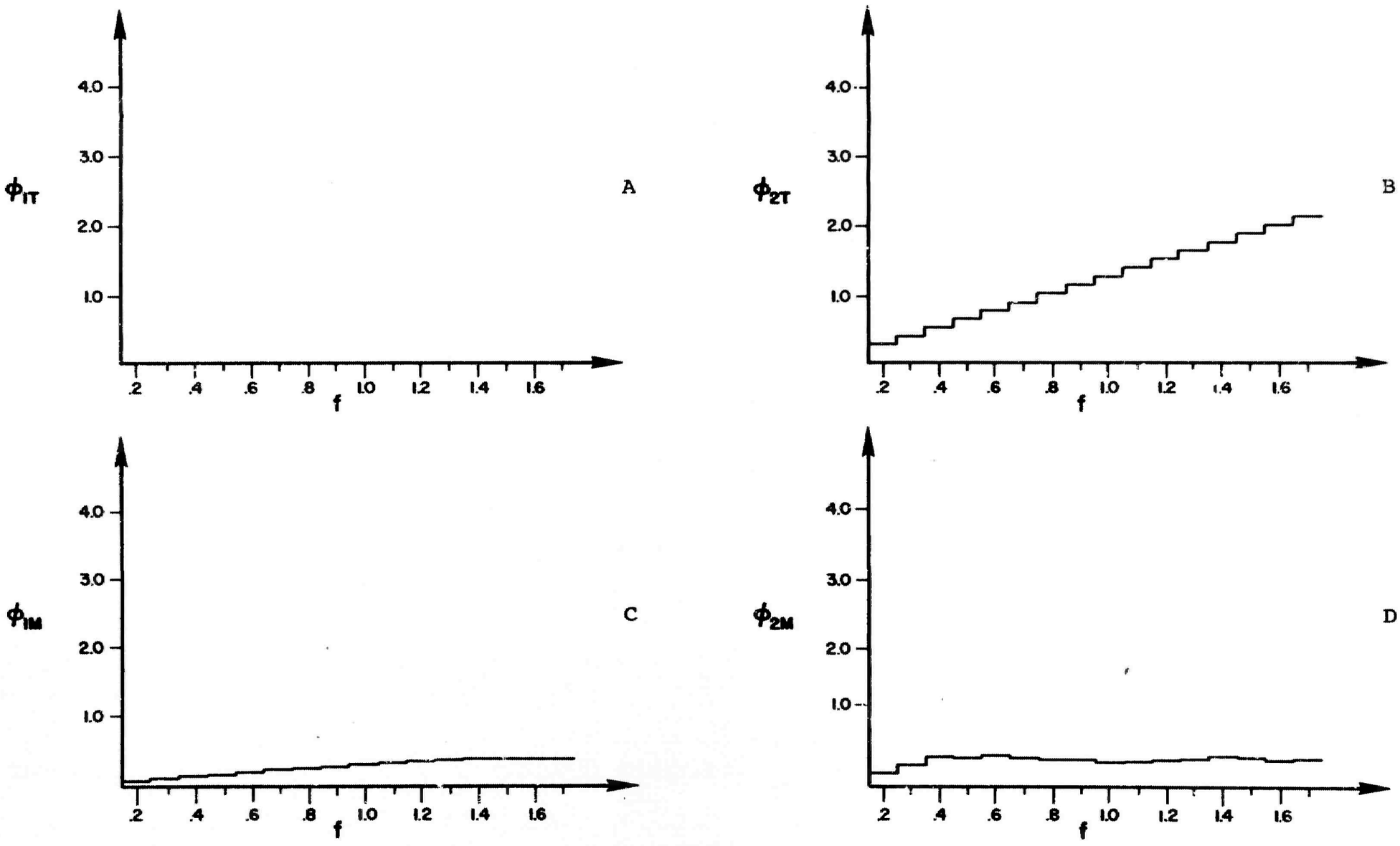

Figure III-5B

the output y(t) since in this case the output y(t) is made up primarily of $x_1(t)$. Hence, large errors are introduced. This is illustrated in both the gain and the phase factors of the frequency response between $x_1(t)$ and $x_2(t)$ as illustrated in Figure III-5. The ordinary coherency between $x_1(t)$ and $x_2(t)$ now reflects the correlation that was induced between the two inputs. For Case I(a), it was, of course, zero for all frequencies; however, now for Case I(b) it becomes quite large - in fact, nearly one for some of the higher frequency ranges. Actually, values very slightly larger than one were obtained for the two highest frequency points which reflected the negative spectral estimates that were obtained in $G_{zz}(f)$. The ordinary coherencies between each of the inputs $x_1(t)$ and $x_2(t)$ with the output y(t) exhibits some more behavior to the ordinary coherency between the two inputs. All of this is illustrated in Figure III-6. Figure III-7 again gives the plots of the ordinary coherencies, which again all turn out to be unity. This reflects the existence of the true linear relations between the variables. Again, the full linear relationship between the two inputs $x_1(t)$ and $x_2(t)$ is not totally a direct relation, but is partially the relation induced via the third variable y(t)

2.3 CASE I(c) RESULTS

Case I(c) carries Case I(b) one step further in that it differs only in that the inputs are more highly correlated. For this case the parameter α is chosen to be equal to 0.8 which induces a stronger correlation between the two inputs $x_1(t)$ and $x_2(t)$. This will be reflected in larger errors in

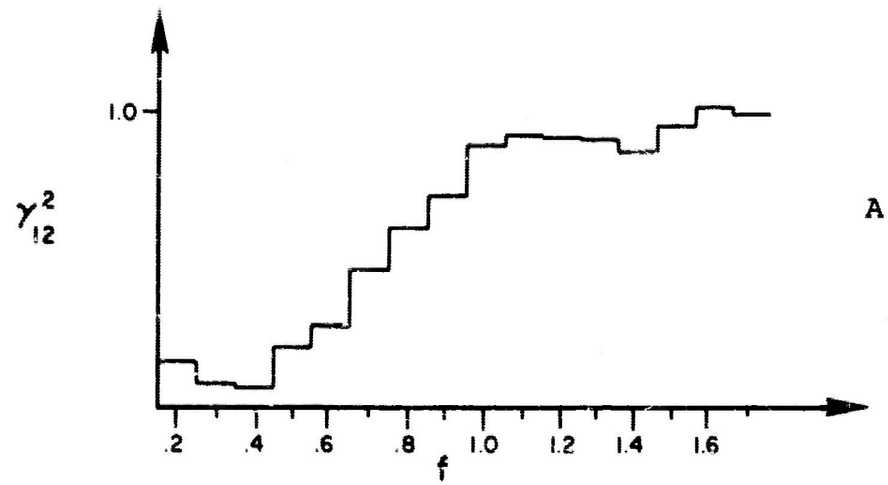

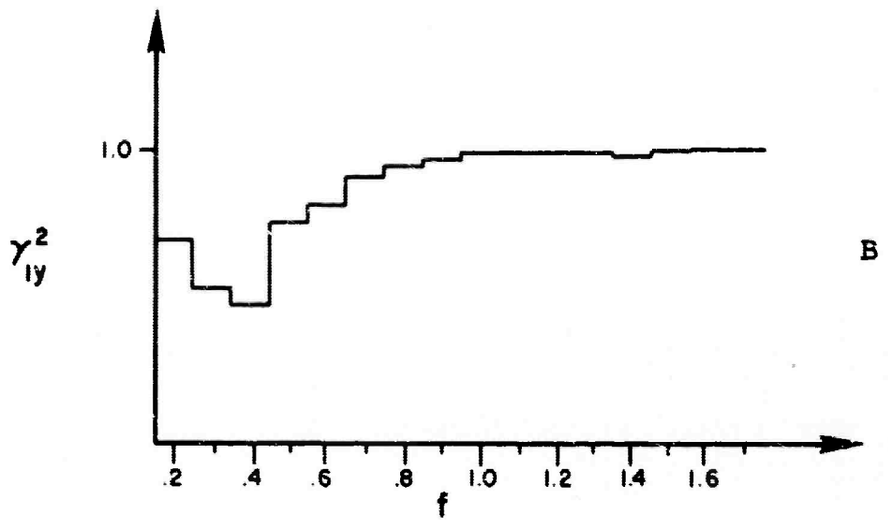

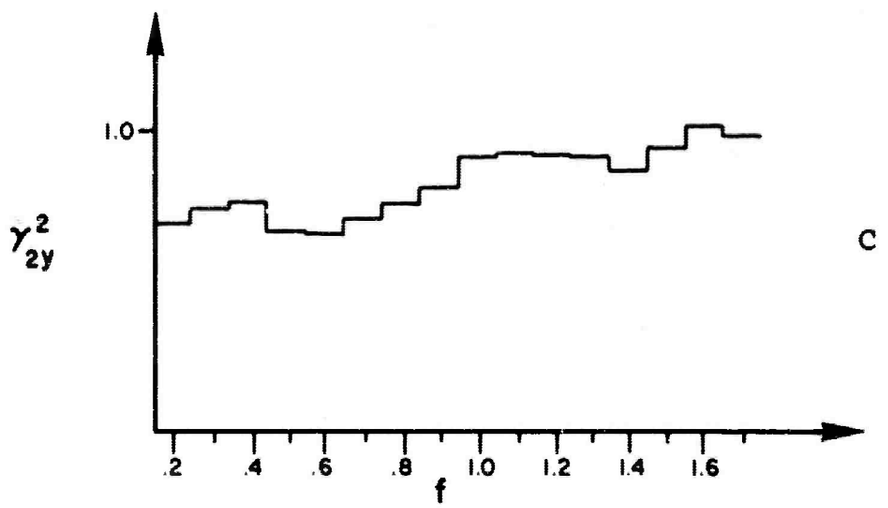

Ordinary Coherence Functions for Case I(b)

Figure III-6

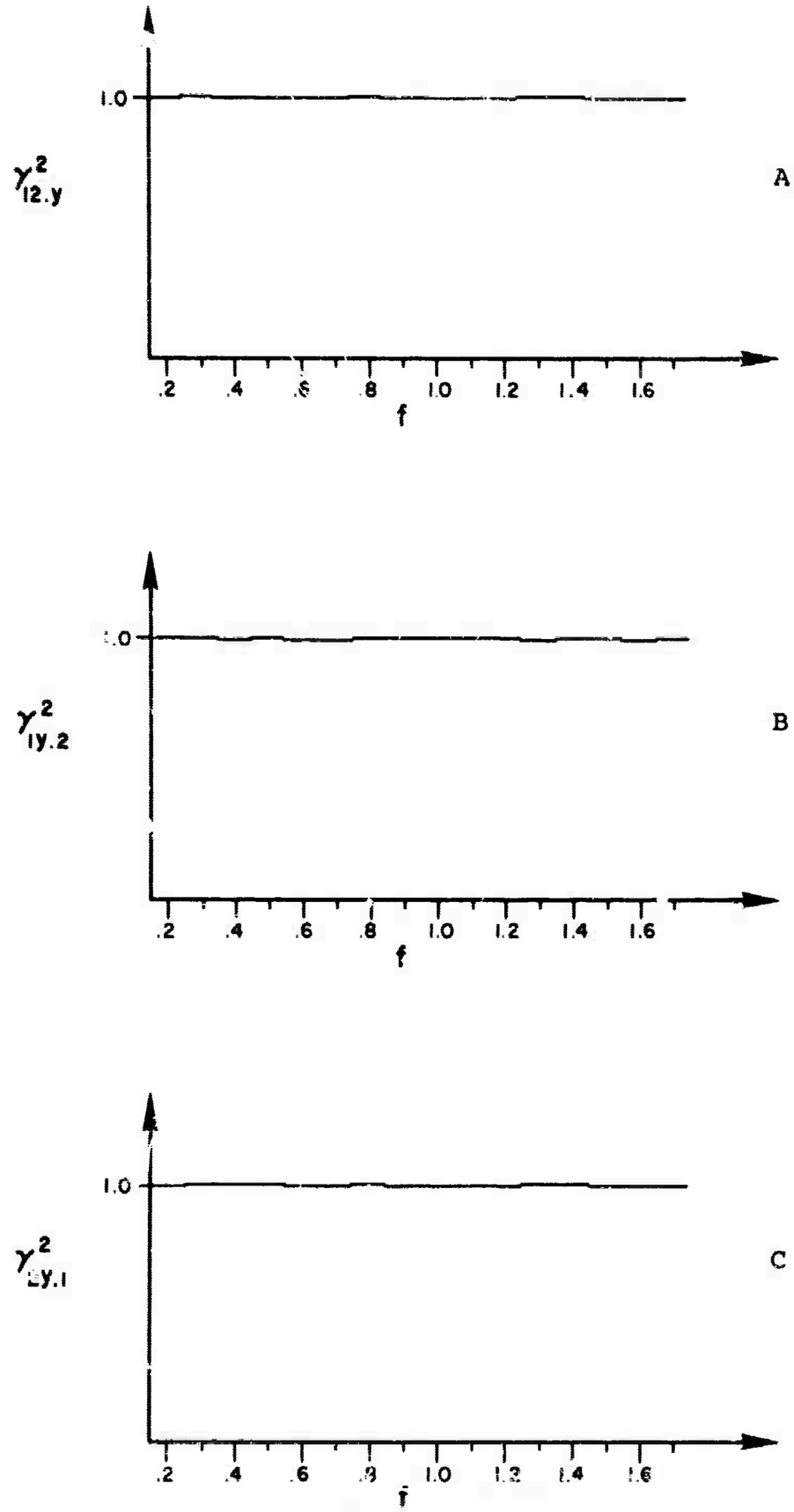

Partial Coherence Functions for Case I(b)

Figure III-7

the computation of the frequency response function between $x_1(t)$ and $y(t)$. Figure III-8 gives the gain and phase factors of the true and measured versions of the frequency response functions of Case I(c).

As can be seen by comparing the gain factor for the true and measured versions of the frequency response function, there is a considerable difference. As a matter of fact, almost an 80% error is introduced at the lower frequencies. The phase factor is also in error by a fairly considerable amount going to about .88 radians at the higher frequency end which would indicate a phase change of almost 50° when done, in fact, exists. The frequency response function between $x_2(t)$ and $y(t)$ is not in error in this case quite as much as it was in Case I(b). This is due to the fact that in this case more of the output $y(t)$ results from the second input $x_2(t)$. The coherence functions are all very close to unity as can be seen from inspecting Figure III-9. The coherence between the two inputs is, of course, high because a very high correlation was induced between the two inputs and their construction. The correlation between each of the inputs and the output is also high because in this case nearly all of each input is made up of $x_1(t)$ and the output is hence also made up of $x_1(t)$. Hence, $y(t)$ is highly coherent with both $x_1(t)$ and $x_2(t)$.

Again, as in the previous case, the partial coherencies are all unity since all the inputs are accounted for and subtracted out when these are computed.

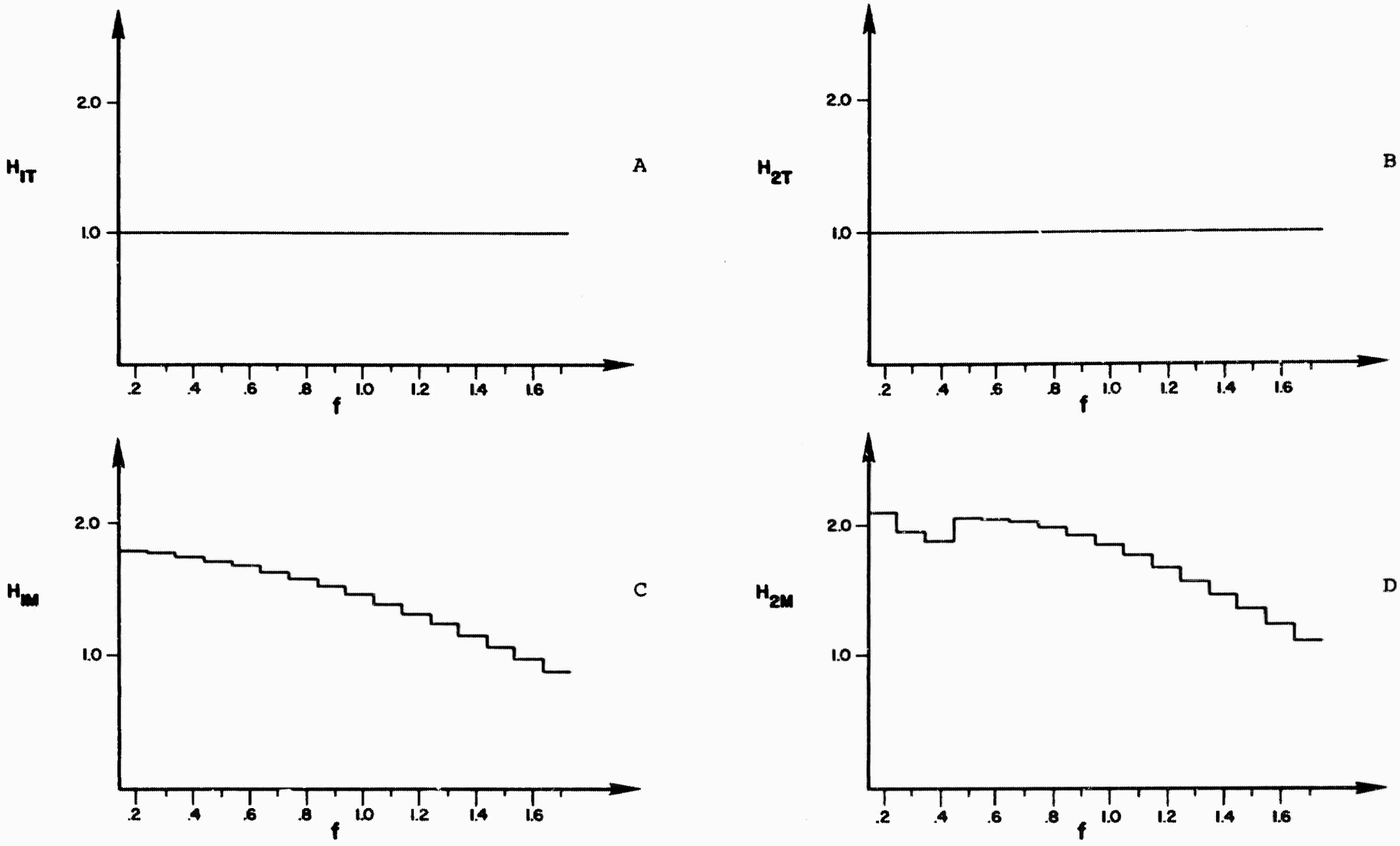

Frequency Resp. nse Functions for Case I(c)

Figure III-8A

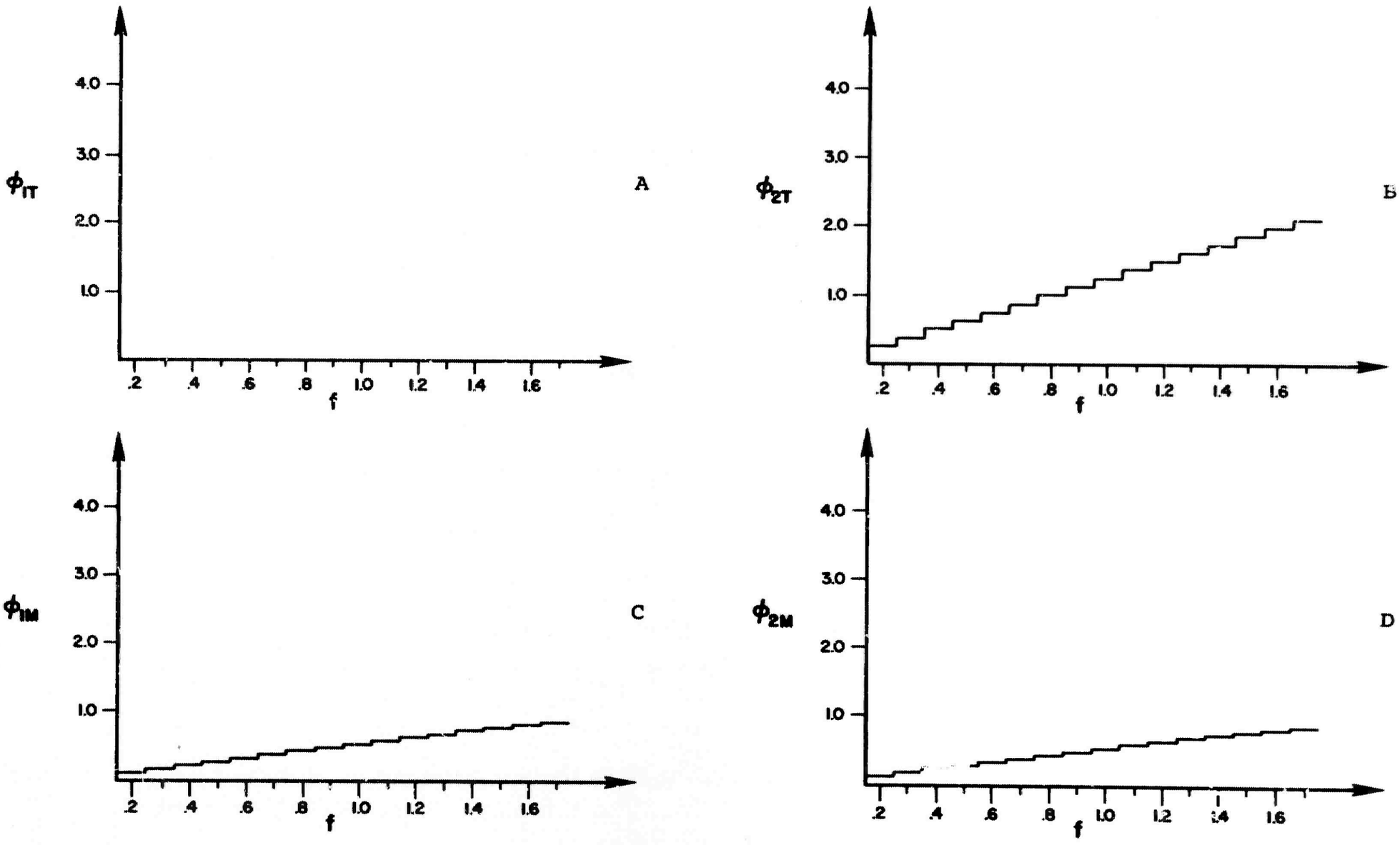

Figure III-8B

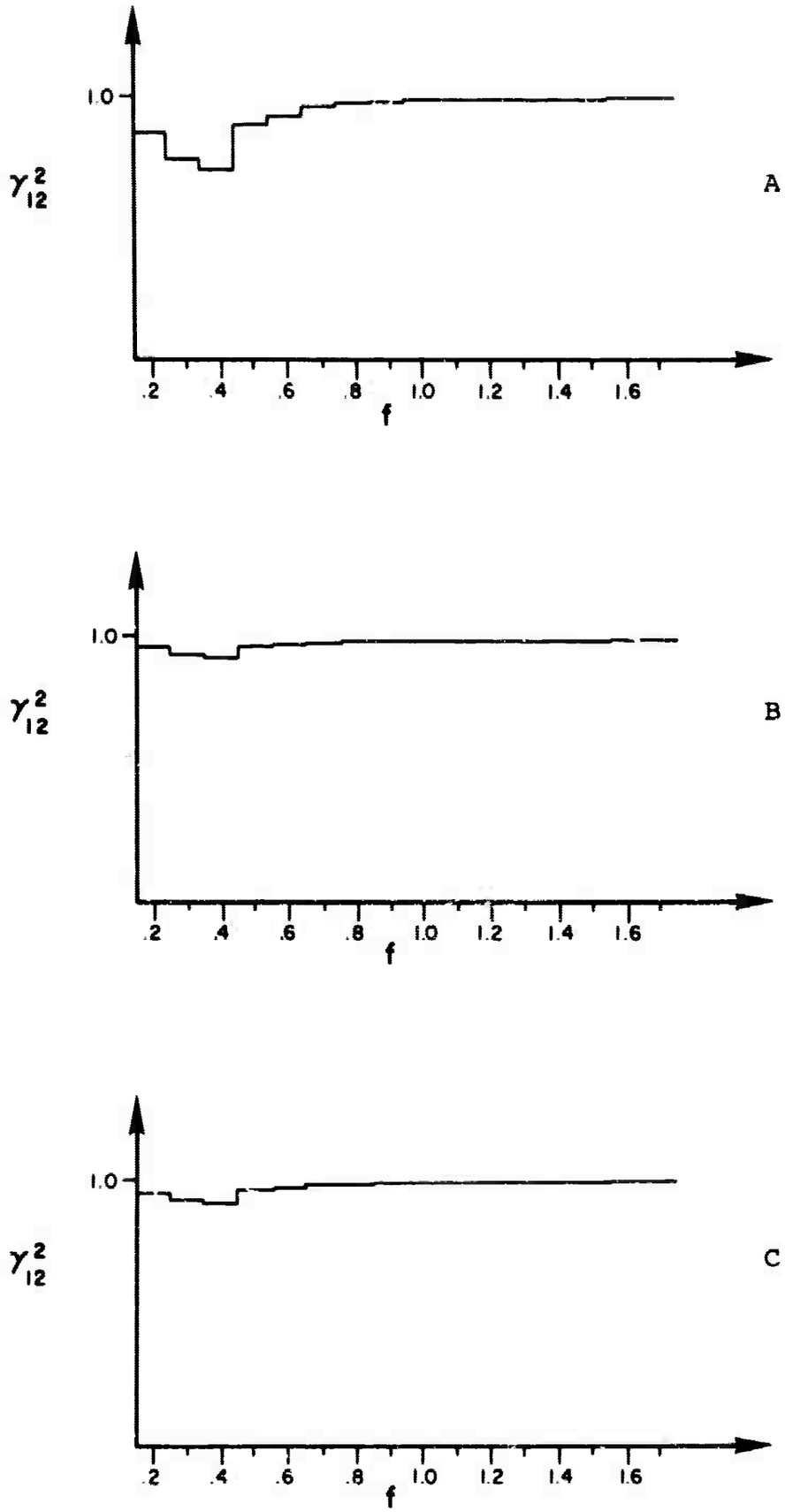

Ordinary Coherence Functions for Case I(c)

Figure III-9

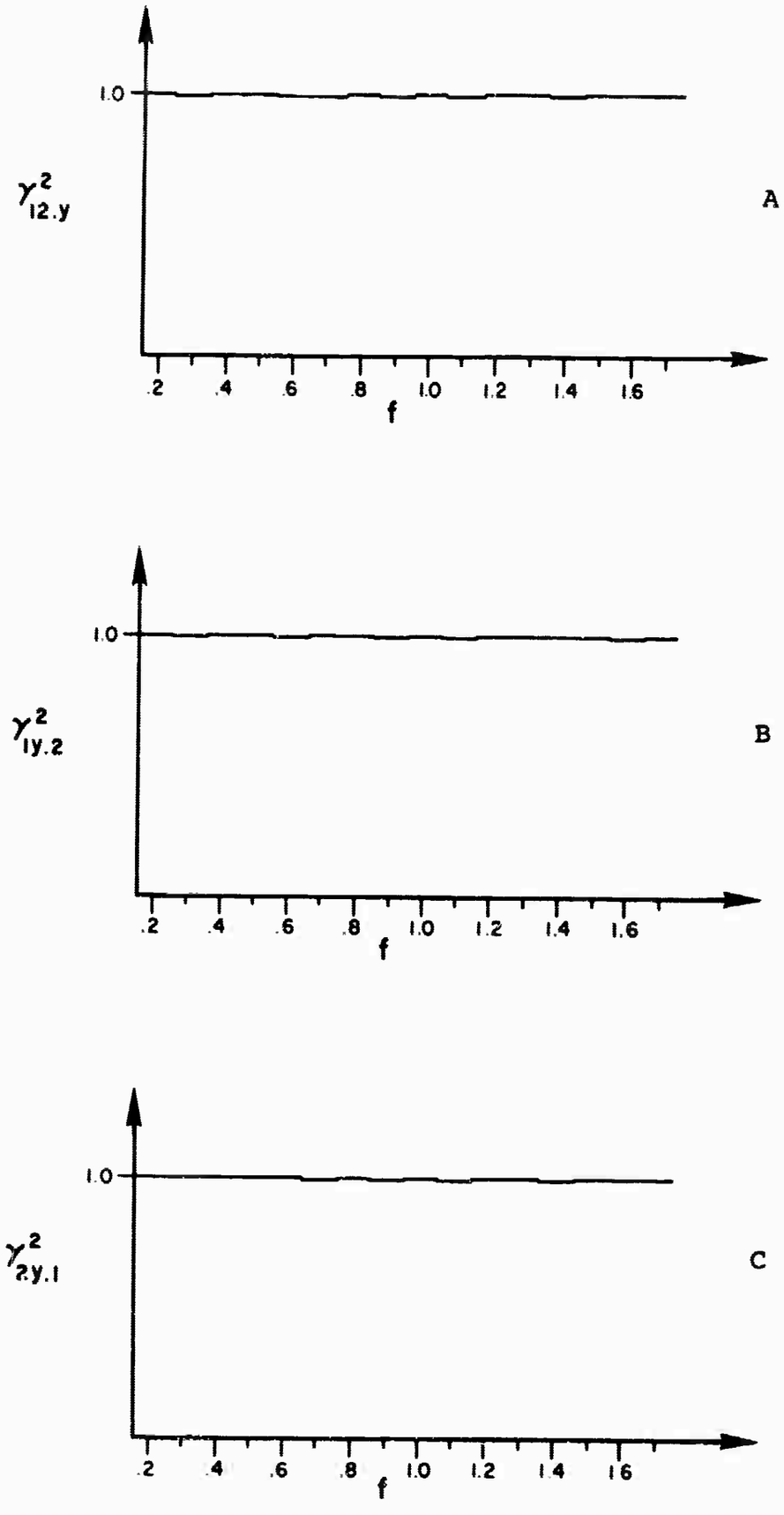

Partial Coherence Functions for Case I(c)

Figure III-10

3. CASE II RESULTS

Case II differs from Case I in that a third input is generated in the data; however, the computations are performed assuming only a two input-single output system. This will correspond to the physical situation where one is unknowingly neglecting to measure a contributing variable. For this case, the correlation between the three inputs was maintained constant in that the parameters α and β were set to 0.4 and 0.6, respectively, for all three versions of Case II. The contribution of the extraneous input $x_3(t)$ to the output was controlled by varying the gain factor a_3 between three values which were 0.2, 0.5, and 1.0. For small a_3, $x_3(t)$ can be thought of as correlated measurement noise. For the larger values of a_3, $x_3(t)$ can be thought of more as a third input which was not being properly considered.

One major difference that will occur throughout the Case II results is that the partial coherencies will not come out to be perfectly unity since in this case not all the inputs are being accounted for. However, in general, they will come out higher than the corresponding ordinary coherencies since they will more closely reflect the true situation in that as many as possible of the variables are being accounted for properly.

3.1 CASE II(a) RESULTS

This case represents small contributions from the third input to the output. That is, the coefficient a_3 which controls the contribution of the third input to the output y(t) is set equal to 0.2 for this case. Figure III-11 presents the true and

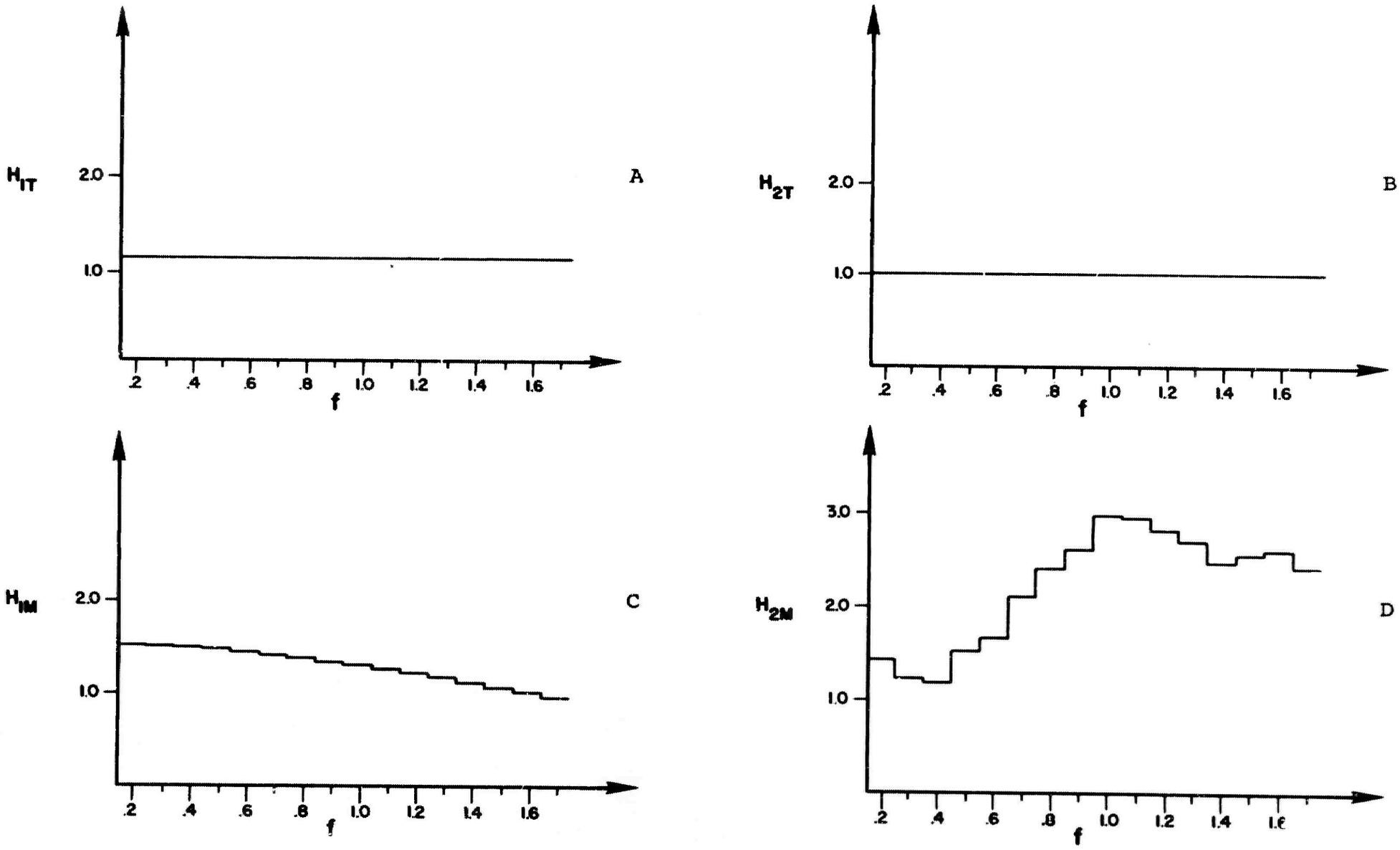

Frequency Response Functions for Case II(a)

Figure III-11A

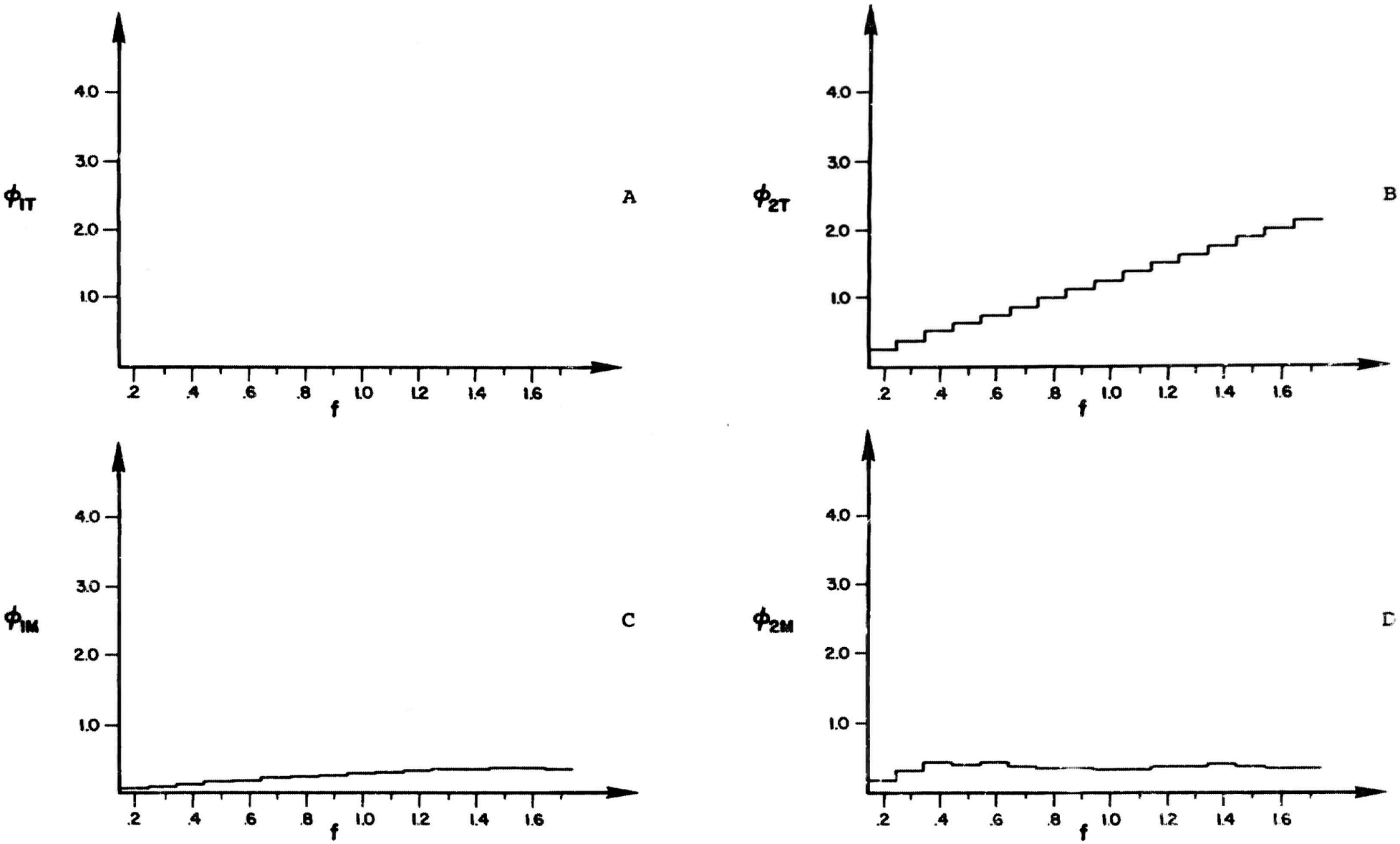

Figure III-11B

measured frequency response functions for this case. Here it should be noted that the so-called true gain factor will be in error although not so much in general as the measured gain factor. This is due to the existence of the third input which is not being accounted for. The true gain factor for the frequency response between $x_1(t)$ and $y(t)$ in this case actually was 1.12, which is an error of 15% from the expected value of 1.0. As can be seen from Figure III-11, the measured value varies with frequency althought not too greatly. The true gain factor for the second frequency response function is computed correctly as 1.0 since the second input $x_2(t)$ is independent of the extraneous input $x_3(t)$. This part of Case II (a) is therefore similar to Case I (a). The measured frequency response function gain factor is, however, in error by a considerable amount which is to be expected since α, which dictates the correlation between $x_2(t)$ and $x_1(t)$, is fairly small and hence the output $y(t)$ is made up primarily of $x_1(t)$ rather than $x_2(t)$.

The ordinary coherence functions are illustrated in Figure III-12 for Case II (a). As can be seen they are considerably in error at the lower frequency ranges, but approach the correct values of near unity at the higher frequency ranges. This is due mainly to the fact that the power spectrum for $x_1(t)$ dominates at the higher frequency, and since the output is made up primarily of $x_1(t)$, the high coherence come through.

The partial coherence functions are shown in Figure III-13 and as can be seen they are very close to one throughout the entire frequency range. But they are definitely slightly less than one. This reflects the fact that the third extraneous input that is not being considered has relatively little effect

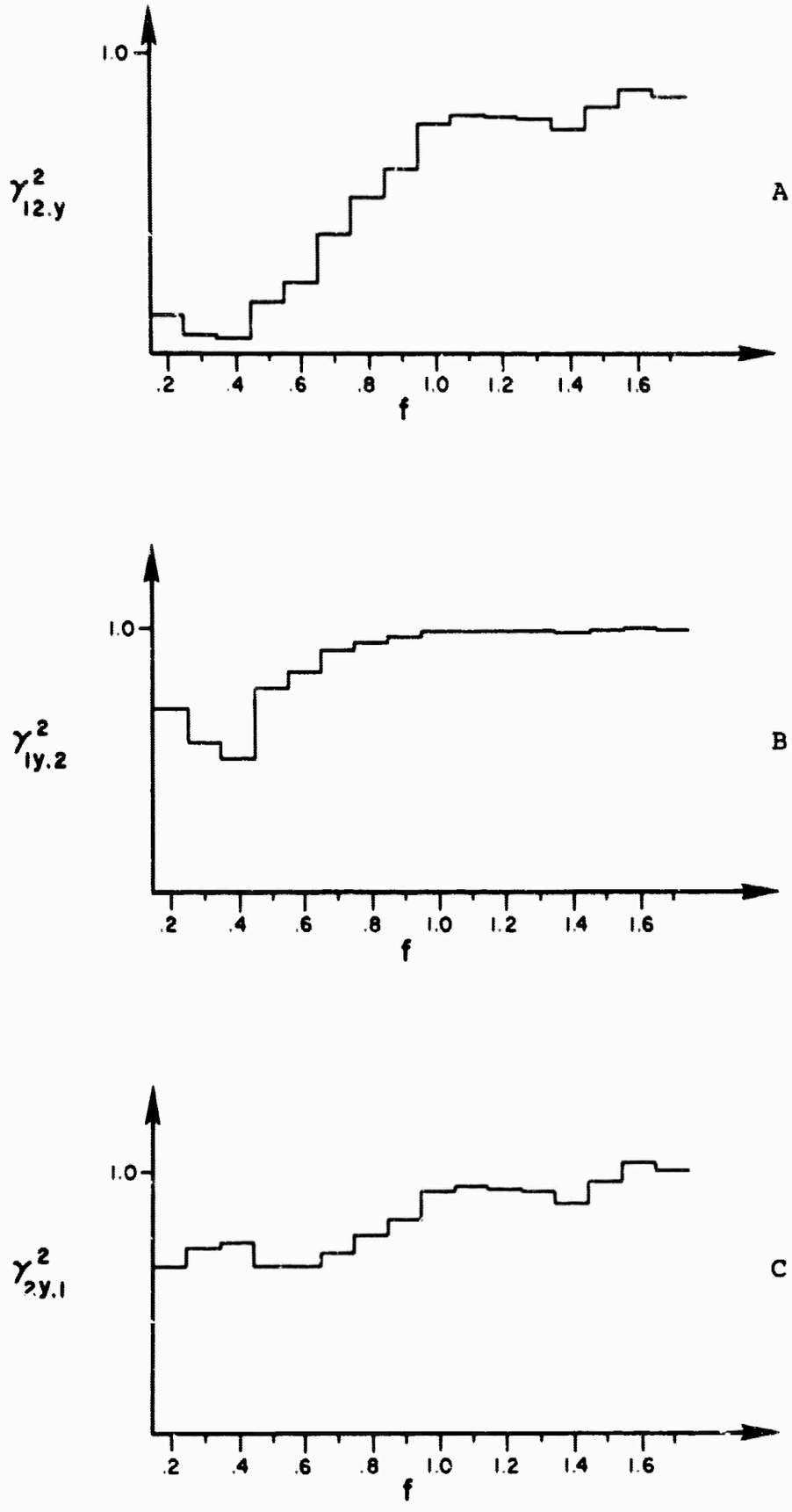

Ordinary Coherence Functions for Case II(a)

Figure III-12

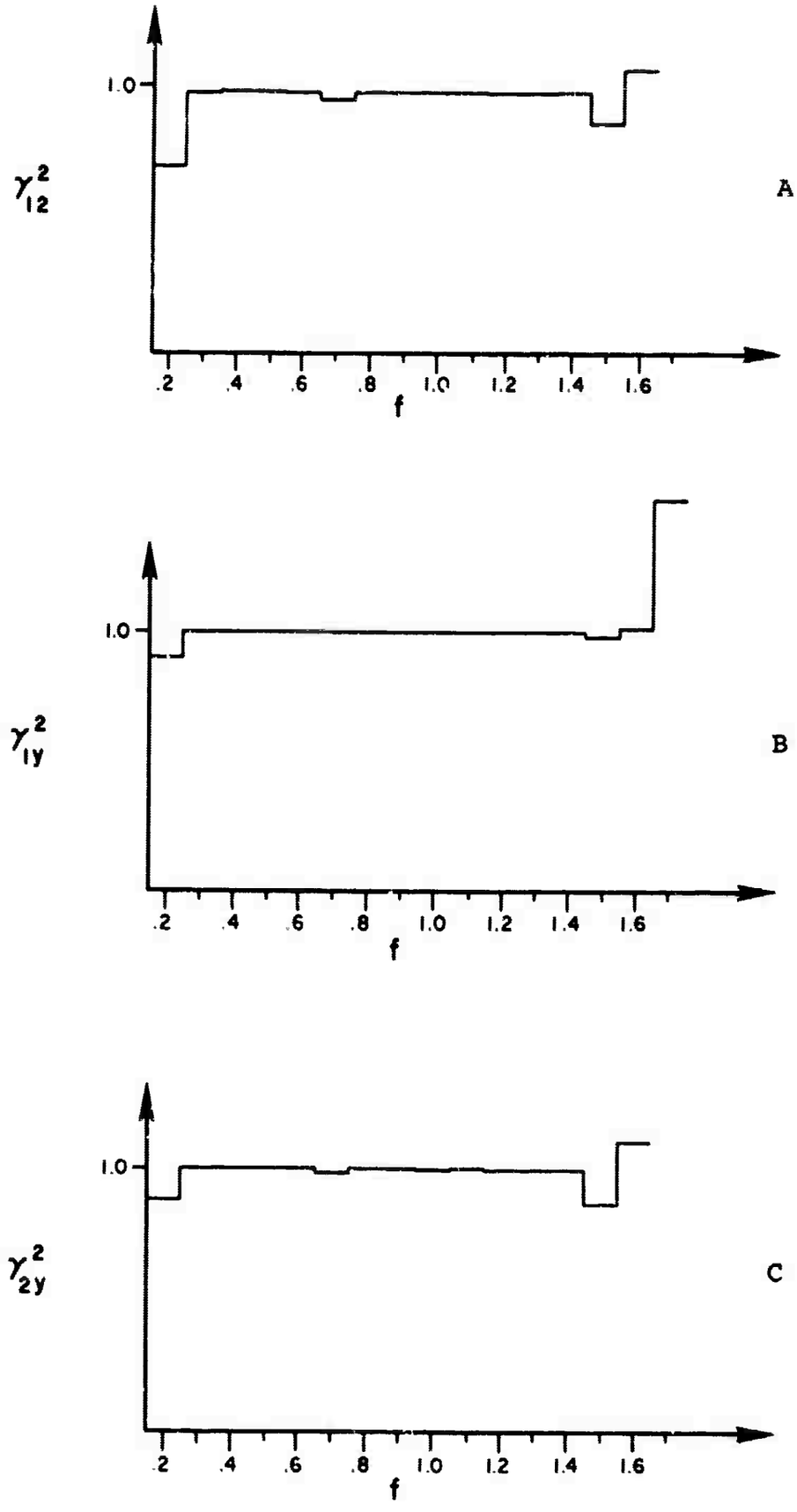

Partial Coherence Functions for Case II(a)

Figure III-13

on the output in this case. Larger discrepancies will occur for Cases II(b) and II(c) which are discussed subsequently.

3.2 CASE II (b) RESULTS

Case II(b) differs from Case II(a) in that the effect of the extraneous third input $x_3(t)$ is allowed to have larger effect on the output y(t). This is accomplished by setting the parameter a_3 equal to 0.5. This will cause slightly larger biases in just about all of the computations. The true gain factor will be in error by somewhat more for the frequency response function between $x_1(t)$ and y(t) as will the various measured values and the coherencies. The frequency response functions are illustrated in Figure III-14.

In Figure III-14, the value for the gain factor for the true frequency response between $x_1(t)$ and y(t) actually comes out to 1.3 instead of the expected value 1.0. This indicates the increasing bias error that occurs when the effect of the third unaccounted for input is magnified. However, since this third input is uncorrelated with the second input $x_2(t)$, the gain factor or the true frequency response function between $x_2(t)$ and y(t) remains correctly computed. This figure also illustrates the slightly larger errors that occur in the measured phase factors and gain factors.

The coherence functions are again in error, of course, and are illustrated in Figure III-15 and III-16. The errors in the ordinary coherence functions remain about the same as in Case I(a); however, this time the errors in the partial coherence functions b gin to be increased due to the more pronounced effect of the extraneous input. In fact, at the three highest frequency points, meaningless results begin to be obtained due to the

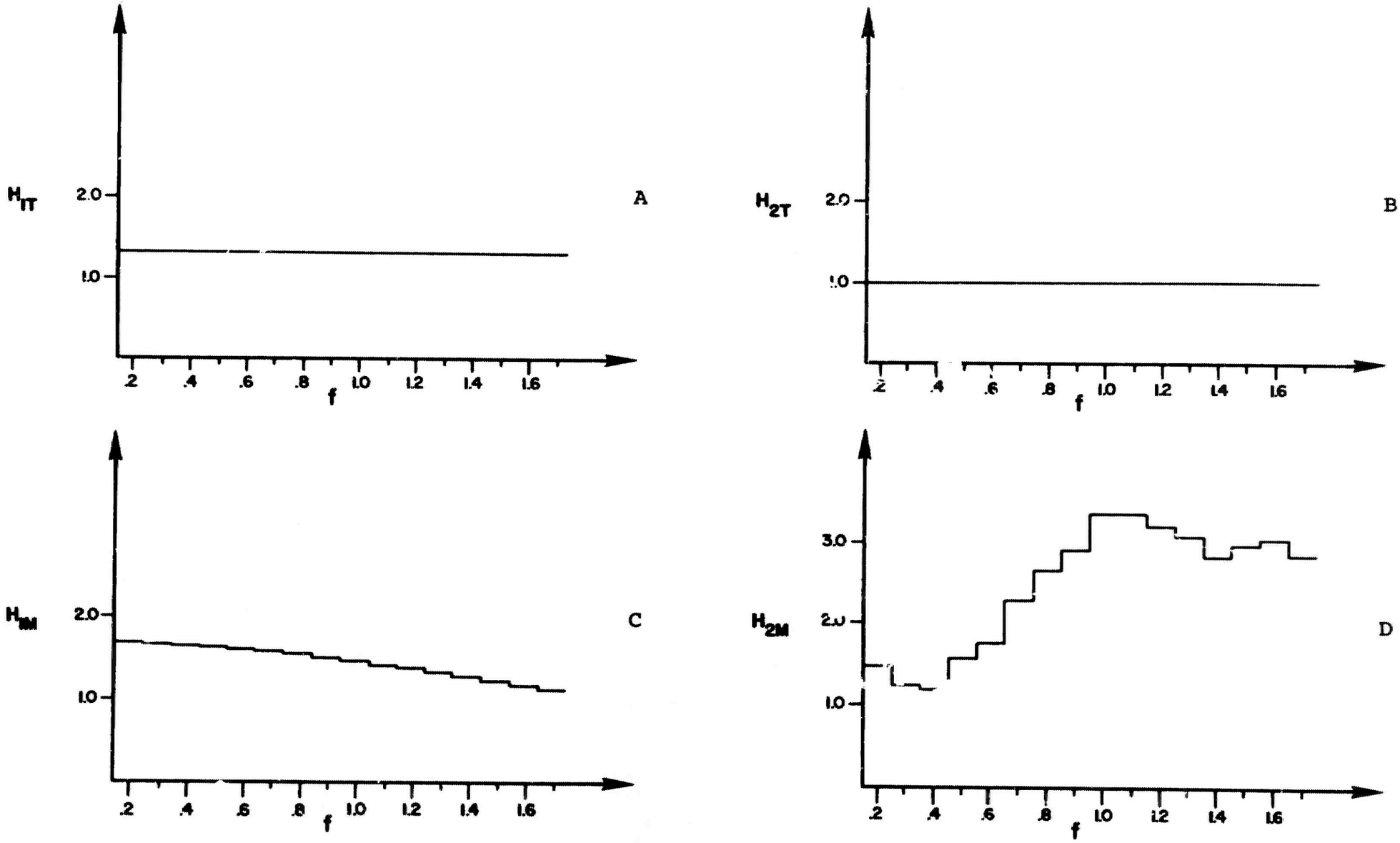

Frequency Response Functions for Case II(b)

Figure III-14A

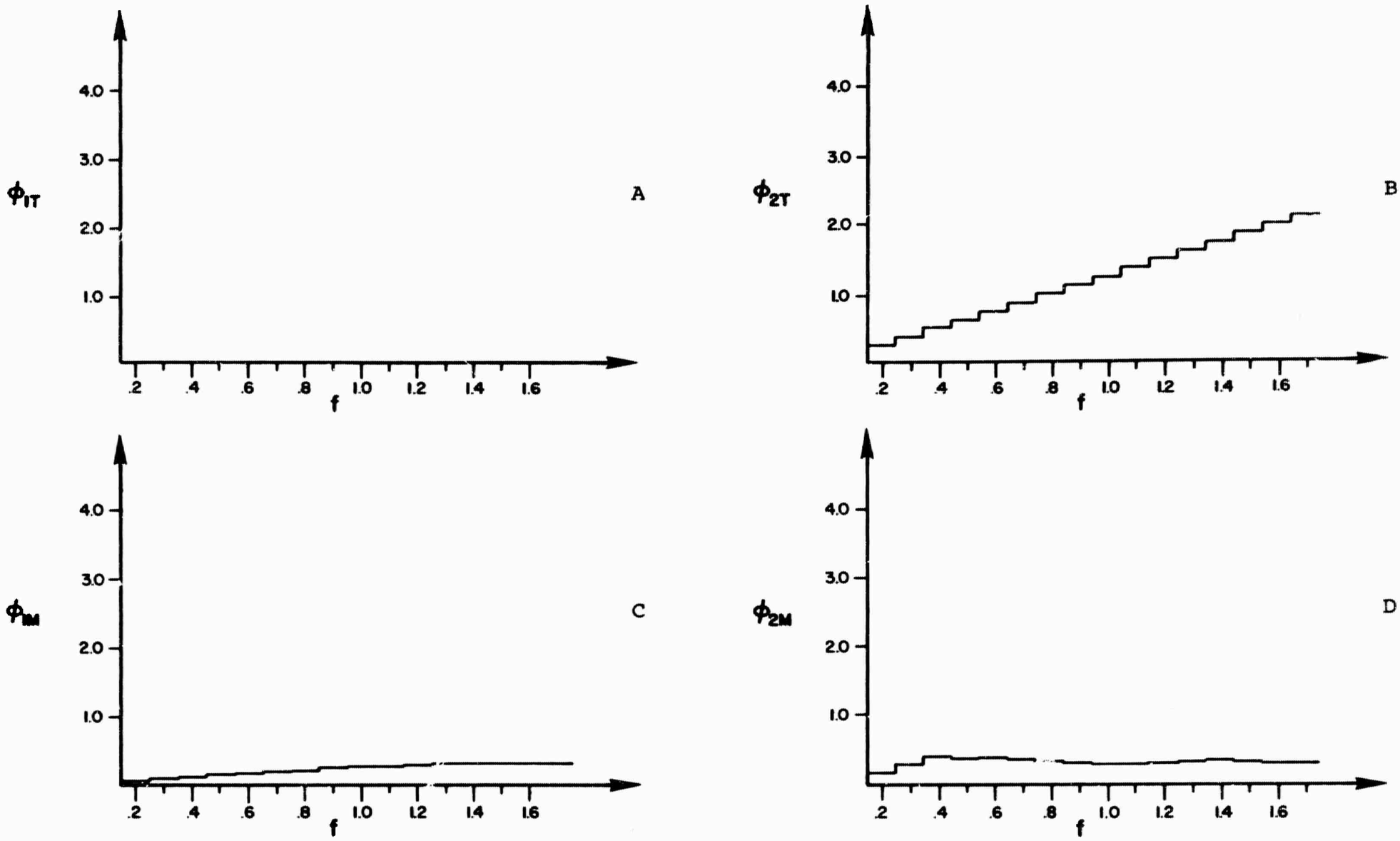

Figure III-14B

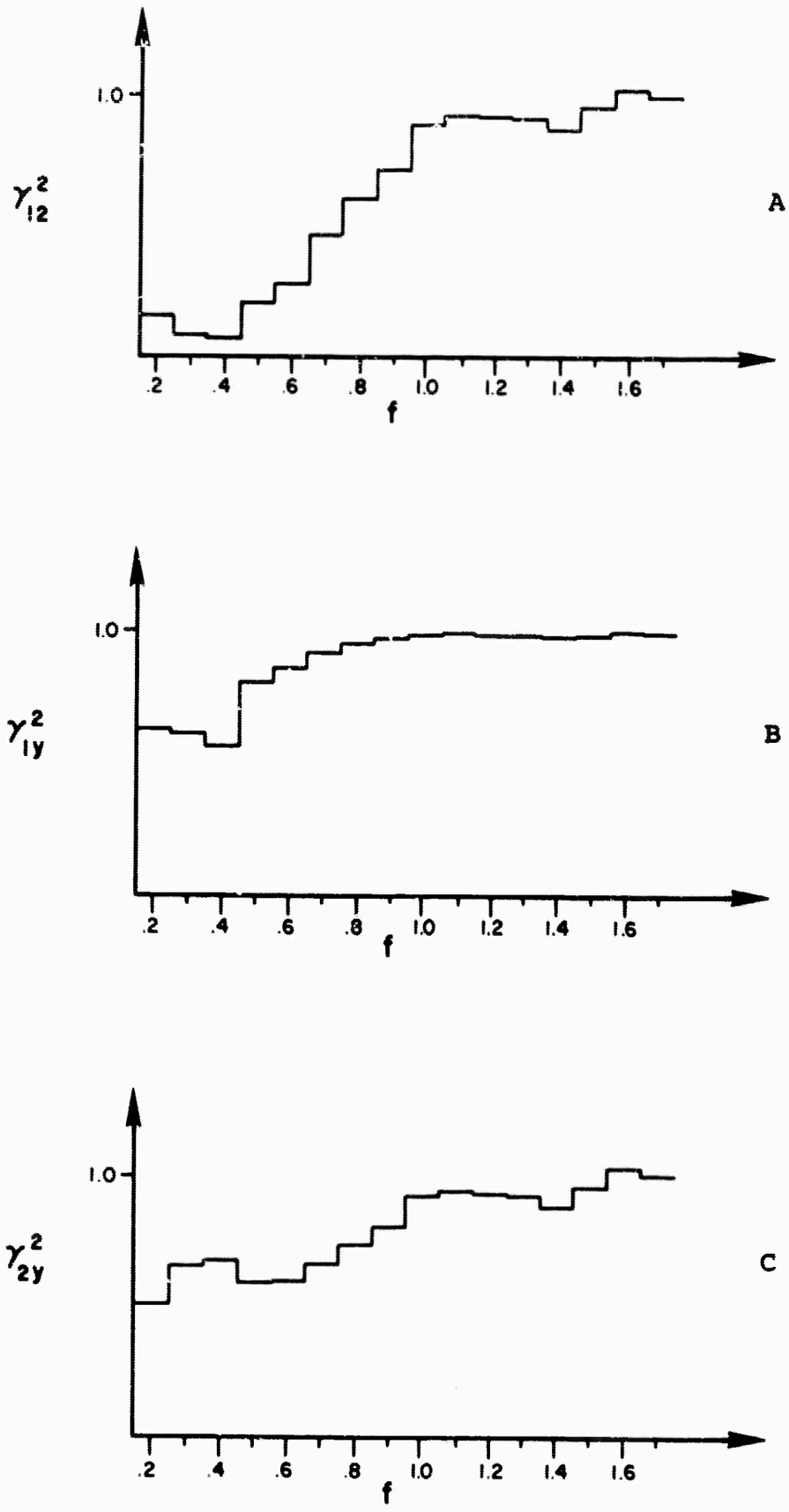

Ordinary Coherence Functions for Case II(b)

Figure III-15

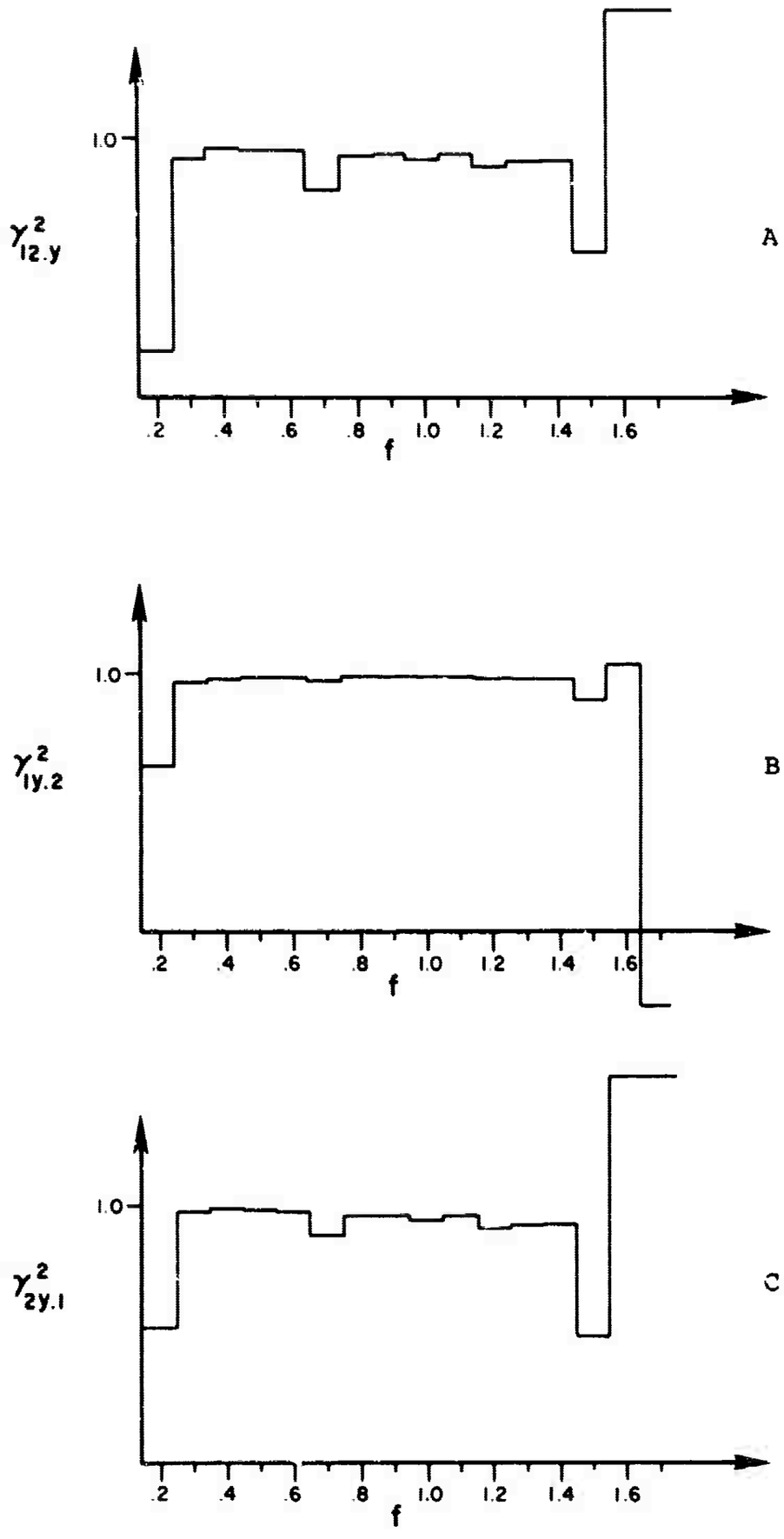

Partial Coherence Functions for Case II(b)

Figure III-16

fact that the power spectrum of z(t) which serves to make up $x_3(t)$ and part of $x_1(t)$ has two negative estimates which tend to invalidate the computations at that point. In general, the partial coherence functions are now deviating farther from unity than previously which is to be expected. Of course, the fact that they are deviating farther and farther from unity can be used as an indicator of the magnitude of the third neglected input which should be one of the general applications for the partial coherence function.

3.3 CASE II(c) RESULTS

Case II(c) differs from Case II(a) and II(b) in that the effect of the third extraneous input is magnified further yet. In this case, the parameter a_3 which controls the contributing as much as each of the other two. Hence, one expects the true gain factor for the frequency response function between $x_1(t)$ and y(t) to be in error by a larger amount yet. This, in fact, happens as do the increased errors in the partial coherence functions.

The gain and phase factors for the true and measured frequency response functions are plotted in Figure III-17. In this case, the gain factor for $H_{1T}(f)$ is computed to be 1.6, which is a 60% error from the expected value of 1.0. The measured gain factor actually varies from almost 2.0 to about 1.4, which is a considerable error. The true gain factor computations for $H_{2T}(f)$, of course, remains correct at 1.0 since the third input $x_3(t)$ is still uncorrelated with $x_2(t)$. However, the measured gain factor varies considerably as does the measured phase factor.

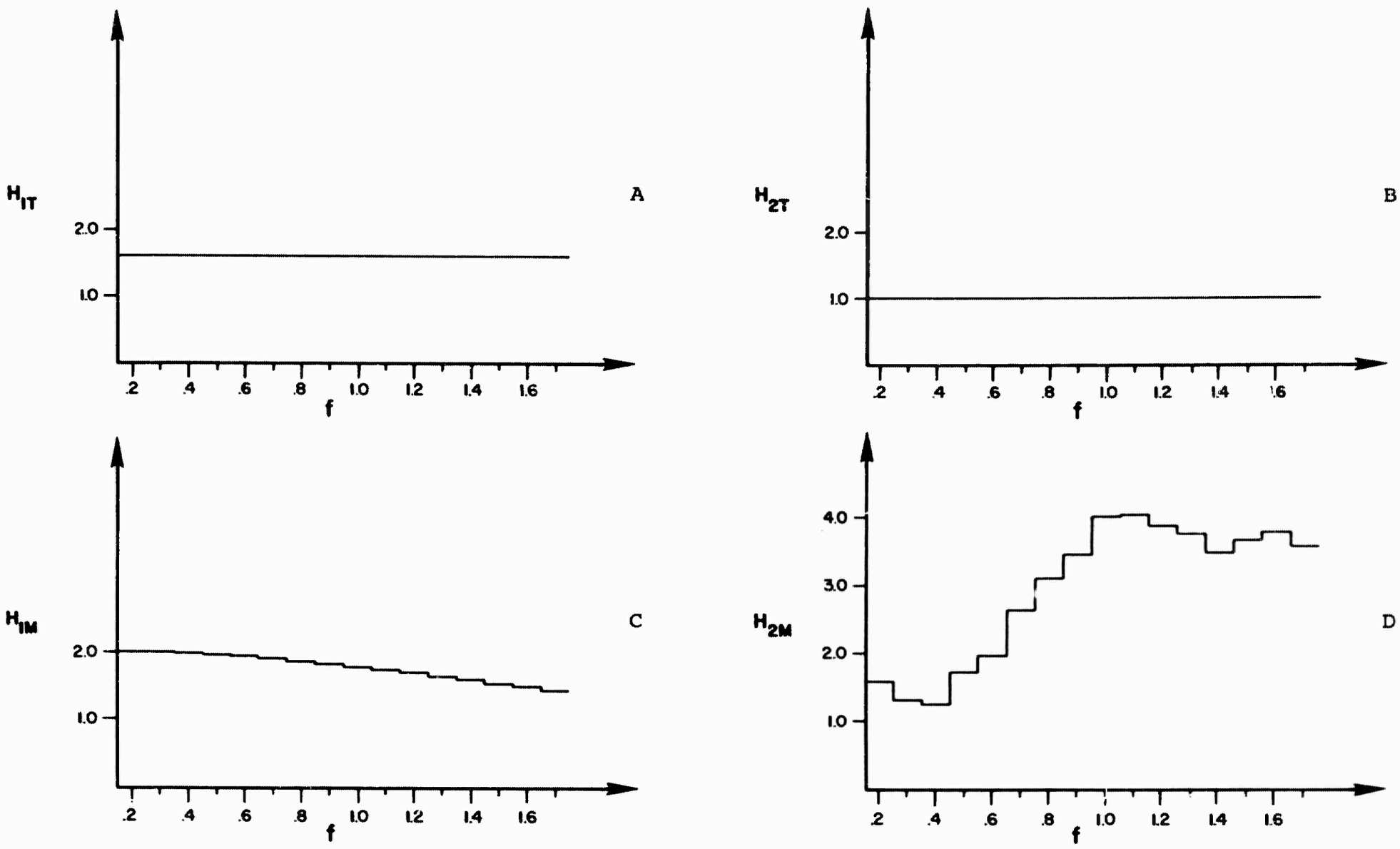

Frequency Response Functions for Case II(c)

Figure III-17A

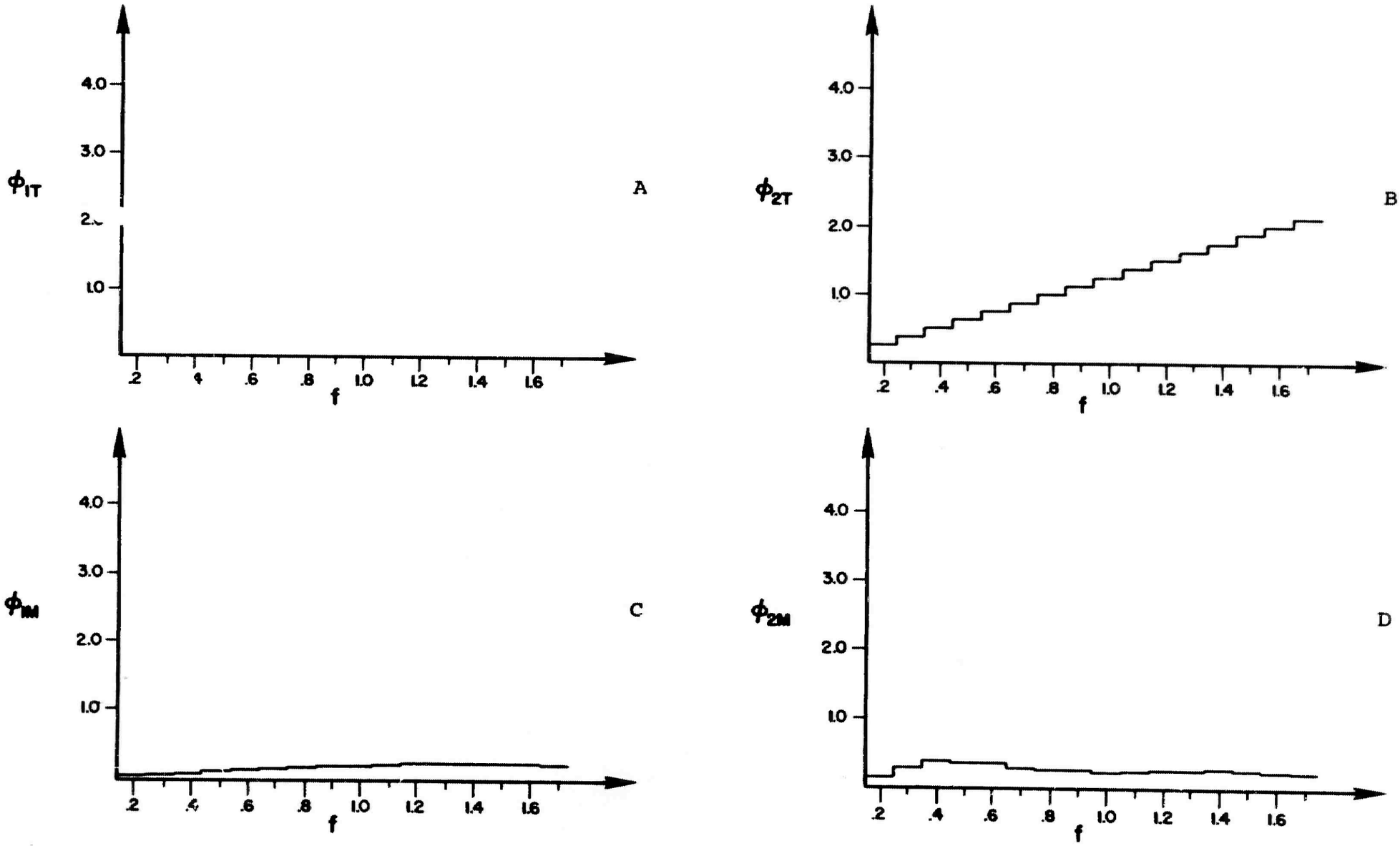

Figure III-17B

The ordinary coherence functions and partial coherence functions for Case II(c) are illustrated in Figures III-18 and III-19. The over-all errors in the ordinary coherence functions remain much the same as in the previous two cases. However, the errors in the partial coherence functions become more and more pronounced, again exhibiting the increased effect of the third input $x_3(t)$. In fact, in some cases, the partial coherence functions are in error more than the ordinary coherence functions which is due to the relatively large effect of the third input. The same instability in the last two or three points of the partial coherence function which results from negative spectral density estimates again occurs for this case.

This concludes the presentation of the numerical results for the computational experiments. The over-all results come out essentially exactly as expected. The Case-I computations illustrate that the frequency response functions are determined correctly when all the inputs are accounted for. In addition, the Case I results illustrate numerically the inaccuracies that occur when only a single input and a single output are used in computing frequency response between an input and output function. Case II illustrates the degeneracy that occurs when a third input is introduced which is unaccounted for in the computations. In general, the increasing inaccuracies which occur with an increasing effect due to a third unaccounted for input are demonstrated numerically.

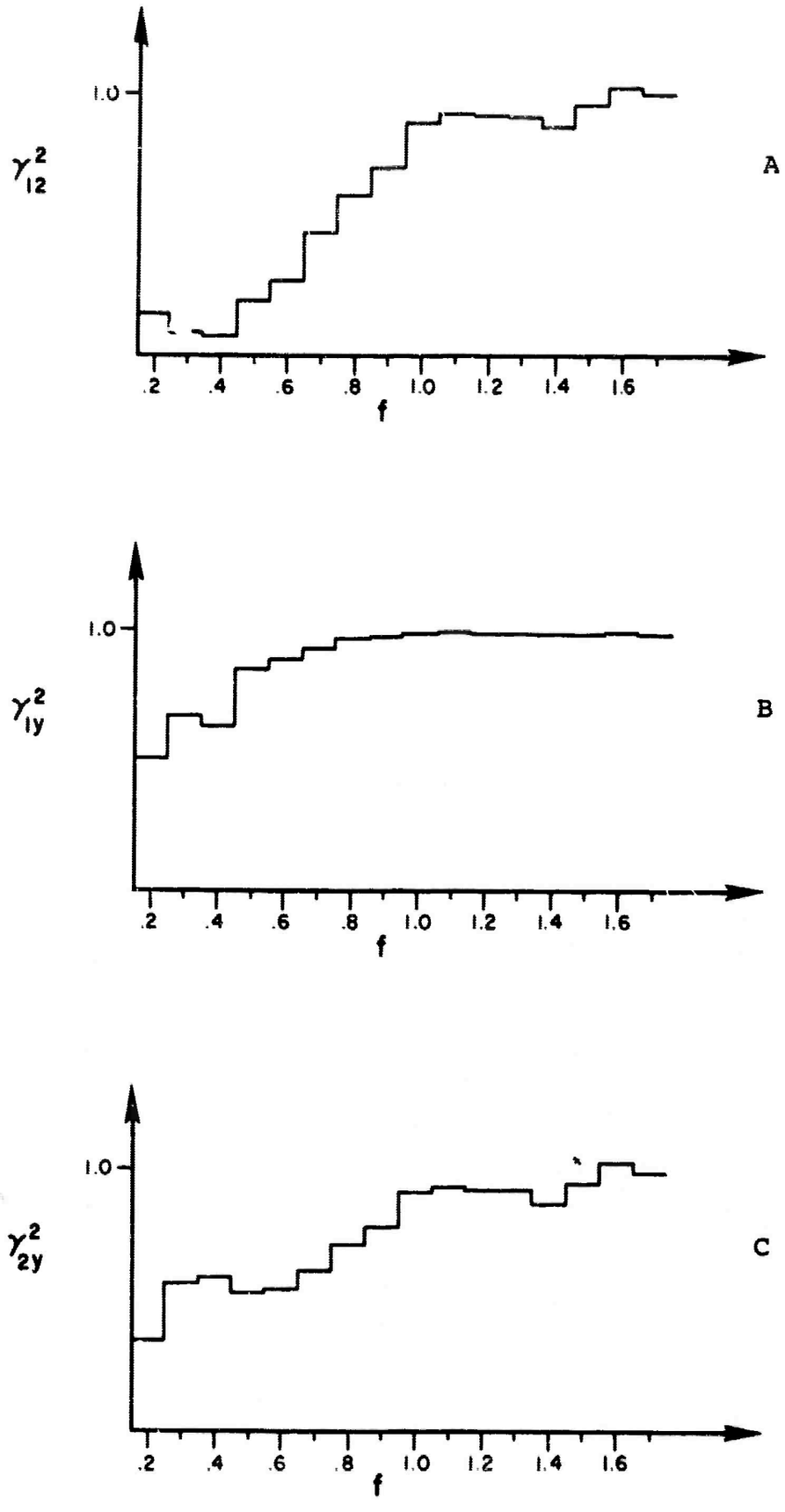

Ordinary Coherence Functions for Case II(c)

Figure III-18

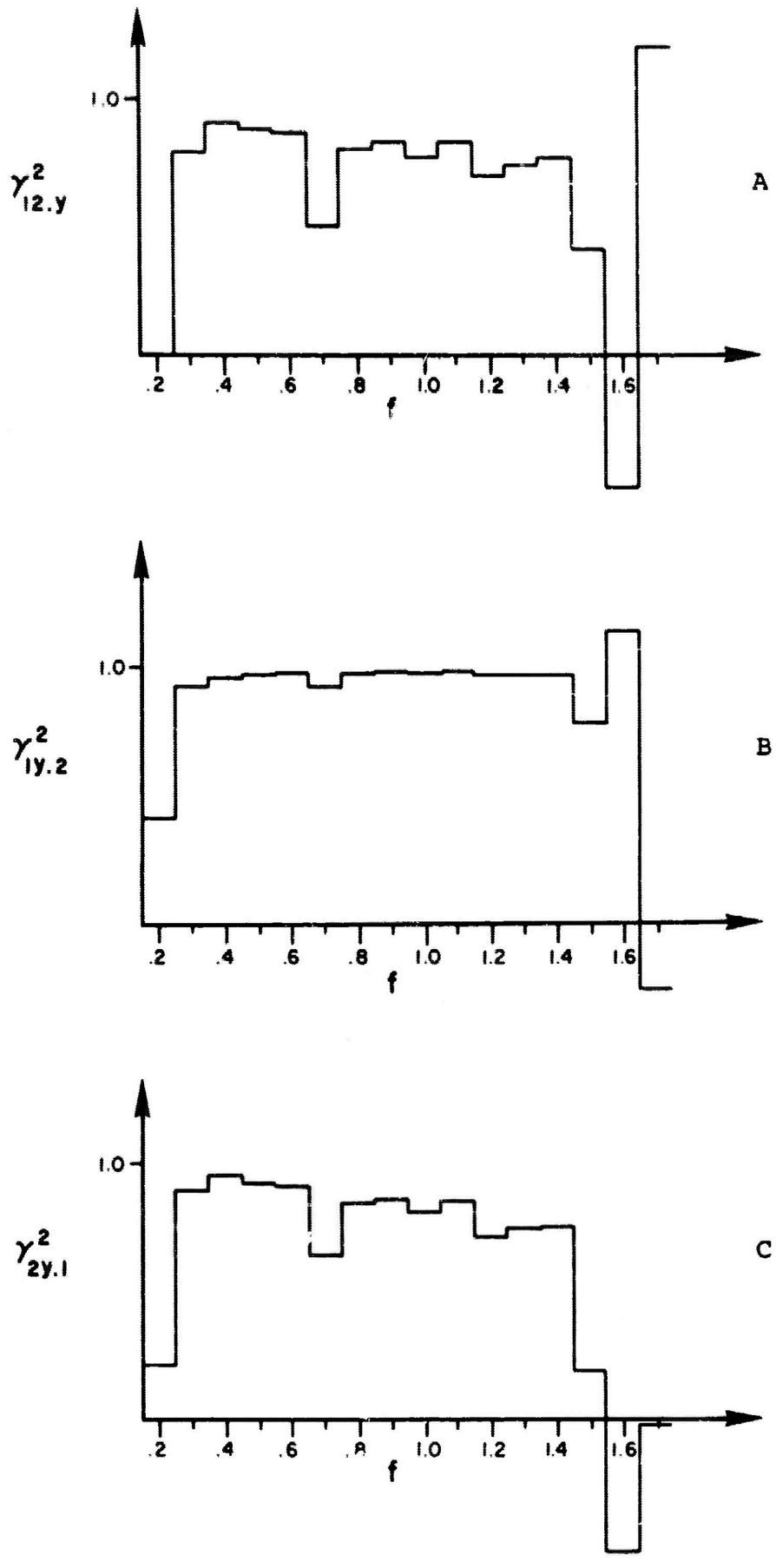

Partial Coherence Functions for Case II(c)

Figure III-19

APPENDIX IV

CONFIDENCE BANDS FOR THREE DIMENSIONAL LINEAR SYSTEM STATISTICS

CONFIDENCE BANDS FOR THREE DIMENSIONAL LINEAR SYSTEM STATISTICS

1. INTRODUCTION

The general form of the distributions of frequency response function and coherence function estimates for the multivariate Gaussian case has been developed in Ref. [1] and in more detail in other as yet unpublished MAC memos.

Comprehensive tables for the exact sampling distribution of coherence functions based on relatively small number n of degrees-of-freedom (d.f.) (up to n = 25) and dimension (total number of records of data) up to p = 10 have been computer generated, Ref. [2]. A study has been performed at MAC under a USAF contract to develop a Gaussian approximation for sample coherence. The results of this study are not yet published but are summarized in this report. A key result of Ref. [1] is that all types of sample coherencies (marginal [ordinary], conditional [partial], and multiple) have identical distributions with certain adjustments in the d.f. which is employed. Hence, one set of tables and one Gaussian approximation is sufficient for all types of coherence.

The F distribution arises in the computation of the frequency response function estimates. This distribution is, of course, well tabulated hence confidence limits are obtained in a straightforward manner.

2. CONFIDENCE LIMITS FOR COHERENCE FUNCTIONS

The tables of Ref. [2] give the (cumulative) distribution function (c.d.f) as a function of n and p when $n \leq 25$ and $p \leq 10$. For ordinary coherence between two variables one enters the tables with p = 2 and n = 2BT as the number of d.f. in the spectrum and coherence estimates. The quantity $B=1/\tau_{max}$ is the analysis bandwidth and T is the record length.

For the test cases which have been run for the seismic experiments the d. f. are

$$n = 2(.1\text{cps})\ (250\ \text{sec.}) = 50$$

The confidence limits for sample coherence may not be obtained from these tables since the limits are exceeded.

A transformation which is a very accurate normal approximation for moderate values of true coherence ($.4 \leq \gamma^2 \leq .95$) and useful for more extreme values is

$$z = \tanh^{-1} \gamma = \frac{1}{2} \ell n \frac{1 + \gamma}{1 - \gamma} \qquad (1)$$

where γ is the positive square root of sample coherence. It has been empirically determined that z is approximately normal with an approximate mean value

$$\mu_z = \frac{1}{2} \ell n \frac{1 + \gamma}{1 - \gamma} + \frac{p - 1}{2(n - p + 1)} \qquad (2)$$

where γ is the square root of true coherence. The variance of z is approximately

$$\sigma_z^2 = \frac{1}{2\ (n - p + 1)} \qquad (3)$$

From the above equations, if one is given a value of γ^2 then

$$P\left[\mu_z - \sigma_z Z_{1-\alpha/2} < z \leq \mu_z + \sigma_z Z_{1-\alpha/2}\right] = 1 - \alpha \qquad (4)$$

Let μ_z be broken into two parts

$$\zeta = \frac{1}{2} \ell n \frac{1 + \gamma}{1 - \gamma} \qquad (5)$$

$$b = \frac{p - 1}{2(n - p + 1)} \qquad (6)$$

Then, Eq. (4) can be rearranged to give $(1 - \alpha)$ confidence bounds on γ which are defined by the inequality

$$\tan h\ (z - b - Z_{1 - \alpha/2}\sigma_z) \leq \gamma \leq \tan h\ (z - b + Z_{1-\alpha/2}\sigma_z) \qquad (7)$$

where $Z_{1-\alpha/2}$ is the $(1 - \alpha/2)$ percentile of the normal distribution.

The adjustment that has to be made for partial coherence is straightforward. In general, one must subtract from the d.f. of the analysis the number of variables whose effect has been subtracted out. In general, one uses n' d.f. where

$$n' = n - (p - 2) \quad ; \quad n = 2\ BT \qquad (8)$$

In the two input single output case, one uses $n' = n - (3 - 2) = (n - 1)$ which will be a minor adjustment for large d.f. Table

I gives a few values of the 99% confidence limits for 2BT = 50. The values given in Table I are plotted in Figure 1. These apply for both the ordinary and partial coherence functions computed in the seismic experiments.

3. CONFIDENCE LIMITS FOR FREQUENCY RESPONSE FUNCTIONS

The confidence bands for the frequency response functions depend on the sample multiple coherence function, the sample multiple coherence function between the inputs (ordinary coherence for two inputs), the sample frequency response functions, and the sample input and output spectral densities. Alternatively, the confidence bands may be given in a form which is a function of the sample frequency response functions, the sample conditioned spectral density of the output y(t) and the elements of the inverse of the input sample spectral density matrix. It is this second form which is most convenient here and will be described.

Consider the two input $\left[x_1(t) \text{ and } x_2(t)\right]$ single output $\left[y(t)\right]$ system being studied. Let the matrix of spectral densities be represented by

$$\hat{S} \equiv \left[\begin{array}{cc:c} \hat{S}_{11} & \hat{S}_{12} & \hat{S}_{1y} \\ \hat{S}_{21} & \hat{S}_{22} & \hat{S}_{2y} \\ \hdashline \hat{S}_{y1} & \hat{S}_{y2} & \hat{S}_{yy} \end{array}\right] \equiv \left[\begin{array}{c:c} \hat{S}_{xx} & \hat{S}_{xy} \\ \hdashline \hat{S}_{yx} & \hat{S}_{yy} \end{array}\right] \qquad (9)$$

where $\hat{S}_{xx}$ is 2 x 2, $\hat{S}_{xy}$ is 2 x 1, $\hat{S}_{yx}$ is 1 x 2, and $\hat{S}_{yy}$ is 1 x 1. The function argument (f) is dropped for notational simplicity. Also, $\hat{S}_{12}$ is simplified notation for the cross-spectral density $\hat{S}_{x_1x_2}$ between the two inputs $x_1(t)$ and $x_2(t)$, etc. Let $\hat{S}^{jk}_{xx}$ represent elements of $\hat{S}^{-1}_{xx}$. The formulas for

confidence bands may then be written in the form

$$\text{Prob}\left[\begin{array}{c} |H_1 - \hat{H}_1|^2 \leq \left(\frac{1}{a_0} - 1\right) \hat{S}_{y|x}\, S_{xx}^{11} \\ \text{and} \\ |H_2 - \hat{H}_2|^2 \leq \left(\frac{1}{a_0} - 1\right) \hat{S}_{y|x}\, S_{xx}^{22} \end{array}\right] \geq P_0 \qquad (10)$$

The definitions of the above quantities are as follows. First the "conditioned" output spectral density is

$$\hat{S}_{y|x} = \hat{S}_{yy} - \hat{S}_{yx}\hat{S}_{xx}^{-1}\hat{S}_{xy} \qquad (11)$$

$$= \hat{S}_{yy} - \hat{S}_{y1}\hat{H}_1 - \hat{S}_{y2}\hat{H}_2$$

The term a_0 is obtained as follows. First letting a prime denote transpose, define the quantity

$$\hat{B} = (\hat{H} - H)\, \hat{S}_{xx} (\hat{H} - H)' \qquad (12)$$

where

$$H \equiv (H_1, H_2) \qquad (13)$$

Then it can be shown that the quantity

$$F = \frac{n-p}{p} \quad \frac{\hat{B}}{\hat{S}_{y|x}} \qquad (14)$$

is distributed as an F statistic with 2p and 2(n-p) d.f. Now a_0 is that constant which satisfies

$$\text{Prob}\left[a_0 < \frac{\hat{S}_{y|x}}{\hat{S}_{y|x} + B}\right] = p_0 \qquad (15)$$

Hence, one chooses a confidence level p_0. Then from tables of the F distribution one finds the percentile value $F_{p_0}\left[2p,\ 2(n-p)\right]$ and this quantity is $\left[(n-p)/p\right]\left[(1/a_0)-1\right]$. Operations on Eq. (15) lead one to Eq. (10) which provides the simultaneous confidence levels given as radii around the points H_1 and H_2 in the complex plane.

The confidence formula given by Eq. (10) may be interpreted in terms of the gain factor H(f) and the phase factor $\Phi(f)$ by considering the sketch in Figure 2.

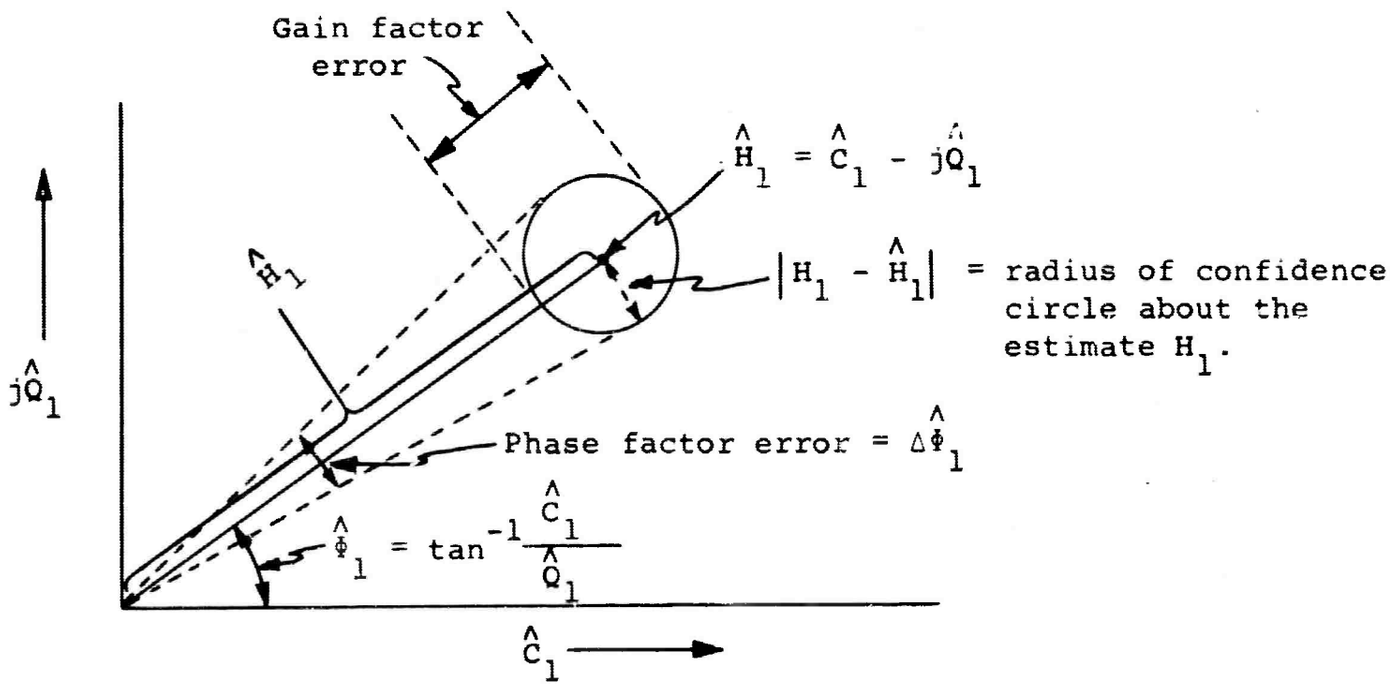

Confidence Bands for Gain and Phase Factors
Figure 2.

From Figure 2 one sees that $|\hat{H}_1|$ is bounded by $|\hat{H}_1| \pm \hat{r}_1$ where $\hat{r}_1 = |H_1 - \hat{H}_1|$ and the phase factor is bounded with confidence p_0 by $\hat{\Phi}_1 \pm \Delta\hat{\Phi}_1$ where

$$\Delta\hat{\Phi}_1 = \arcsin \frac{\hat{r}_1}{|\hat{H}_1|} \tag{16}$$

All these statements hold simultaneously for $|H_2|$ and $|\hat{\Phi}_2|$.

The preceding confidence formulas may be directly extended to p variables by defining the matrix $\hat{S}$ of Eq. (9) for p variables.

$$S = \left[\begin{array}{ccc:c} \hat{S}_{11} & \hat{S}_{12} \cdots & \hat{S}_{1,p-1} & \hat{S}_{1y} \\ \hat{S}_{21} & & & \\ \vdots & & & \\ \hat{S}_{p-1,1} & \cdots & \hat{S}_{p-1,p-1} & \hat{S}_{p-1,\,y} \\ \hdashline \hat{S}_{y1} & \cdots & \hat{S}_{y,p-1} & \hat{S}_{yy} \end{array}\right] = \left[\begin{array}{c:c} \hat{S}_{xx} & \hat{S}_{xy} \\ \hdashline \hat{S}_{yx} & \hat{S}_{yy} \end{array}\right] \tag{17}$$

Equation (10) becomes

$$\text{Prob} \left[\begin{array}{l} |H_1 - \hat{H}_1|^2 \le \left(\frac{1}{a_0} - 1\right) \hat{S}_{y|x} S^{11}_{xx} \\ \vdots \\ |H_{p-1} - \hat{H}_{p-1}|^2 \le \left(\frac{1}{a_0} - 1\right) \hat{S}_{y|x} S^{p-1,\,p-1}_{xx} \end{array}\right] \ge p_o \tag{18}$$

and Eq. (11) is written

$$\hat{S}_{y|x} = \hat{S}_{yy} - \hat{S}_{yx}\hat{S}_{xx}^{-1}\hat{S}_{xy}$$

$$= \hat{S}_{yy} - \hat{S}_{y1}\hat{H}_1 - \ldots - \hat{S}_{y,p-1}\hat{H}_{p-1} \qquad (19)$$

Due to the fact that several variables exist in the confidence formulas, it is not practical to prepare tables. The computations should be added to the basic computing program and given as a part of the normal output. A table of F values for varying n and p could be included in the computer.

REFERENCES (Appendix IV)

1. Goodman, N. R., "Statistical Analysis Based on Certain Multivariate Complex Gaussian Distribution (An Introduction)," Annals of Mathematical Statistics, Vol. 34, No. 1, March 1963, pp. 152 - 177.

2. Alexander, M. J. and Vok, C. A. "Tables of the Cumulative Distribution of Sample Multiple Coherence, "Rocketdyne Division, North American Aviation, Inc,, Research Memorandum 972 - 351, October 1963.